Functional Investigation of SERCA-Regulatory Subunits: The “Regulins”

by

Jessi Jordan Bak

A thesis submitted in partial fulfillment of the requirements for the degree of

Master of Science

Department of Biochemistry
University of Alberta

Abstract

Calcium homeostasis is essential and central to a variety of cellular processes from cell life and death pathways to metabolism to muscle contraction. One component that is essential to intracellular calcium regulation is known as the sarco(endo)plasmic reticulum Ca-ATPase, or SERCA. SERCA resides in the sarcoplasmic reticulum (SR) membrane and is responsible for pumping calcium ions across the SR membrane to be stored in the SR, the calcium storage organelle. SERCA is expressed in almost all cell types, is involved in many physiological processes, and is also regulated by a variety of single-pass transmembrane peptides, which mostly act to lower SERCA's apparent calcium affinity. The structure and function of two regulatory peptides in relation to SERCA has been well studied over the years, and excitingly, these studies can now be expanded to a family of peptide regulators. Recent bioinformatic investigations have shed light on new SERCA-regulators expressed throughout the body collectively referred to as the "regulins." In this family there is myoregulin (MLN) in skeletal muscle, ubiquitously expressed another-regulin (ALN), endoregulin (ELN) in endothelial and epithelial tissue, and DWORF (Dwarf open reading frame) in cardiac muscle. Interestingly, Ca-ATPase regulation is not isolated to mammals and a variety of invertebrate regulators, known as sarcolambans (SLB), have also been identified and found to regulate the invertebrate Ca-ATPase. While initial studies have been published to show physiological roles and their effect on SERCA, specific kinetic details of these effects have not been established. Thus, one goal of the work presented here was to characterize the effect of MLN and ALN on the maximal activity and apparent calcium affinity of SERCA in a controlled, *in vitro* system. The second goal of this study was to determine if sequence variation among regulators, SLB peptides in this case, could influence SERCA regulation. To do this, purified SERCA, regulatory peptide, and lipids were reconstituted to form isolated proteoliposomes from which SERCA activity could be measured through a coupled-enzyme ATPase assay. Since this was the first time these regulators were put in this system, a series of experiments to confirm the incorporation and orientation of these

peptides in proteoliposomes was done. From this, it was found that MLN incorporated into proteoliposomes in the correct orientation and acted to lower the maximal activity of SERCA. ALN also lowered the maximal activity in addition to lowering the apparent calcium affinity of SERCA. The four SLB peptides used in this study all had distinct effects indicating that sequence variation does have a role in the way SERCA is regulated. The work presented here is the first to elucidate the specific kinetic effect of newly identified regulatory peptides of SERCA.

Preface

This thesis is an original work by Jessi Bak. No part of this thesis has been previously published.

Acknowledgements

First off, I would like to thank my supervisor, Dr. Howard Young, for welcoming me to the lab not once, but three separate times- twice as a summer student and once as a graduate student. Without this I would not have been able to learn as much about science, research, and myself as I have over this part of my education and career. I am so grateful for our long meetings about experimental updates that usually derailed into dealing with the unavoidable frustrations of research. Thank you for being understanding when I was frustrated and for never getting upset as I struggled through my first projects. I hope to carry what I have learned forward without forgetting where that knowledge came from.

This section would not be complete without thanking those that directly supervised, trained, and worked alongside me in the lab. Without you I would definitely not be the person and scientist that I am today. Joseph Primeau- thank you for being my first official supervisor when I initially joined as a summer student and for showing me that science and research don't have to be completely serious all the time. Gareth Armanious- thank you for supervising my second summer term, for always challenging me, and for taking the time to understand and listen to my gripes. M'Lynn Fisher- thank you for being another productive and helpful person in the lab. Bashir Khan- Thank you for always taking the time to answer my questions with your vast knowledge of everything biochemistry. Nish Rathod- thank you for having such a determined attitude towards your research, it is a nice energy to have around. Mary Hernando- thank you for keeping me company at the back of the lab while writing (and at the gym)! Graeden Winkelaar and Steffane McLennan- thank you for tackling a project that I couldn't and for successfully making parts of it work! Of course, thank you to my committee members, Joanne Lemieux and Emmanuelle Cordat for the guidance, advice, and questions that ultimately made me a better researcher.

I would also like to thank Ivy Porter and Maggie Wang, both students that I supervised for a 499 and 298 project. It was such a great experience to share what I know with each of you. I wish both of you the best with wherever life takes you.

A huge thank you should also be extended to Dean Schieve, Lisa Dublin, and Kelsey Robertson for all their technical and administrative help through my time here. Without them a lot of computer meltdowns and paperwork issues would have ensued and that would have been terrible.

Another group that I can't forget are those that worked alongside me in the BCGSA and MPDRG student group. It was an outstanding experience and I am so grateful to have joined these groups. I feel like I have made some lifelong friends and I can't wait to hear about what you will all accomplish in the future

Last, but not least, I would like to thank those in my life who are not in science but were helpful from afar. Thank you, Mom, Dad, and Spencer for your encouragement and support in making sure I was comfortable and happy in Edmonton (deadmonton).

Table of Contents

List of Tables

List of Figures

List of Abbreviations

AAV	Adeno-associated virus
A-domain	Actuator domain of SERCA
ADP	Adenosine diphosphate
ALN	Another-regulin
AMP	Adenosine monophosphate
AMPK	AMP activated kinase
ANOVA	Analysis of variance
ATP	Adenosine triphosphate
B. terrestris or Bt	*Bombus terrestris* or bumblebee
BC_3H1	Smooth muscle cell line
BCA assay	Bicinchoninic acid assay
$C_{12}E_8$	Octaethylene glycol monododecyl ether
CAMKII	Calmodulin dependent protein kinase II
Ca-P60A	Invertebrate calcium-transporting ATPase SR/ER type gene
CD spectroscopy	Circular dichroism spectroscopy
CHCl3	Chloroform
CK2	Casein Kinase 2
COS-7	Kidney tissue cell line derived from African green money
D. melanogaster or Dm	*Drosophila melanogaster* or fruit fly
D. pulex or Dp	*Daphnia pulex* or water flea
DWORF	Dwarf open reading frame
E. coli	*Escherichia coli*
ELN	Endoregulin
ER/SR	Endoplasmic or sarcoplasmic reticulum
EYPA	Egg yolk phosphatidic acid
EYPC	Egg yolk phosphatidylcholine
EYPE	Egg yolk phosphatiylethanolamine
FRET	Fluorescence resonance energy transfer
FXYD	Phe-X amino acid-Tyr-Asp motif of the FXYD peptide family
GPCR	g-protein coupled receptor
GSK3	Glycogen synthase 3
HAX1	Hematopoietic cell-specific lyn substrate 1 associated protein X-1
HEK293	Human embryonic kindey cells
HPLC	High performance liquid chromatography
IPTG	Isopropyl β-D-1-thiogalactopyranoside
K_{Ca}	Apparent calcium affinity
LB	Luria broth, Lysogeny broth, Luria-Bertani medium
LDH	Lactate dehydrogenase
MBP	Maltose-binding protein
M-domain	Transmembrane domain of SERCA
MEF2	Myocyte enhancement factor
MgtA	Magnesium transporter A
MLN	Myoregulin
mRNA	Messenger RNA
MST	Microscale Thermophoresis
MyoD	Myogenic differentiation 1 transcription factor
NAD^+	Nicotinamide adenine dinucleotide (oxidized form)
NADH	Nicotinamide adenine dinucleotide (reduced form)
NCX	Sodium/calcium exchanger

N-domain	Nucleotide-binding domain of SERCA
nH	Cooperativity of calcium binding or hill coefficient
NHS-linked	N-Hydroxysulfosuccinimide ester linked
NMR	Nuclear magnetic resonance
OG	Octylpyranoglucoside
PCR	Polymerase chain reaction (pipette cry repeat)
P-domain	Phosphorylation domain of SERCA
PK	Pyruvate kinase
PKA	Protein kinase A
PLN	Phospholamban
PMCA	Plasma membrane calcium ATPase
PP1	Protein phosphatase 1
PSE	Phosphate/sodium buffer
PVDF	Polyvinylidene fluoride
RyR	Ryanodine Receptor
SDS-PAGE	Sodium dodecyl sulfate-polyacrylamide gel electrophoresis
SERCA	Sarco(endo)plasmic calcium ATPase
SLB	Sarcolamban
SLN	Sarcolipin
smORF	Small open reading frame
T. cancriformis or Tc	*Triops cancriformis* or tadpole shrimp
TEV	Tobacco etch virus
TFE	Trifluorethanol
TM	Transmembrane
TMHMM	Transmembrane domain prediction software
T-tubule	Transverse tubule
UV/Vis	Ultraviolet/visible light
V_{max}	Maximal activity
WT	Wild-type

List of common amino acids

Alanine	Ala	A
Arginine	Arg	R
Asparagine	Asn	N
Aspartic acid	Asp	D
Cysteine	Cys	C
Glutamic acid	Glu	E
Glutamine	Gln	Q
Glycine	Gly	G
Histidine	His	H
Isoleucine	Ile	I
Leucine	Leu	L
Lysine	Lys	K
Methionine	Met	M
Phenylalanine	Phe	F
Proline	Pro	P
Serine	Ser	S
Threonine	Thr	T
Tryptophan	Trp	W
Tyrosine	Tyr	Y
Valine	Val	V

List of amino acid motifs mentioned

SXXE/D	CK2 recognition motif
SXXXP	GSK3 recognition motif
RRXS	PKA recognition motif
RXXS	AMPK recognition motif
WLL	Conserved motif in SLN-like SLB peptides
RSYQY	Inhibitory SLN C-terminal tail

Chapter 1: Introduction

1.1: Calcium

Calcium cycling and signalling and the associated regulatory parts of these processes are essential for a multitude of physiological processes (Figure 1). Almost all a mammal's calcium is stored in bones and teeth, however, about 1% of mammal's total calcium is found in intracellular stores in tissues like muscle and epithelial tissue and is greatly important for the function of those tissues[1]. While calcium is not the most abundant ion in an organism, it is still a primary signalling ion compared to the more abundant ion, magnesium. This is because calcium is a larger ion, which allows for it to bind many different biomolecules in a cell. Additionally, binding of calcium to a protein causes a change in shape and charge in the protein, two aspects which make up the basis for signal transduction in a cell. With this, the use of calcium as a messenger or signalling molecule in a cell became more favoured by evolution, eventually leading to intracellular calcium homeostasis having integral role in cell life and death pathways, regulation of gene expression, cellular metabolism, neuron signalling, and in muscle function and metabolism[2–5].

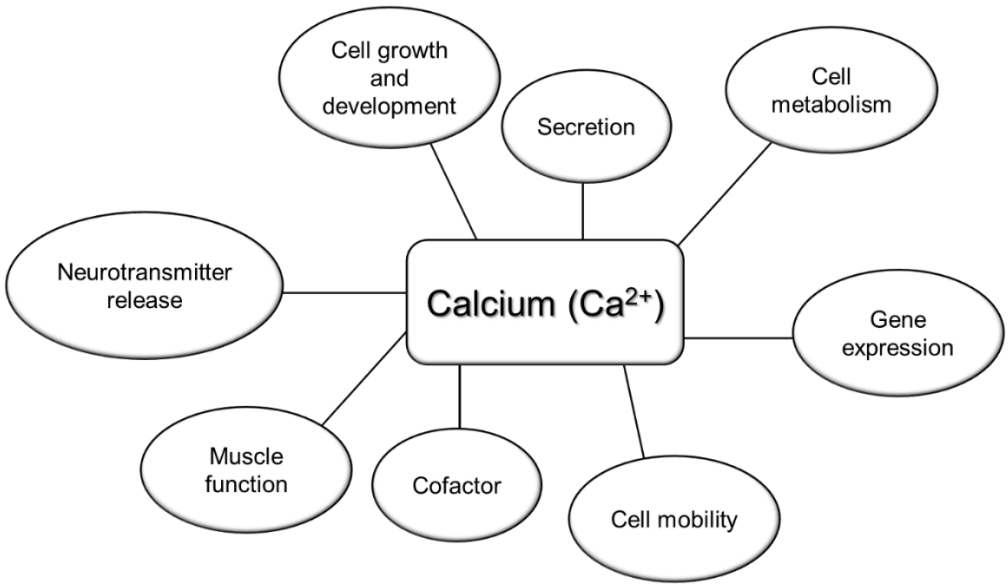

Figure 1: Web diagram placing calcium to be central in a plethora of cellular processes

1.1.1: Calcium and muscle

Calcium has a key role in many processes, particularly in the contraction/relaxation cycle of muscle- the tissue that allows our bodies to move and function. There are different types of muscle, from cardiac, to skeletal, to vascular smooth muscle, with the former two being of focus for this work. Muscle is composed of specialized contractile cells that are arranged as longitudinal myofibrils to generate a pattern of aligned bands that contain the contractile machinery: troponin, tropomyosin, actin, and myosin filaments[6]. The myofibrils of muscle are surrounded by the sarcolemma which contains collections of mitochondria, lipid droplets, glycogen granules, sections of Golgi apparatus, along with the endoplasmic/sarcoplasmic reticulum (ER/SR). The sarcolemma is further arranged to contain transverse tubules, or T-tubules, which form folds that allow for electrical stimuli to travel within the cell and stimulate calcium-mobilizing components and consequent contraction[6,7] (Figure 2). Cardiac muscle shares the same general striated architecture as skeletal muscle with some differences[8]. The components of muscle are arranged in organized repeating units, allowing for the biochemical changes to be translated into mechanical movement as muscle contracts and relaxes.

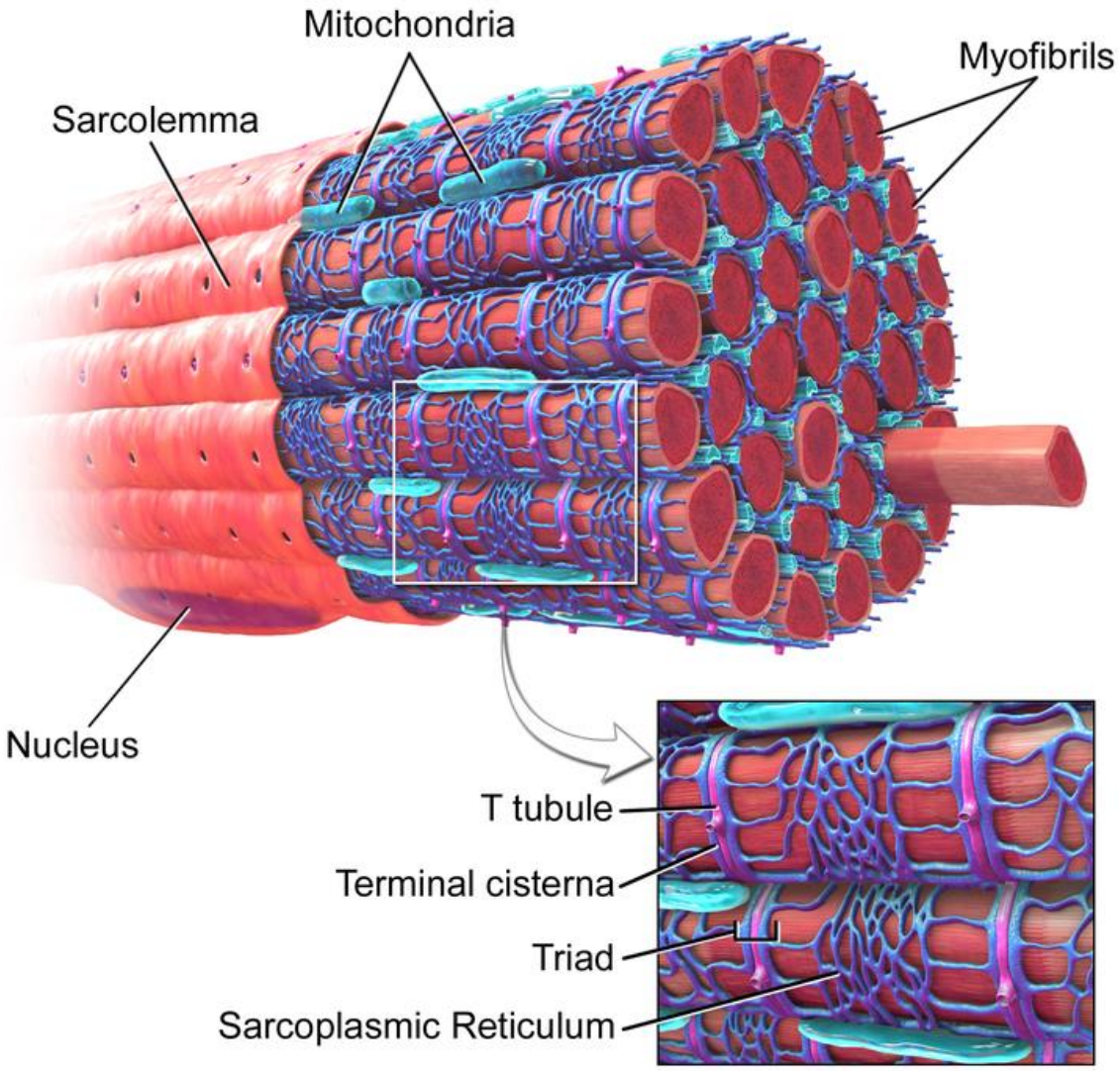

Figure 2: Schematic of skeletal muscle
Top panel shows a muscle fibre encapsulated by the sarcolemma. Many mitochondria are also seen to surround the myofibrils. The bottom panel (zoomed in from top panel) shows the sarcoplasmic reticulum (blue webbed structure) that surrounds the myofibrils[9]. Image used under Creative Commons Attribution Unported License[10].

1.1.2: Intracellular calcium signalling

Since calcium has an essential role in muscle contraction/relaxation in addition to other physiological processes, calcium cycling throughout the entire cell is important and carried out by multiple biomolecules. In line with calcium having a role in many pathways, four different calcium channels exist in the plasma membrane of the cell, each of which acts to import calcium initiated by different systems or stimuli[1,11]. In muscle cells, the L-type voltage-gated calcium channel resides in the T-tubule of the plasma membrane[12]. Inside the cell, free calcium exists in the cytoplasm at around 100 nM, with any remaining calcium being buffered or sequestered by calsequestrin or calreticulin in the ER or SR[1]. Calcium is transported out of the cell via the Plasma Membrane Calcium ATPase (PMCA) or the sodium/calcium exchanger (NCX). Mitochondria also store calcium and utilize a uniporter to take up calcium. While calcium cycles throughout the cell, most of the intracellular calcium is stored in the endoplasmic or sarcoplasmic reticulum[1] (Figure 3).

The calcium that is stored in and cycles through the ER/SR is the most relevant to my studies and with that, the molecular components involved in this will be explained in more detail. When there is an external stimulus present, like an action potential to a muscle cell, it travels down the T-tubule to signal the L-type voltage-gated calcium channel to open and release a small amount of calcium into the cell[7,12]. This then signals the ryanodine receptor (RyR) to open, allowing calcium to exit the SR, enter the cytoplasm, interact with the contractile machinery of muscle, and cause the muscle to contract[13,14]. Following contraction, muscle relaxation occurs as calcium is pumped across the SR membrane against its concentration gradient via the sarco(endo)plasmic reticulum calcium ATPase, or SERCA (Figure 3).

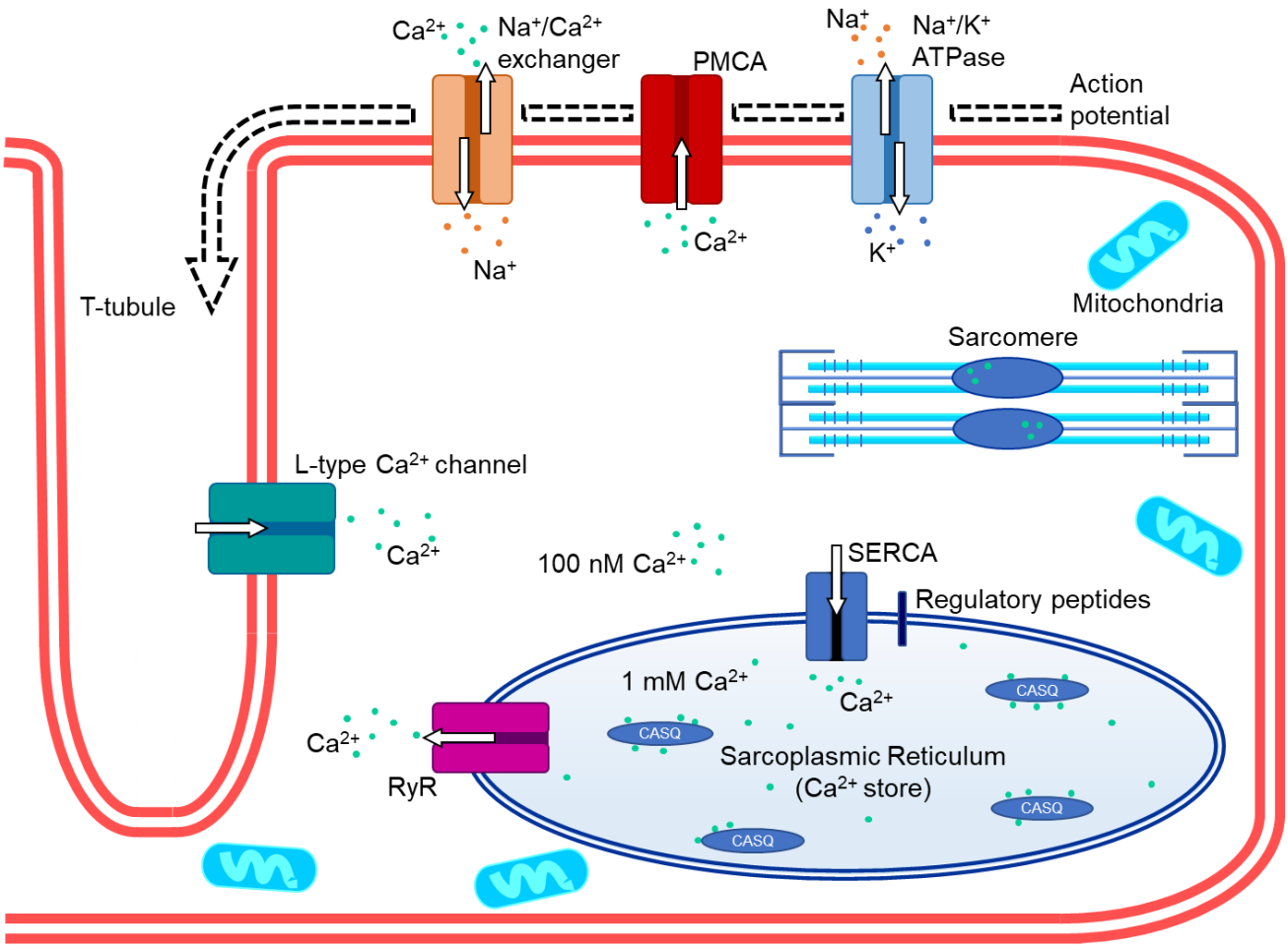

Figure 3: General schematic of calcium homeostasis and trafficking in a muscle cell. In a relaxed state, the Ca^{2+} concentration in the cytoplasm is 10, 000 times lower than in the SR, where free calcium exists along with Ca^{2+} bound to Ca^{2+}-sequestering proteins. When an action potential travels across the plasma membrane and into the transverse tubule, the L-type Ca^{2+} channel is activated, allowing a small amount of Ca^{2+} into the cell. This influx then triggers the ryanodine receptor to open and for Ca^{2+} to exit the SR. This overall increase in Ca^{2+} in the cytosol leads to muscle contraction and triggers the sarco/endoplasmic reticulum Ca^{2+}-ATPase to pump calcium across the SR membrane back into storage causing the muscle to relax. Regulatory peptides of SERCA are also present in the SR membrane and regulate SERCA's ability to pump Ca^{2+}. Additional membrane transport proteins in the plasma membrane are responsible for maintaining other cellular ion concentrations in addition to Ca^{2+}.

1.2: P-type ATPases and SERCA

P-type ATPases are a large family of membrane proteins that function to transport a variety of ions across cell and organelle membranes in all types of life. Because of this, P-type ATPases have a role in a multitude of physiological processes. This family includes enzymes like the PMCA, Na^+/K^+ ATPase, and, H^+/K^+ ATPase all of which couple the transport of ions across the membrane to the hydrolysis of ATP[15,16]. The P-type ATPases are separated into five different subfamilies based on the ions they transport: P1A ATPases are bacterial K^+ pumps, P2A ATPases are Ca^{2+} pumps, P2B ATPases are calmodulin-binding Ca^{2+} ATPases, P2C ATPases are Na^+/K^+ pumps, P3 ATPases are plasma membrane H^+ ATPases, P4 ATPases are phospholipid flippases, and P5 ATPases are orphan transporters. Each member does have unique characteristics, but each subfamily shares common conserved motifs and sequences that make up the similarities in the structure and reaction mechanism[17]. With this, the P2A ATPase, SERCA, is the focus of this work and its general structure and reaction mechanism will be discussed in more detail.

SERCA is a 110 kDa P-type ATPase that exists throughout the body, acting to pump calcium ions from the cytoplasm of the cell across the SR membrane back into storage. SERCA specifically functions to transport two calcium ions at the expense of one ATP[17]. Since Ca^{2+}-ATPase has a central role in intracellular calcium cycling and regulation so the details of this enzyme and its role will be described in the following sections.

1.2.1: Structural information on SERCA

All P-type ATPases contain 4 domains with slight variations in size amongst domains of different sub family members. SERCA is made up of the P-domain (phosphorylation), N-domain (nucleotide binding), A-domain (actuator), and M-domain (transmembrane helices) (Figure 4). The P-domain is globular with a series of β-sheets in the centre of the domain, flanked by α-helices, which join to neighbouring domains and as the name suggests, is the site of

autophosphorylation. This domain is considered the catalytic core and contains the most sequence conservation among the domains, alluding to its importance in the P-type ATPase reaction mechanism[18]. Phosphorylation occurs at a conserved Asp residue in a reversible manner and forms a transient phosphoenzyme intermediate. Of note is the importance of a Mg^{2+} cofactor, which is important in balancing the charge repulsion between the negative Asp and phosphate group, and specifically coordinating the enzyme so that the Asp residue can be phosphorylated[18–20].

The N-domain is an insert that extends off of the P-domain and is connected by a conserved link of anti-parallel strands. It also contains a central β-strand structure which has a conserved motif and Lys reside, making up the nucleotide-binding domain. The adenosine is the only part of ATP to reside in the binding domain and that the triphosphate moiety extended toward the P-domain to phosphorylate the catalytic Asp residue[21,22].

The A-domain is divided into two smaller sections connected to M1, M2, and M3 transmembrane helices of the M-domain. Initially, its function was unknown as it does not have a cofactor or ion binding site. However, a series of structural studies investigating the various reaction intermediates of P-type ATPases showed that the A-domain goes through a dramatic conformational change through the reaction cycle[18,23]. These large movements by a single domain is one of the unique characteristics of P-type ATPases.

The M-domain makes up the transmembrane domain; in SERCA there are ten α-helices, namely M1-M10, that make up this domain and house the binding sites for two Ca^{2+} ions. The TM helices are unique in terms of their length, tilting, and rigidity and that the helices directly involved in calcium binding have different folding patterns to create spaces for Ca^{2+} to bind[22]. Of the helices involved in calcium binding, M4-M6 and M8, M4 is partially unwound to accommodate the binding and translocation of Ca^{2+} ions[23]. Also, the structural rearrangements of the transmembrane helices allow for the transport of counter ions for SERCA, which are

protons[23,24]. Another aspect that is unique to the M-domain is that it has the least amount of sequence conservation compared to the other domains of P-type ATPases. This is to account for the difference in atomic radii of the various ions that each P-type ATPase can transport and potentially to accommodate different regulatory peptides of these ATPases[18].

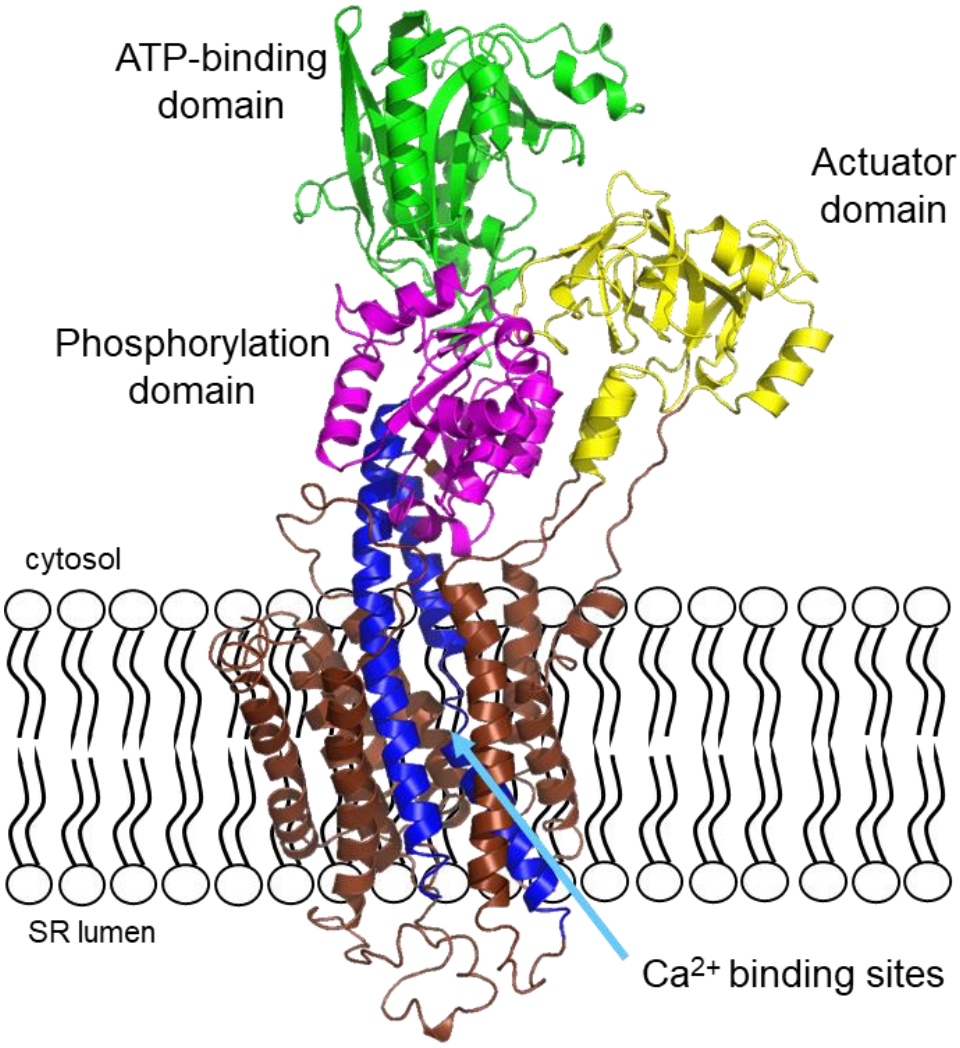

Figure 4: General SERCA structure
Shown above is the crystal structure of SERCA2a with the ATP-binding domain (green), the actuator domain (yellow), and the phosphorylation domain (pink). The TM helices are shown in brown and blue, with the blue helices representing where the Ca^{2+} binding sites are located.

1.2.2: Mechanism of Ca^{2+} pumping by SERCA

All P-type ATPases share a general reaction scheme known as the Post-Albers Scheme, though Ca^{2+} transport by SERCA will be discussed in more detail here. This process is highlighted by three main features: the sequential transfer of ions across the membrane against their concentration gradient, the ion binding sites are in the TM region, and a common set of steps that make up ion transport[25]. Generally, this reaction mechanism includes a high affinity state and a low affinity state for ion binding with multiple intermediate steps in between[17].

The ion pumping reaction cycle that SERCA goes through includes 6 steps (Figure 5). First, Ca^{2+} binds in a sequential and cooperative manner to the high-affinity E1 state of SERCA in exchange for 2-3 H^{+}[26]. This ion binding leads to a TM helix rearrangement which propagates to the P-domain, allowing for Mg^{2+} to bind to this domain as a cofactor. Phosphorylation will not occur if this does not happen, as the Mg^{2+} is responsible for negating the electrostatic repulsion between the Asp in the phosphorylation site and γ-phosphate on ATP[17,27]. Once these components are in place, phosphorylation occurs, generating a phosphorylated intermediate with Ca^{2+} and ADP occluded, or $(Ca^{2+})_2$-E1P-ADP. Following this, ADP is exchanged for ATP and the phosphorylated E1 state is changed to a phosphorylated low-affinity E2 state with Ca^{2+} and ADP, or $(Ca^{2+})_2$-E2P-ADP. Ca^{2+} is then exchanged for protons, where the Ca^{2+} exits SERCA's ion binding site into the lumen of the SR. Dephosphorylation occurs, resulting in an intermediate where calcium can again bind in exchange for H^{+} ions and SERCA can continue with another pumping cycle[25].

Also, of note is that the rate-limiting step of this reaction is thought to be between the E1P to E2P transition or the return from E2 to E1 (Figure 5). Additionally, the rate-limiting step was thought to include the large rotational movement of the A-domain during the E1P to E2P transition. This movement is to help protect the phosphoryl group from hydrolysis as a conserved loop in the A-domain is brought in close contact with the phosphorylation site. The

other cytoplasmic domains also go through conformational movements as a result of the movement of the A-domain and it has been observed that TM helices rotate or incline. The movement of the cytoplasmic domains and rotation of the TM helices are linked, tightly regulated, and coordinated, and they all must occur to ensure the P-domain is in the correct orientation so that phosphorylation can take place[18,25]. Structures for almost all of SERCA's reaction cycle intermediates have been determined[28]. Studies utilizing single-molecule FRET have also provided mechanistic details into the timescale and domain movements of P-type ATPases[29,30]. Single-molecule FRET studies showed that the rate-limiting intermediates of the reaction are those that occur before the E1P formation[29.30]. These studies provide a means to understand individual transition states in the reaction cycle and will help to elucidate complete details of the reaction mechanism when paired with other structural studies of P-type ATPases.

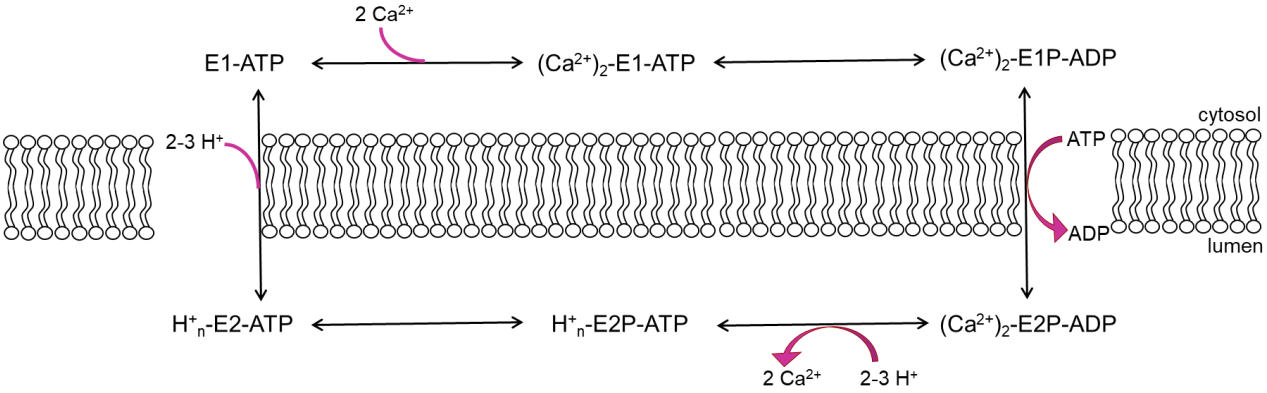

Figure 5: General outline of SERCA's reaction mechanism to pump calcium
The cycle begins with Ca^{2+} binding to the high affinity E1 state, forming a calcium and ATP-bound intermediate. This intermediate is then phosphorylated and transferred to the E2P state. Following this, H^+ (n=2-3) is exchanged for Ca^{2+} (n=2). The cycle concludes with dephosphorylation, resulting in a return to the low-affinity E2 state awaiting Ca^{2+} binding.

1.3: SERCA gene isoforms and expression patterns

In vertebrates, SERCA exists as three different genes and multiple splice variants (Table 1). Briefly, SERCA1 is expressed in fast-twitch skeletal muscle as two different isoforms, a and b, which are the adult and neonatal forms, respectively[31]. SERCA2a is expressed in cardiac and slow-twitch skeletal muscle and SERCA2b is present in all tissues at low levels. SERCA3 is expressed in non-muscle tissue and only isoforms a-c include evidence of protein expression. Finally, SERCA2c has also been identified in cardiac muscle.

Table 1: Tissue expression of various SERCA isoforms

Isoform	**Tissue Expression**
SERCA 1a	Fast-twitch skeletal muscle, Adult
SERCA 1b	Fast-twitch skeletal muscle, Neonatal
SERCA 2a, 2c	Cardiac and slow-twitch skeletal muscle
SERCA 2b	All tissues at low levels: skeletal, cardiac, smooth, non-muscle
SERCA 3a-f	Non-muscle tissues

Ca-ATPases are also present in invertebrates and they are encoded by a single gene that can be alternatively spliced to form two isoforms. These isoforms in *C. elegans* slightly resemble SERCA2a and 2b in vertebrates and that these isoforms in both *C. elegans* and *D. melanogaster* are essential to the organism. In *C. elegans*, SERCA is required for proper development and muscle function and in *D. melanogaster*, SERCA is also essential for muscle function and for maintenance of heartbeat frequency[32,33]. Ultimately, this shows that SERCA's expression and function is conserved through different domains of life.

As alluded to in Table 1 of SERCA distribution, the developmental stage of an organism dictates the isoform and level of SERCA expression. For example, SERCA1b and SERCA2a are co-expressed in developing skeletal muscle, but in adult tissue these isoforms are replaced by SERCA1a. Some isoforms maintain expression during development, like SERCA2a, which remains expressed in slow-twitch skeletal muscle and cardiac muscle, but not in any other

forms of skeletal muscle in adulthood[16,34]. The reason for this is unclear and it has been suggested that the individual calcium transport features of each SERCA isoform are what make up the characteristics of muscle at that stage of life[16]. Increases in SERCA expression are due to development of the SR in the tissue, which would then lead to greater muscle activity[34]. Other age-related changes have been observed, showing that SR calcium uptake decreases in aging cardiomyocytes[31,34]. While the exact reason for these differences between the isoforms is unknown, SERCA is a necessary player in maintaining intracellular calcium homeostasis.

Along with being expressed in different tissues, each SERCA isoform has unique structural and functional characteristics. Overall, the various isoforms do share the same general primary structure and tertiary structure, indicating that the differences in expression patterns may be connected to distinct functional characteristics that would ultimately govern calcium homeostasis in a cell type[16]. In cells, SERCA1a had a higher turnover rate compared to SERCA2a, hinting that perhaps the skeletal muscle isoform is specialized to accommodate greater contractile action[35]. SERCA2b has a higher affinity for calcium and slower turnover rate than SERCA2a. Of note, SERCA2b has an extended C-terminal tail that may be the reason for the kinetic difference between isoforms[36,37]. SERCA3 showed a decreased affinity for calcium and a higher pH dependence from the other isoforms[38]. With regard to the neonatal isoform, SERCA1b has a lower level of activity compared to SERCA1a with a comparable affinity for calcium[39]. By combining the unique expression patterns and kinetic properties of SERCA isoforms, studies have begun to deduce subtle physiological features of each isoform.

1.4: Physiological role of SERCA isoforms

In line with the knowledge that SERCA isoforms show tissue-specific expression, some isoforms have been implicated in physiological processes with clinical relevance for disease. Specifically, defective calcium signalling has been shown to lead to heart failure, muscular

dystrophy, sarcopenia, sepsis, and cancer, as examples[40]. The most-studied isoforms of SERCA and their associated physiological roles will be discussed here.

SERCA1a, expressed in fast-twitch skeletal muscle, is essential to contraction/relaxation coupling in muscle and is thought to be associated with muscular dystrophy and Brody Myopathy. Briefly, muscular dystrophies are a group of disorders characterized by the breakdown or weakening of muscle over time and Brody myopathy is defined by excessive cramping of skeletal muscle[41,42]. Both disorders have links to altered calcium regulation in muscle. Extensive studies of mutations in SERCA1a showed that mutations caused decreased expression or lowered maximal activity, lessening the amount of calcium to be pumped back into the SR and consequently, decreasing the relaxation of muscle[43–45].

SERCA1b, the neonatal isoform, was implicated in muscle growth and development based on the observation of insufficient diaphragm development in rats and mice lacking SERCA1b. This implication was further supported by the finding that isolated BC_3H1 cells, which differentiate into myocytes, would not express SERCA1b but would express SERCA1a[46]. A decrease in mRNA transcript levels of SERCA1b in rabbit muscle 2-weeks after birth and into adult development was also observed[47]. In combination, these findings show that SERCA1b is a key component in muscle differentiation and development, but not in adult muscle.

SERCA2a is expressed in slow-twitch skeletal muscle and cardiac muscle, with the majority of literature focusing on SERCA's role in the heart. In slow twitch skeletal muscle, SERCA2a is not as highly expressed as the isoform in fast-twitch skeletal muscle, indicating that rapid calcium transport is not as important in slow-twitch muscle[45]. SERCA2a, the cardiac isoform, has a role in cardiac ischemia, hypertrophy, and dilated cardiomyopathy in the case of lower-than-normal expression levels. Elevated expression levels have also been linked to hypertrophy and congestive heart failure[48]. A SERCA2a knock-out mouse is embryonic lethal, but the heterozygous offspring could live with impaired SERCA2a expression and function,

eventually leading to heart failure. This indicated that another mechanism is available to maintain some level of calcium regulation[49]. Nonetheless, SERCA2a is considered a therapeutic target in heart failure. Multiple therapeutic approaches have been explored to improve the expression or function of SERCA2a in humans, but no potential treatment has made it though clinical testing yet[48].

SERCA2b has an overarching calcium housekeeping function as it is expressed in all tissues at low levels[48]. In line with its widespread expression, SERCA2b has been implicated in in many pathways such as the cell surface expression of GPCRs, to cell differentiation in liposarcomas, and store-operated calcium entry in platelets[50–52]. In addition to this, it has been proposed that the kinetic differences between the SERCA2 isoforms is due to the interaction of the 2b tail with calreticulin or calnexin[53]. In this model, it is suggested that in resting conditions, the tail of SERCA2b interacts with the luminal tail of calnexin leading to a decrease in activity and increase in sensitivity of SERCA. During active conditions, this interaction shifts to the opposite scenario leading to the higher activity and lower sensitivity that is previously reported for SERCA2b[45,53]. SERCA2b mutations have also been linked to Darier's disease, a skin disorder characterized by a decreased epidermal cell adhesion and altered keratinization, which is caused by altered calcium homeostasis in skin cells[54,55]. While these links are not completely defined, SERCA2b mutations may be linked to neurological disorders, but not cardiovascular function in humans[56,57]. Adding to its widespread expression and physiological role, SERCA2b has also been implicated in ER stress response, apoptosis, and cell growth. A complete map of the interactions of other cellular components with SERCA2b has not been done, but SERCA2b does have a broad and important role in calcium homeostasis[45,58].

SERCA3 exists as 6 different isoforms and is the least conserved SERCA isoform; it is expressed in non-muscle tissues, has a much lower affinity for calcium, and functions at a higher pH. Initially, no obvious phenotype was observed from SERCA3 ablation studies but

some disturbance to non-muscle cell relaxation was seen[59,60]. It is also co-expressed with SERCA2b, hinting towards a housekeeping function, but SERCA3 behaves differently and follows a unique expression pattern in endothelial cells[61]. In pancreatic beta cells, calcium homeostasis is an important regulator of insulin release and overall glucose metabolism[62,63]. With this, SERCA isoforms have been implicated in diabetes. SERCA3 is presumed to have a role in glucose metabolism because of a noticeable decrease in SERCA3 in type-2 diabetes, but not SERCA2b in diabetic rats. This would indicate that it is SERCA3 that has the main role in maintaining calcium homeostasis for proper insulin secretion and glucose metabolism[64]. SERCA2a also has a role in diabetic cardiomyopathy through modes that are not well understood, but theorized, nonetheless. In type 1 diabetes, hyperglycemia leads to the oxidization of SERCA, decreasing its activity, ability to pump calcium, and consequently, altering the contraction/relaxation cycle of the heart. In type 2 diabetes, decreases in calcium uptake, contractility, and expression were all seen, though it is unclear whether this is a cause or consequence of the disease[65]. Similarly, studies have linked altered calcium homeostasis to skeletal muscle function and diabetes[66]. All in all, SERCA has widespread physiological importance, making it a valuable potential therapeutic target in many conditions. Because of this, all aspects surrounding SERCA-dependent calcium homeostasis and, regulation are considered important research targets.

1.5: Regulatory subunits of SERCA

SERCA is regulated by multiple single-pass transmembrane peptides. These regulatory peptides have been identified through a variety of means and so far, they appear to regulate different isoforms of SERCA in unique ways. Historically, the two most well-studied regulators are phospholamban (PLN) and sarcolipin (SLN).

1.5.1: Phospholamban (PLN)

PLN was discovered in the 1970's through experiments that aimed to phosphorylate the cardiac isoform of SERCA, SERCA2a. Instead of phosphorylating SERCA, a small peptide was the target of phosphorylation in crude microsomal vesicles[67,68]. Studies building from this found that PLN has a role in cardiac function by decreasing the calcium affinity of SERCA2a[69]. Furthermore, phosphorylation of PLN by protein kinase A (PKA) or calmodulin-dependent protein kinase ll (CAMKll) led to a decrease in PLN's ability to inhibit SERCA[69–72]. This process is controlled via the β-adrenergic signalling pathway, which is activated by adrenalin, leading to the activation of G-proteins, adenylyl cyclase, cyclic AMP, and consequently PKA, which phosphorylates PLN[73]. These critical studies began to clarify PLN's role in regulating cardiac muscle.

An important next step was the ablation of PLN in mice, which led to increased levels of contractility and an increased apparent calcium affinity of SERCA, indicating that PLN has an essential role in maintaining these two processes[74]. This is important as common indications of heart failure are abnormal calcium transients and disrupted muscle contractions[75]. A number of mutations in human PLN have been identified and shown to alter both of these aspects. Mutations are found throughout the peptide sequence, with notable mutations being R9C, R9L, R14del, and L39stop, each of which has been implicated as lethal or greatly damaging to heart function[76–78]. The focus of the work discussed in the latter part of this thesis is on regulatory peptides homologous to PLN, so it is instructive to note that a peptide regulator of SERCA can have an overall essential physiological function, is held under another level of regulation by phosphorylation, and is found to have disease-associated genetic variants in humans.

Numerous structural and interaction studies have been conducted to explore the relationship between SERCA and PLN. Generally, PLN has both α-helical and β-sheet structure, with the α-helical region corresponding to the transmembrane domain[79,80]. PLN also

exists as a monomer and as a pentamer, though the role of each of these forms in regulating SERCA is still debated in the field[81]. Studies employing NMR, cross-linking, and modelling from X-ray crystal structures of SERCA, all show that there is an interaction between SERCA and monomeric PLN[81]. Again, since PLN is not the focus of this thesis work, details into its structure and interaction with SERCA will not be described here in detail, however, it is important to note that PLN's structure has been determined and that it's structure and interaction with SERCA has been explored through a variety of means like NMR, FRET, and crystallography.

1.5.2: Sarcolipin (SLN)

In addition to PLN, SLN is another regulatory peptide with a plethora of physiological roles, some of which have been uncovered in recent years. SLN was initially discovered because it co-purified with SERCA during purifications from rabbit hind-leg muscle[82]. Later, it was found that SLN is mainly expressed in fast-twitch skeletal muscle with SERCA1a and in the atria of the heart with SERCA2a[83,84]. Additionally, SLN acts to inhibit SERCA's ability to pump calcium across the SR membrane, much like PLN[85]. This inhibitory action on SERCA in combination with varied tissue expression led to a variety of proposed physiological roles for SLN from atrial function and remodelling, to muscle thermogenesis, and to mitochondrial biogenesis[86–90]. Studies involving a SLN knockout mouse model showed increased cardiac contractility and calcium transport rates compared to WT mice, indicating SLN to have an important role in regulating these processes[87]. Studies following this showed that an increase in fibrosis and altered expression of genes encoding for extracellular matrix proteins in the atria, hinting that disrupted calcium cycling due to a lack of SLN leads to changes in atrial tissue[86]. In studies taking an opposite approach overexpression of SLN in cardiac tissue, showed impaired cardiac contractility and inhibition of SERCA, also supporting the notion that SLN is essential to proper atria function and calcium cycling within cardiac tissue[91].

Moving away from SLN's role in the heart, the fact that SLN is also present in skeletal muscle raised questions as to its role there. Initial studies using isothermal calorimetry measured an increase in heat output from ATP hydrolysis by SERCA when SLN was present[92]. By combining this result and the finding that Ca^{2+} tended to accumulate in the presence of SLN, it was proposed that SLN uncouples ATP hydrolysis by SERCA from its ability to pump calcium[93,94]. This is distinct from PLN since SLN likely binds to SERCA throughout its transport cycle, whereas PLN only binds to the Ca^{2+}-free E2 state of SERCA[94,95]. On a more physiological note, this uncoupling and consequent heat production and increase in energy expenditure has been implicated in non-shivering thermogenesis and is potentially a mammalian adaptation to colder temperatures[89,96]. SLN in skeletal muscle has a role in metabolism, and consequently, obesity, as a lack of SLN leads to an increase in obesity in mice[88,96]. Altered Ca^{2+} regulation in the presence of SLN has been shown to increase signals to activate mitochondrial biogenesis[90]. With the results of each of these functional explorations, it is clear that SLN has a role in muscle thermogenesis and metabolism.

SLN also has unique characteristics in terms of residues that are essential to its mode of regulating SERCA. One important aspect of SLN to note is that its main inhibitory function is encoded in the last five residues of its C-terminal tail, consisting of the residues RSYQY. Removal of this sequence resulted in a loss of inhibition by SLN and the addition of this sequence to PLN resulted in super-inhibition of SERCA[97]. X-ray crystal structures of SLN and SERCA together have also been determined, showing that it interacts with SERCA in the same site as PLN[98]. Although SLN is not the focus of this thesis, its most noteworthy aspects are its varied physiological function in different tissues and its distinct set of residues that contribute to function compared to PLN.

1.5.3: Small regulators, growing family: General “regulin” introduction

While both of these regulators interact with SERCA, they each have their own pattern of expression, physiological consequences, and unique structural features. What’s more, we now know that SERCA regulation, and Ca-ATPase regulation overall, does not stop with only PLN and SLN. Technological advances in bioinformatic screening have led to the discovery of additional small peptide regulators[99,100]. What is especially unique about these new regulators is that they were initially hidden in sequences of RNA that were annotated as long, non-coding. With the identification of these various regulatory peptides, we have taken to referring to this family as the “regulins” (Figure 6).

The expansion of the family of SERCA-regulatory began with identification of the sarcolamban peptides, which are found in insects and are orthologues to the mammalian regulators. Some of these peptides have been found to be more similar to PLN and others to SLN in terms of sequence identity and their effect on SERCA[101]. These regulators have a specific role in modulating the activity of insect Ca-ATPase, hinting at roles to modulate cardiovascular function or temperature regulation[102]. More details into the insect orthologues will be discussed in Chapter 4.

In addition to these inhibitory regulins, a peptide with a unique effect on SERCA was identified; Dwarf open reading frame (DWORF), was identified and found to enhance SERCA activity in the heart (Figure 6). The mode in which DWORF enhances SERCA activity is debated, though it has been suggested that it acts by displacing the other regulators, particularly PLN, since it is also expressed in the heart[103].

Another muscle-specific regulator, myoregulin (MLN), was identified in skeletal muscle, found to impair SERCA’s ability to pump calcium back into the SR, and to have a role in muscle performance[104] (Figure 6). Details into this regulator will be discussed further in Chapter 3.

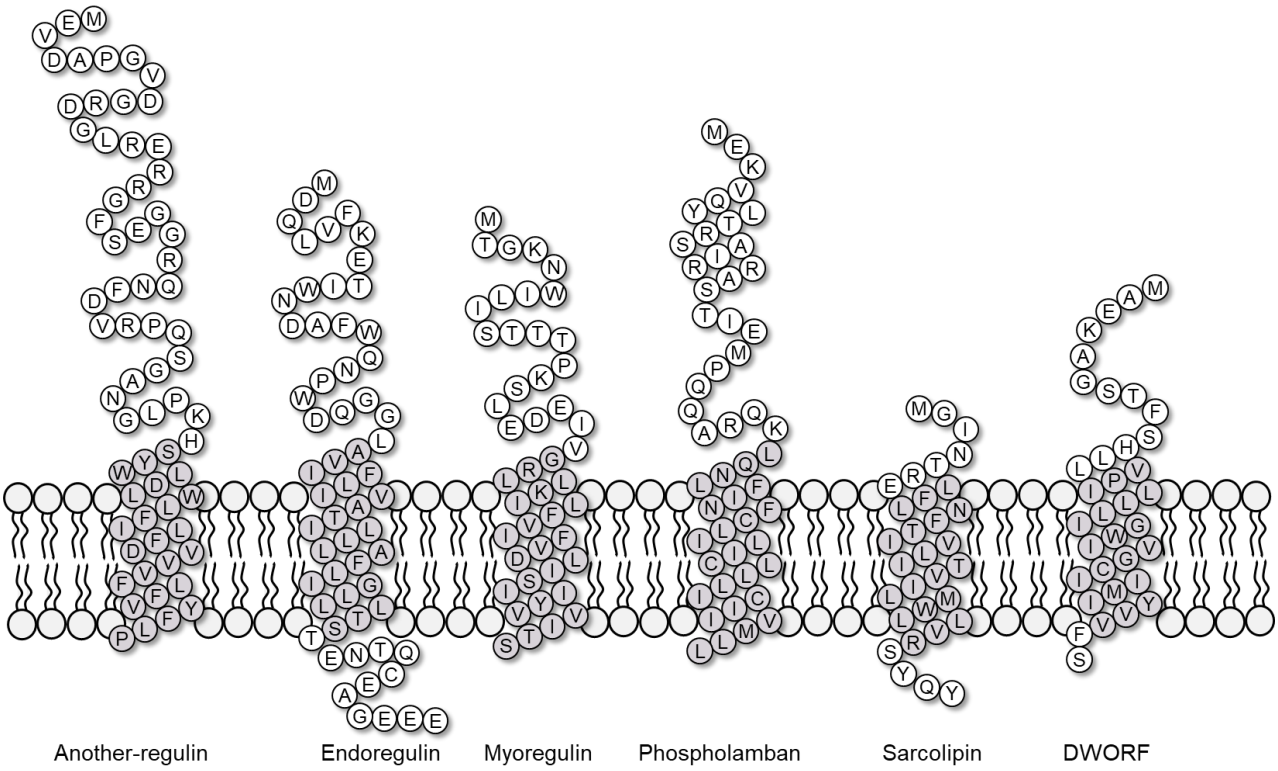

ALN MEVDAPGVDGRDGLRERRGFSEGGRQNFDVRPQSGANGLPKHSYWLDLWLFILFDVVVFLFVYFLP
ELN MDQLVFKETIWNDAFWQNPWDQGGLAVIILFITAVLLLILFAIVFGLLTSTENTQCEAGEEE
MLN MTGKNWILISTTTPKSLEDEIVGRLLKILFVIFVDLISIIYVVITS
PLN MEKVQYLTRSAIRRASTIEMPQQARQKLQNLFINFCLILICLLLICIIVMLL
SLN MGINTRELFLNFTIVLITVILMWLLVRSYQY
Dworf MAEKGSTFSHLLVPILLLIGWIVGCIIMIYVVFS

Figure 6: Topology and sequences of the mammalian regulin family.
(A) Topology diagrams of each regulin peptide. Transmembrane domains (grey) were predicted using TMHMM[105]. (B) Sequence alignment of the human sequences of the regulin peptides. Alignments were done using Clustal omega software and adjusted manually to maximize for overlap of the transmembrane domains (grey highlight)[106]. It can be seen that there is a lot of variation between these peptides in terms of sequence identity and length.

Lastly, the first SERCA regulators in non-muscle tissue have been identified as well; endoregulin (ELN) and another-regulin (ALN) have been discovered to regulate isoforms of SERCA in non-muscle tissue[107] (Figure 6). Details into ALN will be discussed in Chapter 3. Each regulator has been shown to localize to the ER membrane and is co-expressed with the tissue-specific isoform of SERCA[103,104,107]. Additionally, each regulator is predicted to have α-helical structure in the transmembrane domain and is either unstructured or β-sheet in the remaining domains of the peptide. Detailed structural studies combining techniques like NMR, CD spectroscopy, or co-crystallization with SERCA have yet to be done for these new regulins and remain as something to be explored[101,103,104,107]. To date, the studies exploring these new regulators have been conducted in mice or in whole-cell systems. These studies are useful in providing insight to the physiological role of the peptide and for providing details like localization, expression, and activity in a cell. While the existence of these peptides is known and some details into their regulatory effect on SERCA have been explored, a full and detailed understanding of their structure, kinetic effect, and physiological role remains unknown.

1.6: Aims and hypotheses

The expansion of SERCA-regulatory peptides has consequently opened many doors in this field of research. Specific information into the structure of the regulators and their interaction with SERCA along with physiological roles or disease-association in humans remains largely unknown. In addition to this, detailed kinetic information into how these regulators alter SERCA's activity in an isolated system is yet to be explored. Thus, the overarching goal of my thesis is to characterize the kinetic effect of six different regulatory peptides on SERCA's maximal activity and apparent calcium affinity in isolated proteoliposomes. The work carried out to address these aims is separated into two different chapters; one chapter will address the regulatory effect of MLN and ALN on SERCA and the other chapter will address the effect of sequence variation through four SLB peptides on SERCA.

1.6.1: Myoregulin and another-regulin will regulate SERCA

The first studies of MLN and ALN showed that both of these peptides lowered SERCA's affinity for calcium without altering the maximal activity[104,107]. The aim of my work is to determine the effect of MLN and ALN on SERCA in an isolated proteoliposome system. To do this, purified SERCA, regulatory peptide (MLN or ALN), and lipids are co-reconstituted into proteoliposomes at varying molar ratios of SERCA to regulatory peptide. To address this aim, the majority of work presented in this thesis was to optimize and confirm the reconstitution process in addition to characterizing the kinetic effects on SERCA. As background knowledge, a previous study that MLN and ALN lower SERCA's calcium affinity in whole-cell homogenates. In addition, the underlying assumption was that the regulins will function as tissue-specific SERCA inhibitors, much like PLN and SLN. Thus, it was hypothesized that the same inhibitory effect will be seen in isolated proteoliposomes for each regulatory peptide.

1.6.2: Sequence variation will alter SERCA regulation

Another aspect of SERCA regulation that is yet to be clearly defined is the role of sequence variation. So far, it can be concluded that peptides with different sequences can interact with and regulate SERCA in a similar manner. It can also be said that Ca-ATPases are regulated by transmembrane peptides in different phyla, as seen with the SLB peptides in *Drosophila* and that these mammalian and insect regulators evolved from a common ancestor. With this, the aim of this part of the thesis is to determine how sequence variation in these transmembrane regulators alters the kinetic effect on SERCA. To do this, four different SLB peptides were reconstituted with SERCA and the kinetic effect was measured through an coupled-enzyme activity assay as for the other peptides mentioned previously. With the understanding that certain residues or motifs in PLN and SLN are essential to their inhibitory function and that combinations of these structural elements lead to increased or altered SERCA

regulation, it was hypothesized that the sequence variation seen in the SLB peptides will provide insight on the range of kinetic effects on SERCA activity.

Chapter 2: Purification and preparation of SERCA, regulatory peptides, and isolated proteoliposomes

2.1: Purification of sarcoplasmic reticulum membrane and SERCA

Sarcoplasmic reticulum (SR) was purified from rabbit hind-leg muscle as reported previously, with some modifications[108]. Tissue (~300 g) was homogenized in 0.1 mM EDTA in a blender for 30 seconds with 1-minute rest to ensure tissue remained ice cold and this cycle was repeated 12 times. The homogenate was then centrifuged at 15 000xg for 20 mins and the supernatant was filtered through 16 layers of cheesecloth. SR membranes were separated from other tissue components using a series of differential centrifugation steps. Solubilized SR (~30 mg/mL) was frozen in liquid nitrogen and stored at -80 ^{o}C for future SERCA purification.

SERCA was purified via Reactive Green, an affinity chromatography dye ligand attached to agarose beads (Sigma Aldrich, ON). This protocol has been adjusted from an original method to accommodate the discontinuation of the original resin[109]. Resin was stored in 2M NaCl and nutated overnight at 4 ^{o}C prior to purification. Resin was then rinsed with 200 mL of water and equilibrated with 25 mL of wash buffer (1 mg/mL $C_{12}E_8$, 1mM $CaCl_2$, 50 mM MOPS pH 7.0, 1 mM DTT, 20% Glycerol v/v). Frozen SR aliquots equalling about 100mg of SR, were gently thawed on ice, added to extraction buffer (10 mg/mL $C_{12}E_8$ v/v, 8mM $CaCl_2$, 50mM MOPS pH 7.0, 5mM DTT, 20% Glycerol v/v), and gently stirred for 1 hour at 4 ^{o}C. The solubilized SR membranes were then centrifuged at 117 734xg for 20 mins (Optima L-90K Beckman-coulter centrifuge, Type Ti70 rotor). The supernatant was added to the resin and nutated for 2 hours at 4 ^{o}C. The column was then washed with wash buffer and elution buffer (1 mg/mL $C_{12}E_8$, 1mM $CaCl_2$, 50 mM MOPS pH 7.0, 1 mM DTT, 20% Glycerol v/v, 20 mM ADP, 100mM KCl, 20mM KOH) was added to the resin and left to incubate for 1.5 hours at 4 ^{o}C. Fractions were collected and protein concentration was estimated through a BioRad Assay and SDS-PAGE visualization (Figure 7). The highest concentrated samples that appeared to be greater than 0.4 mg/mL as a

result of the BioRad Assay were pooled, egg-yolk phosphatidylcholine (EYPC, Avanti Polar Lipids) was added to 0.25 mg/mL and the pool of purified SERCA was frozen in liquid nitrogen and stored at -80 ºC. To quantify the amount of SERCA, one aliquot was thawed and SERCA activity was determined by measuring the ATPase activity in a reaction mixture over a 50 second time period using 1 mL reaction volume on a Perkin Elmer Lambda 35 UV/Vis spectrometer (See Measuring ATPase Activity in Proteoliposomes). The concentration of SERCA was confirmed by assuming a maximum specific activity of 12 µmol/min/mg.

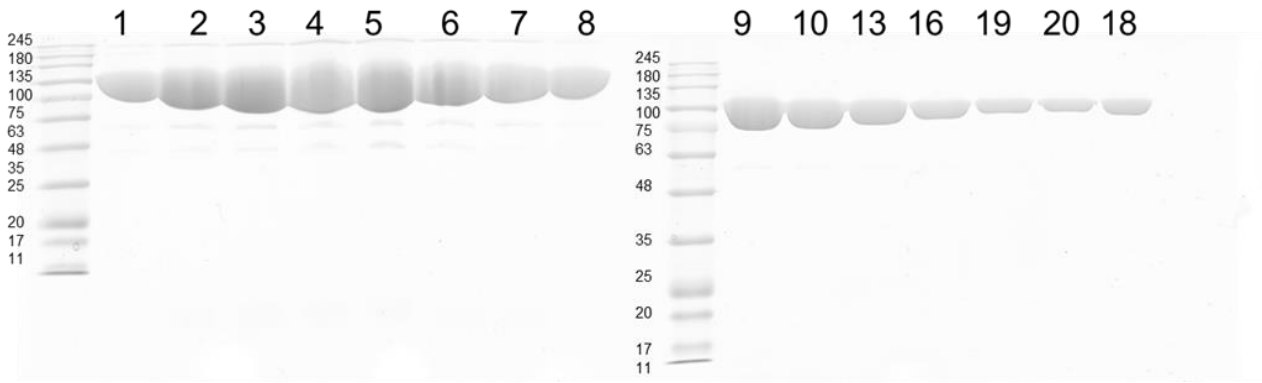

Figure 7: Representative gel of fractions from a typical SERCA purification
For this gel specifically, fractions 2-6 and 7-10 were pooled in two separate batches yielding concentrations of 5.7 mg/mL and 5.5 mg/mL, respectively.

2.2: Synthetic myoregulin (MLN) and another-regulin (ALN) peptides

Myoregulin and another-regulin were purchased from Peptide 2.0 (Chantily, VA). To ensure the peptides were pure and were the correct molecular weight, the peptides were analyzed by mass spectrometry (Proteomics and Mass Spectrometry Facility at the University of Alberta) and assessed via SDS-PAGE (Figure 8). Upon analysis, each peptide was found to be the correct and expected molecular weight (Figure 8). To store for future experiments, peptides were weighed and separated in 1 mg amounts, resuspended in 80 % isopropanol to 1 mg/mL, and aliquoted in amounts suitable for reconstitution at different SERCA to peptide molar ratios (1:2.5, 1:5, 1:7.5). Isopropanol was evaporated via a speed vacuum concentrator (Savant SPD 2010) and dried-peptide aliquots were stored at -80 ºC.

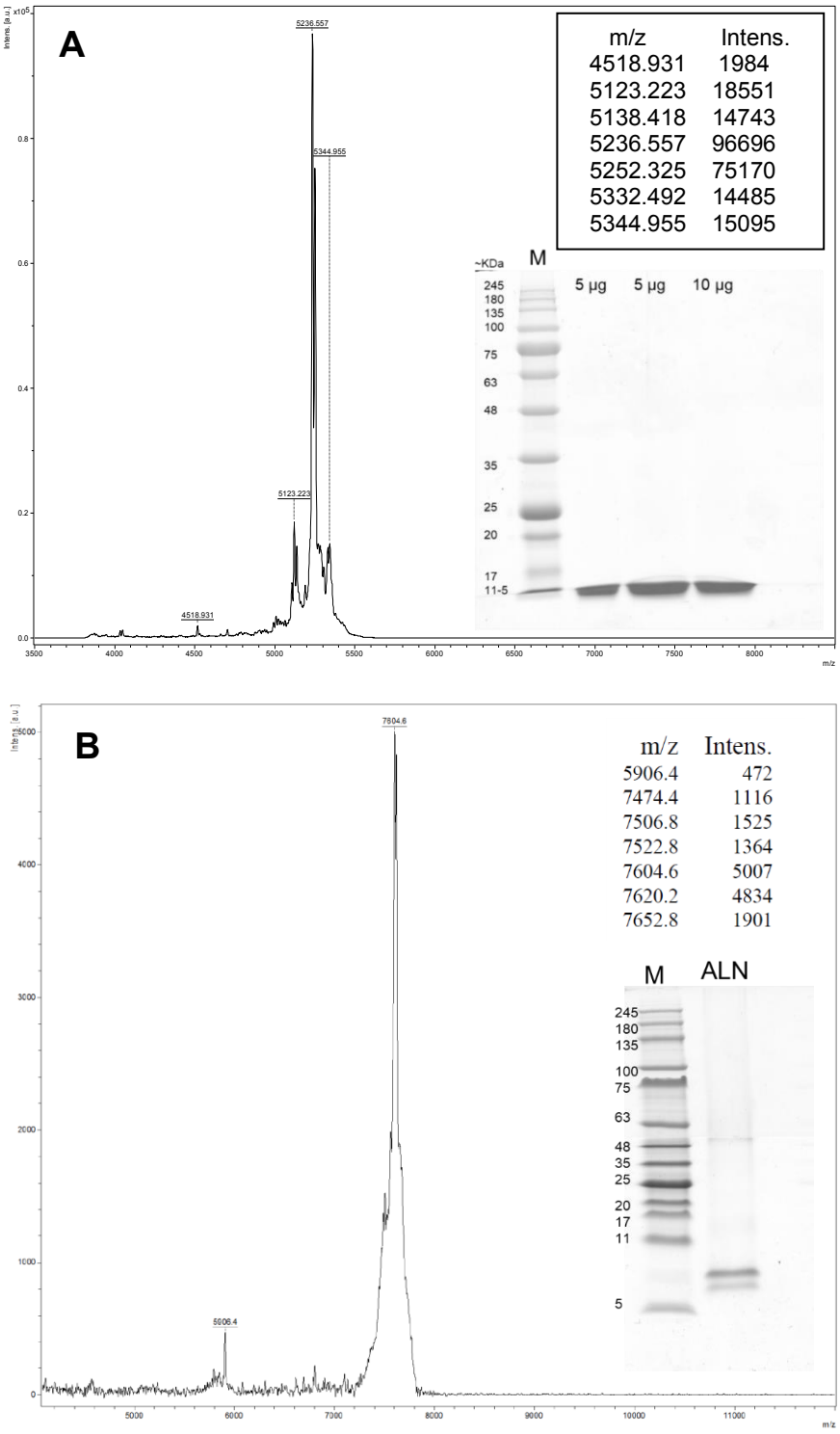

Figure 8: Purity checks for synthetic MLN and ALN
Mass spectrometry and SDS-PAGE (inset) analysis for (A) MLN and (B) ALN. MLN's expected molecular mass is 5194 Da and ALN's expected mass is 7604 Da. Other peaks were attributed to oxygen or sodium adducts.

2.3: Recombinant sarcolamban (SLB) peptides

Genes and primers for SLB peptides were purchased from Integrated DNA Technologies (Coralville, Iowa), resuspended in water and stored at -20 ^{o}C SLB genes were generated using three-step PCR, where two halves of the gene were created and then stitched together (Table 2, Figure 9). Following PCR mutagenesis, PCR product was digested with restriction enzymes BamH1 and EcoR1 (Anza Cloning System, ThermoFisher Scientific) where 1 µL of each enzyme was added to 0.2-1 µg of DNA with 3 µL Anza Enzyme reaction buffer in a total reaction volume of 30 µL. It was then isolated and purified from an agarose gel using GenepHlow GelPCR kit (FroggaBio, North York, ON). Purified PCR product was stored at -20 ^{o}C for future ligation reactions.

The expression vector used for cloning experiments was pMal-C2X (New England Biolabs MA), which contains a maltose-binding protein (MBP) engineered for optimal affinity to amylose resin (used for purification) and an ampicillin-resistant selection marker. This expression vector was also engineered to contain a tobacco etch virus (TEV) protease site for cleavage of the MBP fusion protein product. Expression vector was stored in DH5α *E. coli* glycerol stocks at -80 ^{o}C and used to inoculate cultures to start the expression of the fusion protein. Expression vector was purified with the GeneAid Presto Mini Plasmid Kit (FroggaBio, North York, ON) and stored at -20 ^{o}C until further use. Vector was digested and purified in the same manner as the PCR product (Figure 9).

Digested plasmid and PCR product were ligated overnight using a ligase kit (Anza T4 Ligase Master Mix, Invitrogen, CA) at a 3:1 ratio of insert to vector (Figure 9). Ligated products were transformed into DH5α *E. coli* by adding 1 µL ligated DNA to 50 µL cells, followed by a subsequent incubation on ice for 40 minutes, heat shock at 42 ^{o}C for 30 seconds, addition of 200 µL LB media, and growth at 37 ^{o}C for 1 hour. Cells in media were then plated onto agarose plates containing 100 µg/mL carbenicillin in either 50 µL or 150 µL amounts. Plates were

incubated at 37 ºC overnight. Colonies were screened for positive transformation of vector containing PLN or SLN mutants or SLB peptides by inoculating 2 mL LB media containing 100 µg/mL carbenicillin with a single colony, growing at 37 ºC overnight, then purifying the plasmid using the same method and GeneAid Kit as before.

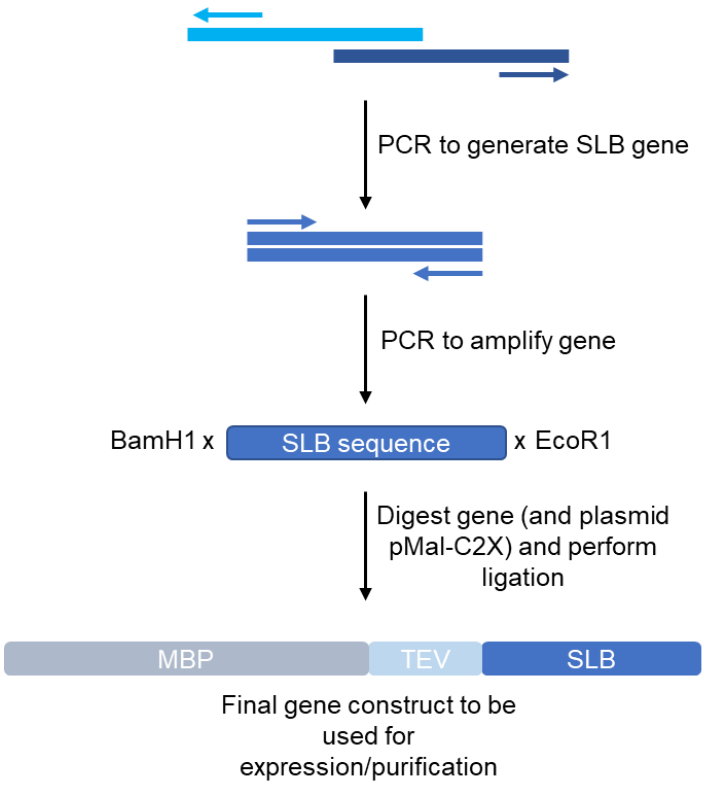

Figure 9: Flow diagram of cloning steps used to generate the SLB gene
Overlapping primers were used to generate the SLB gene, which was then amplified with a separate set of primers (Table 2). This gene product and pMal-C2X were double-digested with BamH1 and EcoR1. Between each of these steps, gel purification was performed. Following digestion and purification, gene products were ligated. The last step in the diagram shows the final gene construct that exists within pMal-C2X, with maltose-binding protein (MBP), a TEV (tobacco etch virus) cleavage site, along with the SLB gene of interest.

Table 2: Primer sequences for the generation and amplication of SLB genes

Primer Name and Use	**Sequence (5'→3')**
MalEF- for sequencing	**5'**GGTCGTCAGACTGTCGATGAAGCC**3'**
MalER- for sequencing	**5'**CGGGCCTCTTCGCTATTACGCCAG**3'**
BtSLB FWD- to make gene	**5'**AGATGCATCCCCGCAGGCGGCGCACGAAACCAAAAACATTCTGAGCACCTACTTCATCCTGATCCTGCTG**3'**
BtSLB REV- to make gene	**5'**ATACCAATTCTCAGAACAGACCAGAGTACAGCAGCCACAGGCAGATCAGCAGCAGGATCAGGATCAAG**3'**
DmSLB FWD- to make gene	**5'**AGATGGATCCTCTGAAGCGCGTAACCTGTTCACCACCTTCGGTATCCTGGCGATCCTGCTGTTC**3'**
DmSLB REV- to make gene	**5'**ATAGGAATTCTCAGAGAACCGCGTAGATCAGGTACAGGAAGAACAGCAGGATCGCCAGGATACC**3'**
DpSLB FWD- to make gene	**5'**AGAAGGATCCAACAACCCGGAACACGCGCACGCGAAATCTCTGATCATCAACTACGTTGTTATCATCCTG**3'**
DpSLB REV- to make gene	**5'**ATAGGAATTCTCACATACCTTCGCACAGCAGCCACAGCAGAGACAGCAGCAGGATGATAACAACGTAGTTG**3'**
TcSLB FWD1- to make gene	**5'**AGATGGATCCGCCGATACCCGTCGTAAATCTATCATGGACCAGGTTACCGCGCTGAAAAACCGTG**3'**
TcSLB FWD2- to make gene	**5'**CCGCGCTGGAAAACCCTCAAGCGAAATCTCTGGTTGTTAACTACCTGGTTATCATCCTGCTGCTG**3'**
TcSLB REV- to make gene	**5'**ATAGGAATTCTCACGCACCAGTGTACAGCAGCCACAGGATACCCAGCAGCAGGATGATAACCAG**3'**
BtSLBF- to amplify gene	**5'**AGATGGATCCCCGCAGG**3'**
BtSLBR- to amplify gene	**5'**ATAGGAATTCTCAGAACAGAC**3'**
DmSLBF- to amplify gene	**5'**AGATGGATCCTCTGAAGCGCGTAA**3'**
DmSLBR- to amplify gene	**5'**ATAGGAATTCTCACAGAACCG**3'**
DpSLBF- to amplify gene	**5'**AGATGGATCCAACAACCCG**3'**
DpSLBR- to amplify gene	**5'**ATAGGAATTCTCACATACCTTC**3'**
TcSLBF- to amplify gene	**5'**AGATGGATCCGCTGATACCC**3'**
TcSLBR- to amplify gene	**5'**ATAGGAATTCTCACGCACCAG**3'**

Sanger sequencing was used to determine the sequence cloned into pMal (TAGC, University of Alberta) and PCR screening was done in concert with this as another method to isolate positive colonies for future purification. A sequencing primer was designed to be in the MBP region of the plasmid to allow for a full reading of the inserted gene (Table 2). PCR

screening was done using the forward and reverse primers corresponding to the gene of interest (Table 2). Positively screened purified DNA was stored at -20 ^{o}C for later large-scale expression and purification.

2.4: Expression and purification of SLB peptides

Expression and purification of SERCA-regulators has been described previously[110]. To start large-scale expression, DH5α *E. coli* was transformed with positively sequenced plasmid DNA corresponding to the pMal plasmid containing one of four SLB sequences. While DH5α is not an expression strain of *E. coli,* previous expression studies with PLN showed that this cell line led to suitable expression levels for purification and thus it was used for the expression of other regulatory peptides. Transformation was carried out as in section 2.3. Single colonies were used to inoculate 100 mL of overnight culture (LB media + Vitamin B1 + 100 μg/mL carbenicillin) and were left to shake at 230 rpm overnight at 37 ^{o}C. Following overnight incubation, 25 mL of overnight culture was added to 1 L media (LB media + Vitamin B1 + 0.1 % Glucose + 100 μg/mL carbenicillin) in a 4 L flask. Cultures were incubated at 37 ^{o}C and shaken at 200 rpm. Optical density at 600 nm was used to monitor growth of cells and when OD600 reached 0.6-0.8, 0.5 mM IPTG was used to induce expression. Following induction, cultures were grown at 22 ^{o}C for 24 hours. Cells were harvested by centrifugation (Sorvall RC 6+) at 8000 x g for 15 minutes. Cell pellets were resuspended in 50 mM Tris-HCl, pH 7.5 and centrifuged again at 4000 xg for 10 minutes (Beckman Coulter Allegra 64R, C0650 rotor). Remaining buffer was removed, cells were flash frozen in liquid nitrogen, and stored at -20 ^{o}C for subsequent purification.

To purify the various peptides, cells were thawed on ice, resuspended in 60 mL of lysis buffer (20 mM NaH_2PO_4/Na_2HPO_4, 120 mM NaCl, 0.5% azide, 0.5 % glycerol, 0.5 % Triton X-100), and homogenized with a Dounce homogenizer. Cells were then lysed via sonication using a Branson Sonicator at 70 % amplitude for 45 seconds, pulsing for 0.5 seconds on and off.

Soluble and insoluble material following cell lysis were separated by centrifugation at 49 000 xg for 25 minutes (Optima L90-x, Beckman-coulter, Type Ti70 rotor). The soluble supernatant fraction containing the MBP-peptide fusion was added to an amylose affinity column and nutated for 1 hour at room temperature. The amylose affinity column was equilibrated with 500 mL PSE buffer (20 mM NaH_2PO_4/Na_2HPO_4, 120 mM NaCl, 0.5% azide). Following nutating and binding, the column was washed with 500 mL PSE buffer to remove contaminating proteins. MBP-fusion protein was eluted by adding 80 mM maltose (dissolved in PSE) and a nutating for 30 minutes, followed by gravity-flow of 200 mL of 40 mM maltose in PSE. Between 200-250 mL of elution was collected and concentrated to 30-50 mL using an Amicon concentrator (Model 402 max, 75 PSI). TEV protease (purified in lab) was added to about 5 U/mg of protein with 1 mM DTT and left to incubate at room temperature overnight. Cleavage was monitored by SDS-PAGE and more TEV protease and DTT was added if cleavage was incomplete If cleavage was complete, MBP was separated by guanidine-hydrochloride extraction or chloroform-isopropanol extraction.

For peptide extraction with guanidine-hydrochloride, cleaved peptide was centrifuged at 117 000 xg for 45 minutes (Optima L-90x, Beckman-coulter, Type Ti70 rotor) to collect precipitated protein. The pellet was resuspended in 1 M guanidine hydrochloride to solubilize MBP from cleaved peptide by homogenization with a Dounce homogenizer, and then incubated at room temperature for 1 hour. The insoluble material was separated by centrifugation at 117 000 xg for 25 minutes (Optima L-90x, Beckman-coulter, Type Ti70 rotor). This pellet was resuspended by homogenization in 7 M guanidine hydrochloride. The solubilized peptide was suitable for purification by high performance liquid chromatography (HPLC, Varian 940 LC).

HPLC was performed using a reverse-phase Zorbax SB-300 C8 silica-based column on a Varian 940 LC HPLC. The 7 M guanidine hydrochloride solution containing protein was injected onto the HPLC column and was purified using gradient consisting of a 20-minute wash

with 0.05 % trifluoroacetic acid and water, then followed by a gradual increase of isopropanol to with 80 % isopropanol over 180 minutes. During the experiment, the column was heated to 60 ^{o}C to accommodate for the viscosity of 7M guanidine hydrochloride. Two mL fractions were collected every minute and fractions were analyzed via SDS-PAGE. The purest and most concentrated samples were pooled, isopropanol was evaporated under nitrogen gas, and the sample was lyophilized overnight. The lyophilized sample was resuspended in 80 % isopropanol and protein concentration was measured via a BCA colorimetric assay. Protein was aliquoted in 50, 75, or 100 µg quantities and solvent was evaporated using a speed vacuum concentrator. Samples were stored at -80 ^{o}C. Purity was confirmed through MALDI-TOF mass spectrometry and SDS-PAGE as with the synthetic peptides (Figure 10). Peptides were found to be of variable purity, though levels determined from mass spectrometry analysis showed that purity was acceptable for further experiments (Figure 10).

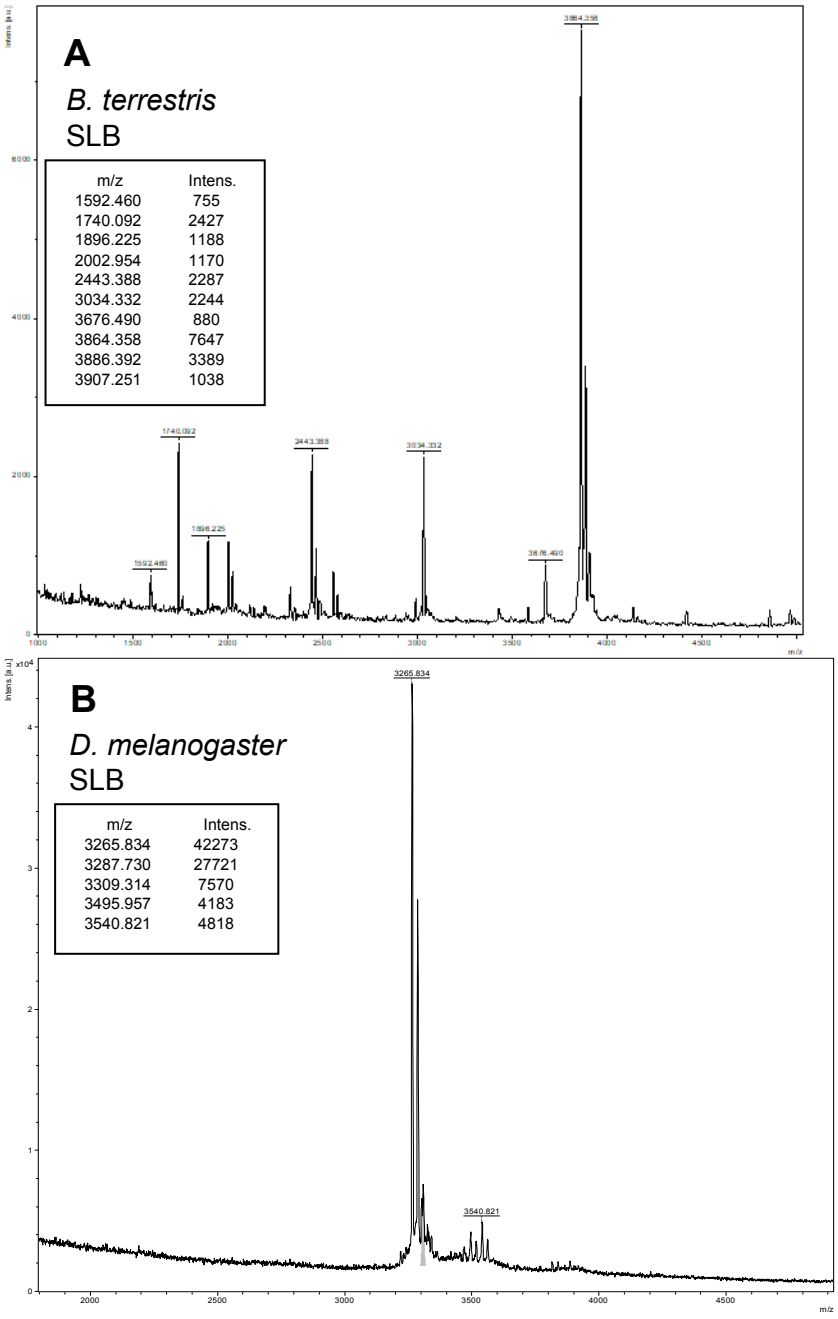
A
B. terrestris
SLB
m/z Intens.
1592.460 755
1740.092 2427
1896.225 1188
2002.954 1170
2443.388 2287
3034.332 2244
3676.490 880
3864.358 7647
3886.392 3389
3907.251 1038
B
D. melanogaster
SLB
m/z Intens.
3265.834 42273
3287.730 27721
3309.314 7570
3495.957 4183
3540.821 4818
m/z

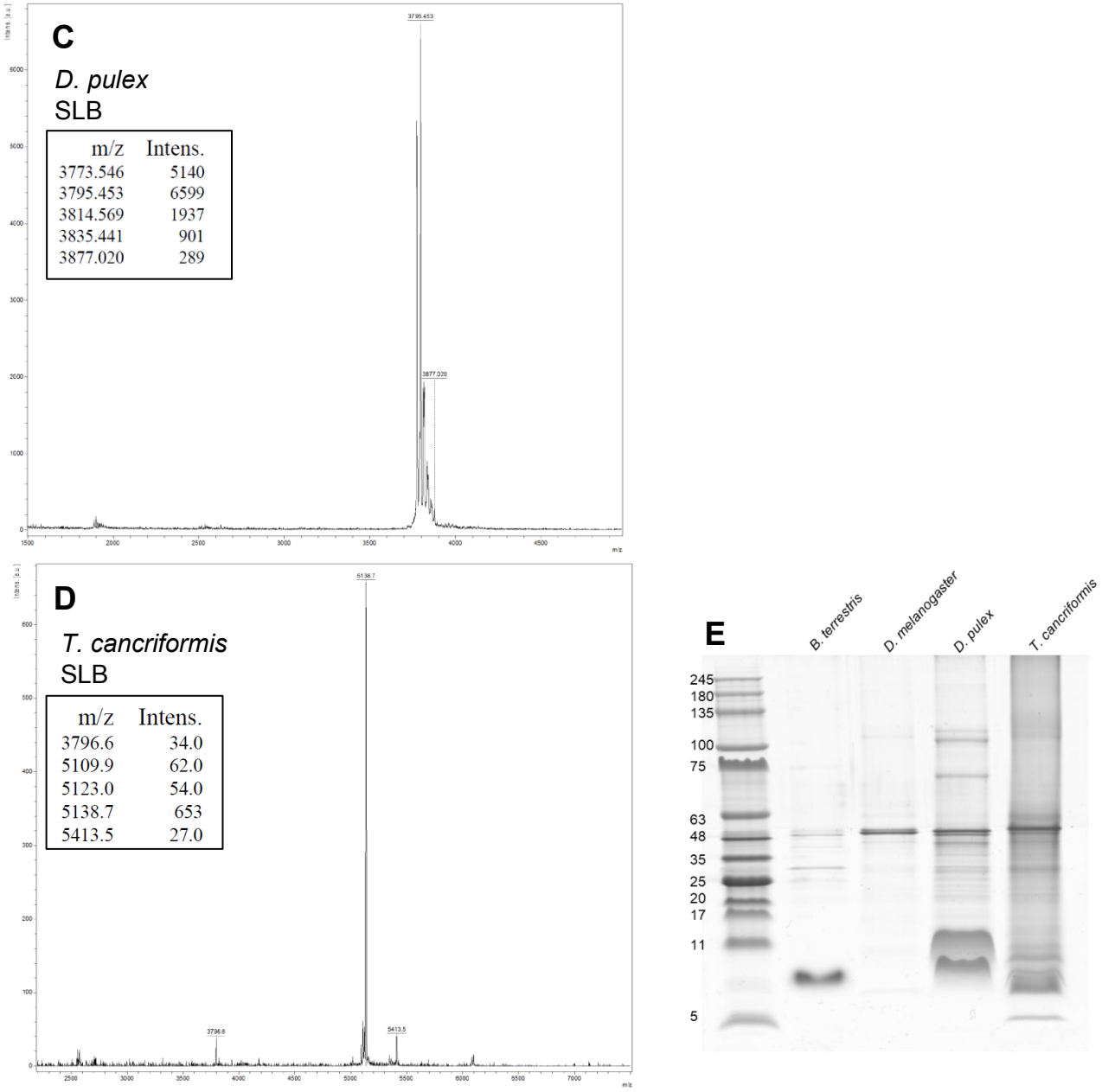

Figure 10: Purity checks for SLB peptides
Each mass spectrometry result from MALDI-TOF analysis (A-D) shows the peaks seen as well as the numerical values obtained (inset). (E) SDS-PAGE of pure peptide. 5 µg of each was added. *B. terrestris* SLB can be seen between 5 and 11 KDa, which could correspond to a dimer from two 3.6 KDa monomers. *D. melanogaster* SLB is difficult to visualize, though faint bands can be viewed between 5 and 11 KDa. *D. pulex* is seen as two major bands below and above 11 KDa, which may correspond to monomers and dimers. *T. cancriformis* is seen as several bands. This peptide was the most difficult to express and purify and was the least soluble, which may explain why this lane was so streaky compared to the others. The expected molecular masses for each peptide are 3853 Da,3253 Da, 3762 Da, and 5106 Da for *B. terrestris, D. melanogaster, D. pulex, T. cancriformis*, respectively.

2.5: Reconstitution of SERCA and peptide into proteoliposomes

Reconstitutions were prepared as described previously[111]. To prepare for reconstitutions, thin-lipid films were generated using egg-yolk phosphatidylcholine (EYPC) and egg-yolk phosphatidic acid (EYPA). Lipid was stored in chloroform as a 25 mg/mL stock and was added to reconstitutions to achieve a weight of lipid to protein final ratio of 9 EYPC to 1 EYPA. Reconstitutions performed for a SERCA alone control and for SERCA in the presence of peptide. For reconstitutions including peptide, stored peptide was resuspended in a mixture of 2 parts chloroform to 1-part trifluoroethanol, to achieve a final concentration of 1 mg/mL. Lipids were then added to the peptide as described above. For some sets of experiments with MLN, half of the detergent $C_{12}E_8$ was added at this stage with the goal of increasing the solubility of MLN for incorporation into the reconstitution. Thin films were generated by evaporating under nitrogen gas while gently vortexing. Prepared films were then stored in a desiccator overnight to remove residual organic solvent before reconstitution (Figure 11).

Following preparation of the lipid-peptide thin films, water was added, and the mixture was incubated at 37^{o}C for 30 minutes. Detergent was then added to achieve a final weight ratio of 1 lipid: 1 protein: 2 detergent and the resuspension was vortexed for 3 minutes. Buffer was added (7 µM imidazole, 33 mM NaCl, 0.006 % azide, and 3.3 mM $MgCl_2$) and the suspension was briefly vortexed again. Reconstitution buffer (1 mg/mL $C_{12}E_8$, 1mM $CaCl_2$, 50 mM MOPS pH 7.0, 1 mM DTT, 20% Glycerol v/v, 20 mM ADP, 100mM KCl, 20mM KOH) and 300 µg of SERCA were added in a total volume of 200 µL. Reconstitutions with SERCA, peptide, lipid, and detergent were gently mixed for about 30 minutes. After this time, SM2 Biobeads (20-50 mesh, BioRad) were added slowly in four 1 mg additions followed by a 5 and 10 mg addition to slowly and then completely remove the detergent in solution and to allow proteoliposomes to form with correctly oriented protein. Proteoliposomes were then isolated through sucrose-gradient centrifugation (106000 xg, 1 hour, Optima TLX, TLS-55 rotor) and collected at the interface

between 20 % and 50 % sucrose layers. Proteoliposomes were mixed, aliquoted, flash frozen in liquid nitrogen and stored at -80 ^{o}C (Figure 11).

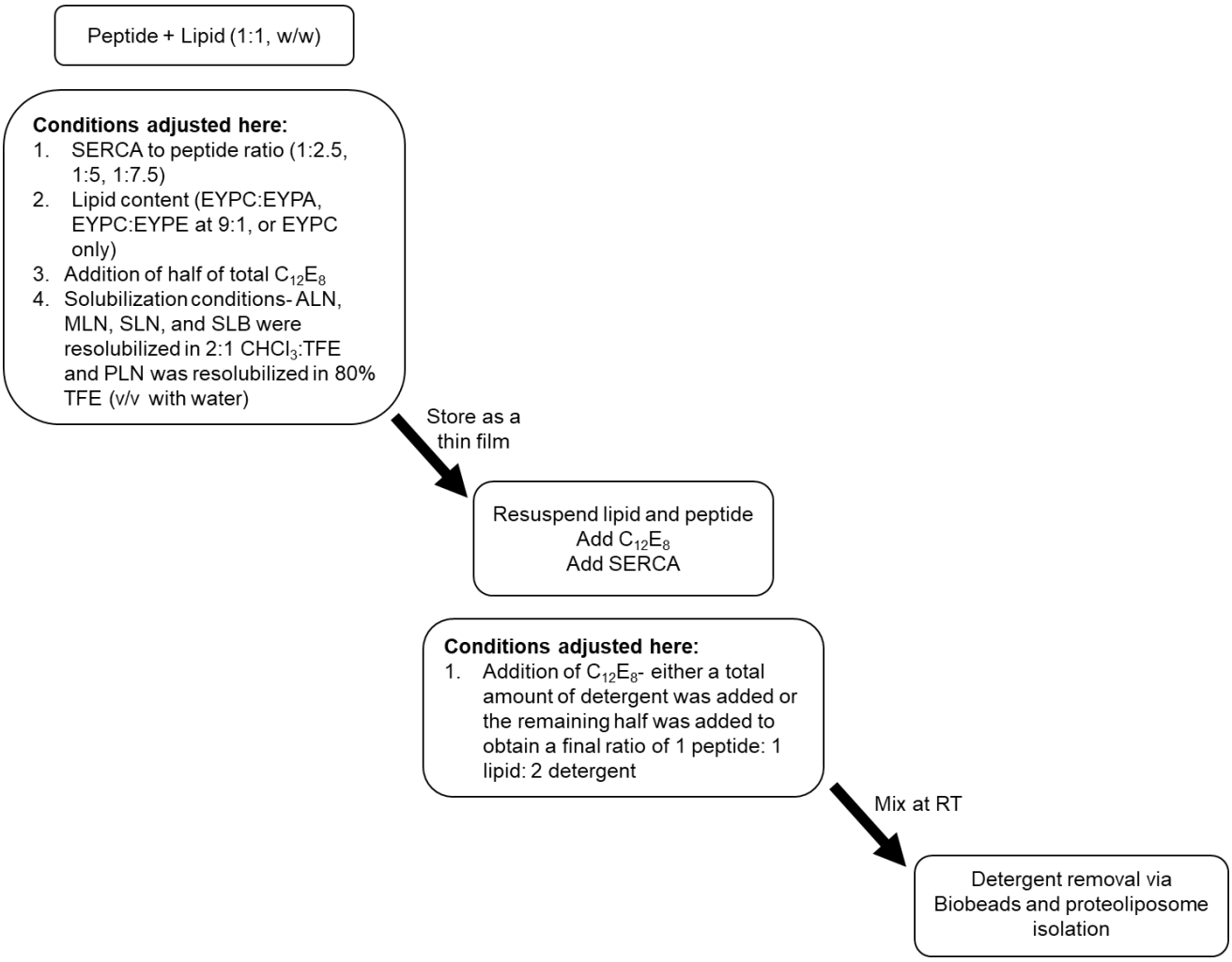

Figure 11: Flow diagram of the main steps of proteoliposome reconstitution
For a typical 1:5 SERCA:MLN reconstitution, 85 µg MLN, 385 µg lipid (38.5 µg EYPA and 346.5 µg EYPC), 300 µg SERCA, and 570 µg $C_{12}E_8$ were used to achieve a final protein: lipid: detergent ratio of 1:1:2, respectively.$CHCl_3$- chloroform, TFE: trifluoroethanol, EYPC- egg yolk phosphatidylcholine, EYPA- egg yolk phosphatidic acid, EYPE- egg-yolk phosphatidyl ethanolamine, RT- room temperature.

2.6: Quantification of protein in proteoliposomes

Protein concentration determination in proteoliposomes was carried out in two different ways: BCA (bicinchoninic acid) colorimetric assay and SDS-PAGE quantification. The former measured total protein concentration and the latter allowed for the quantification of SERCA alone, also allowing for the indirect calculation of peptide present in the proteoliposome.

The BCA assay was carried out using 0.5 mg/mL BSA (bovine serum albumin) to generate a standard curve ranging from 1-5 mg/tube (Figure 12). For the protein samples, 5, 5, and 7.5 µL of proteoliposomes were measured and compared to the standard curve. Here, protein was added to 50 µL of 2 % SDS, vortexed, and then mixed with 1 mL of assay reagent (50 parts Pierce BCA Assay Reagent A from Thermofisher Scientific and 1 part 4% $CuSO_4$). The standard curve and protein samples were then incubated in a 60 ^oC water bath for 30 minutes. Samples were then transferred to a room-temperature water bath and absorbance readings at 562 nm were taken on the UltroSpec 2000 UV/Vis spectrometer. A standard curve was plotted as absorbance against mg of protein per tube using linear regression analysis. From this linear relationship, total protein concentration in each proteoliposome sample was calculated (Figure 12).

Gel quantification by SDS-PAGE was done by loading 5, 6, and 7 µL of each sample as a set onto a 10 % polyacrylamide gel (Figure 12). Electrophoresis was carried out at 160 V for 45 minutes. Gels were stained using Bio-Safe Coomassie G-250 protein stain (Biorad, Hercules, CA). After destaining, gels were digitally scanned using an Epson V800 Scanner and SilverFast Software. Images were uploaded into the image analysis software, ImageQuant. From here, SERCA band density was integrated and the calculated area value was used to measure the relative amounts of SERCA in each reconstitution. SERCA reconstituted alone was considered to have a value of 1 and the SERCA concentrations in the remaining reconstitutions were calculated as ratios of that based on the integrated areas. This ratio was multiplied by the

total protein concentration obtained from the BCA assay to calculate the concentration of SERCA in the proteoliposomes. The values obtained for SERCA concentration were used for further calculation of specific activity (Figure 12).

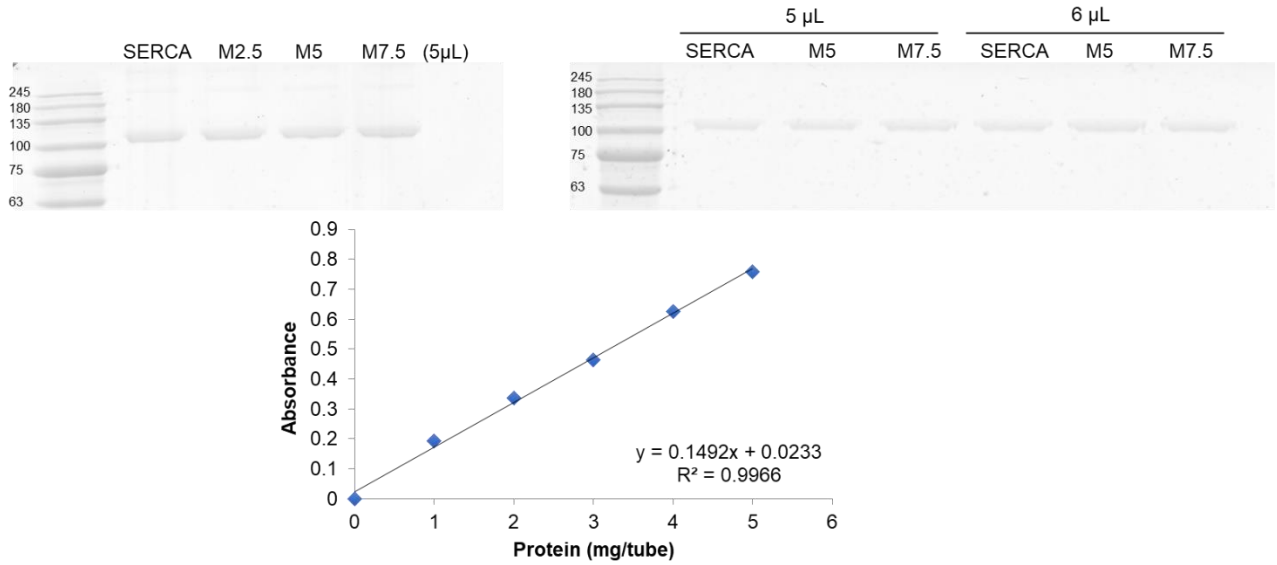

Figure 12: Representative SDS-PAGE and BCA assay curve of reconstituted proteoliposomes
Top panels show results from two separate experiments. The bands seen correspond to SERCA from different reconstitution conditions and different volumes are added to compare and monitor consistency. The bottom panel shows a typical BCA assay result where absorbance is plotted against mg protein per tube. From this, a linear equation is generated and used to calculate mg protein in proteoliposome samples. Concentration in mg/mL can be calculated with the volume added to the tube.

2.7: Measuring ATPase activity in proteoliposomes

ATPase activity of SERCA was measured using a coupled-enzyme assay (Figure 13). The calcium-dependent hydrolysis of ATP to ADP by SERCA was coupled to the oxidation of NADH to NAD^+ by lactate dehydrogenase. The coupled-enzyme assay uses pyruvate kinase, which converts phosphoenolpyruvate to pyruvate and regenerates ATP from ADP. Lactate dehydrogenase then converts pyruvate to lactate and oxidizes NADH (absorbs at 340 nm) to NAD^+ (no absorbance at 340 nm). Thus, the hydrolysis of ATP by SERCA is stoichiometrically

coupled to the decrease of NADH, and the concentration of NADH is easily determined from the absorbance at 340 nm (Figure 13).

The assay contains three main components: assay mix (50 mM imidazole, 100 mM KCl, 5 mM $MgCl_2$, 0.5 mM EGTA, 2.4 mM ATP, 0.18 mM NADH, 0.5 mM PEP, 9.6 U/mL lactate dehydrogenase and pyruvate kinase), calcium solution (1mM $CaCl_2$, diluted from 100 mM with assay mix), and reconstituted proteoliposomes (diluted to 1/6- 1/8) (Figure 14). Measurements were conducted in a 96-well plate format over a range of calcium concentrations (pCa 4.8, 5, 5.4, 5.6, 5.8, 6, 6.2, 6.4, 6.6, 6.8, 7, 7.2) with the central values corresponding to the physiological range of calcium in the cell cytoplasm. Absorbance readings were started immediately after the addition of proteoliposomes and were conducted on either a Molecular Dynamics M3 spectrophotometer or a BioTek spectrophotometer to measure the decrease in absorbance at 340 nm. In the case of the M3 spectrophotometer, readings were taken every 28 seconds with shaking in between, for a total of 50 minutes at 37 ^{o}C. For the BioTek spectrophotometer, readings were taken every 39 seconds, with shaking in between, for a total of 50 minutes. From these reads, specific activity was calculated for SERCA proteoliposomes at each calcium concentration.

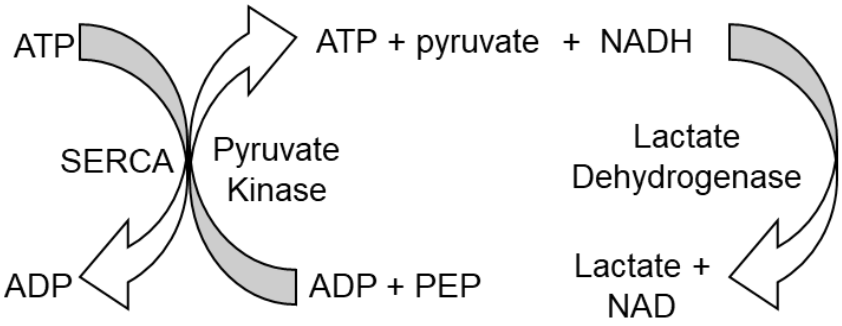

Figure 13: Reaction mechanism of the input and output components of the ATPase activity assay
As SERCA uses ATP, pyruvate kinase regenerates ATP via PEP, forming pyruvate. Lactate dehydrogenase oxidizes NADH to form lactate and NAD^+. Measurements were taken at 340 nm as NADH was depleted.

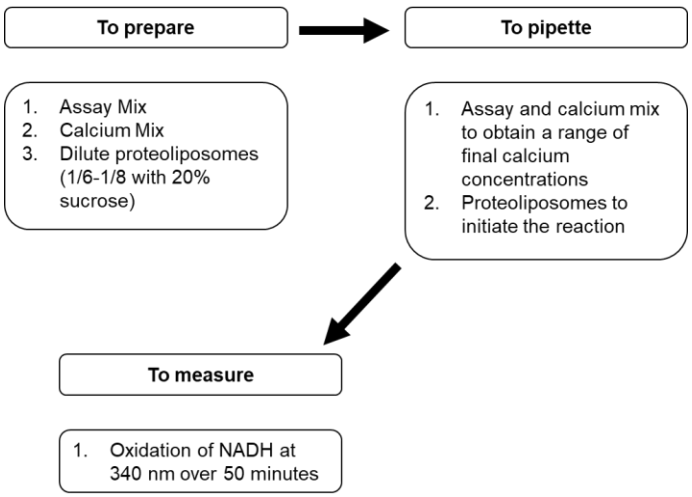

Assay Mix Recipe
50 mM imidazole, pH 7.0
100 mM KCl
5 mM $MgCl_2$
0.5 mM EGTA
2.4 mM ATP
0.18 mM NADH
0.5 mM PEP
9.6 U/mL lactate dehydrogenase
9.6 U/mL pyruvate Kinase

Calcium Mix Recipe
100 mM stock $CaCl_2$
Diluted to 1mM with assay mix

Volume of assay and calcium mix added to obtain specific pCa values

pCa	4.8	5.0	5.4	5.6	5.8	6.0	6.2	6.4	6.6	6.8	7.0	7.2
Volume of Assay Mix (uL)	73.4	75.8	80.8	84.6	89.6	95.8	103.4	112.0	120.6	128.2	134.6	139.4
Volume of Calcium Mix (uL)	76.6	74.2	69.2	65.4	60.4	54.2	46.6	38.0	29.4	21.8	15.4	10.6

Figure 14: Schematic of the preparation and additions for the ATPase assay
The top panel shows what was prepared, the order in which it was pipetted and what was measured. The bottom panel shows specific recipes used to make each component mentioned in the top panel.

2.8: Calculating ATPase Activity

From absorbance values obtained from the spectrophotometer, slopes were calculated from the decrease in absorbance over time corresponding to the oxidation of NADH as SERCA uses ATP to pump calcium. From these slope values, specific activity of SERCA for each reconstitution condition and calcium concentration could be calculated using equation 1. Specific activity was plotted against increasing calcium concentrations on a logarithmic scale and curves were fit using the Hill equation (equation 2) in SigmaPlot software. From this analysis, three important values could be obtained: maximal activity (V_{max}), apparent calcium affinity (K_{Ca}), and the Hill coefficient or cooperativity of SERCA (nH).

$$\text{Specific activity} = \frac{(\Delta \text{O.D.}/\text{min})}{6.22 * [\text{protein}]}$$

Equation 1: To calculate specific activity of SERCA at a single calcium concentration. Where ΔO.D is the change in optical density or absorbance over time, 6.22 M/cm is the extinction coefficient of NADH, and where the protein concentration refers to the concentration of SERCA in a single well.

$$\text{Velocity} = \frac{Vmax * [S]^n}{(K_{Ca})^n + [S]^n}$$

Equation 2: Hill equation. Where V_{max} is the maximal velocity of the enzyme, S is the substrate concentration (calcium), n is the Hill coefficient, K_{Ca} is the apparent calcium affinity. This 3-parameter Hill equation was used via SigmaPlot software to calculate maximal activity, apparent calcium affinity, and cooperativity of SERCA.

2.9: Method to observe the incorporation of protein into proteoliposomes

The incorporation of the various peptides into proteoliposomes was analyzed via tris-tricine SDS-PAGE with 4%, 10%, and 16% acrylamide layers. A sample of 10 µL was taken at the beginning of the reconstitution process before the addition of Biobeads. Using SDS-PAGE, this ‘before’ sample of known composition (300 µg SERCA and 85 µg MLN, for example) was compared to a sample of proteoliposomes after reconstitution and isolation. Equal volumes

were applied to SDS-PAGE so that the amounts of SERCA and peptide before and after the reconstitution could be compared.

To quantify any differences observed here, Image Studio Lite (LiCOR Biosciences) software was used. Identical rectangular boxes were drawn around each band of interest, which allowed for the calculation of band intensity. From the differences in intensity values, percent differences of final reconstitution samples from control or 'before' samples could be calculated.

2.10: Biotinylation and orientation of MLN in proteoliposomes

Biotin labelling to determine the orientation of peptides in proteoliposomes has been done for PLN in the past[112,113]. For labelling, the WT sequence of MLN was used as it has 2 lysine residues on the cytoplasmic region of the peptide, with one more in the transmembrane region. To label these residues, EZ-Link Sulfo-NHS-LC-biotin (ThermoFisher Scientific) was used in combination with IRdye 800CW Streptavidin (LI-COR Biosciences) to visualize and quantify the level of biotinylation. Labelling was carried out by combining 20 µL of reconstitution and 16.7 mM borate-KOH, pH 9.0 along with either 0.5 % octylpyranoglucoside (OG) or water. In these experiments, one set of reactions included a detergent to solubilize the proteoliposome membrane for complete labelling of the peptides, while the other reaction did not contain detergent and only externally oriented peptides. After the addition of 45 mM Sulfo-NHS-LC biotin, reactions were carried out on ice for two hours. Reactions were quenched with 1 uL of 10X Tris/Glycine running buffer without SDS followed by the addition of 30 µL of 2X SDS-PAGE loading buffer.

Biotin labelled samples were analyzed by tris-tricine SDS-PAGE with 4%, 10%, and 16% polyacrylamide and western blotting. Electroblotting was carried out at 100 V for 1 hour onto Immun-Blot PVDF 0.2 µm membrane. Biotinylated protein was probed with 0.2 µg/mL IRdye

800CW Streptavidin (LI-COR Biosciences). Blots were imaged using a LI-COR Odyssey IR scanner and exposures to 700 and 800 nm light lasted for 30 seconds or 1 minute.

Bands were quantified using Image Studio Lite (LI-COR Biosciences). Rectangular boxes of equal size were drawn around each band so that the area and intensity could be calculated. Samples treated with detergent were considered to be completely labelled and the percentage of labelling was calculated for non-detergent samples was based on the ratio of areas determined for each protein band. Three independent experiments were completed in the same manner to determine the amount of labelling.

2.11: CD spectroscopy: sample preparation, measurements, and analysis

Secondary structure of MLN was characterized using a Chirascan circular dichroism spectrometer (Applied Photophysics). For MLN, 500 µL of buffer (10 mM Tris-HCl pH 7.5, 2.5 % dodecylmaltoside (DDM), 0.5 mM DTT) was added to a thin film of 100 µg of MLN peptide. Samples were stirred overnight and centrifuged the following day to remove any precipitate. The concentration of the supernatant was measured via a BCA assay (described previously).

Measurements were taken on a Chirascan CD spectrometer (Applied Photophysics, Surrey, UK). A baseline measurement without any sample or cuvette present was taken to ensure minimal background signal. Following this, 10 scans of the buffer used to solubilize MLN were recorded and then 10 scans of the peptide in detergent micelles were taken. Measurements were recorded between 190-280 nm every 0.5 seconds in a 1 mm cuvette at room temperature. An average of these 10 scans was calculated and smoothed in the Chirascan analysis software. Data was then input into the CD analysis software, Dichroweb (London, UK) under the following input conditions: wavelength range of 190-280nm, step size of 1 nm, input units as mdeg/machine units, and output units of mean residue ellipticity[114]. The K2D analysis algorithm along with the reference data set of SMP 180 optimized for 190-240 nm

was used[113,115]. The K2D analysis program calculates secondary structure by self-organizing the input dataset (CD dichroism wavelength) and generating a topological map in order to calculate protein secondary structure. A reference dataset is not required, though the SMP 180 dataset is generated from a set of membrane proteins, making it the most suitable set of references for the peptides of interest in this study. Following analysis on Dichroweb, data was plotted as mean residue ellipticity versus wavelength.

2.12: Statistical Analysis

A minimum of three independent reconstitutions and activity assays were performed for each sample and the ATPase activity was measured over a range of calcium concentrations (0.1–10 μM). For each individual dataset (single ATPase activity assays), the calcium concentration at half-maximal activity (K_{Ca}) and the maximal activity (V_{max}) were calculated based on non-linear least-squares fitting of the activity data to the Hill equation using Sigma Plot software (SPSS Inc., Chicago, IL). The reconstituted proteoliposomes containing SERCA alone are a well-characterized control for all peptide-containing proteoliposomes. The known V_{max} and K_{Ca} values for SERCA were used to correct for small inaccuracies in the determination of specific activity and calcium concentration, and these correction factors were applied to the individual ATPase activity datasets[76,97,111]. The individual ATPase activity datasets were averaged, and errors were calculated as the standard error of the mean for a minimum of three independent reconstitutions.

To determine statistical significance, the Hill parameters were calculated for each individual assay after correction. These kinetic parameters (V_{max}, K_{Ca}, and nH) were used to determine statistically significant differences between SERCA reconstituted alone and SERCA reconstituted with a regulatory peptide. Calculations were once again completed in Sigma Plot software using a one-way ANOVA on ranks. If there was a significant difference between these

groups ($P<0.001$), Dunn's multiple comparison test was used to determine the statistical probability of the difference between the test group (SERCA reconstituted with peptide) and the control group (SERCA reconstituted alone). A difference was considered significantly different if $P<0.05$.

Chapter 3: Regulation of SERCA by MLN and ALN

3.1: An introduction to MLN and ALN

Improvements in bioinformatic technology have led to the identification of functional peptides encoded by small open reading frames or sequences concealed within RNAs previously annotated as long non-coding RNAs. It is known that SERCA is regulated by transmembrane peptides, two of which are phospholamban (PLN) and sarcolipin (SLN)[103,104,107]. Recently it has become apparent that SERCA is regulated in every tissue it is expressed in by a family of peptides which we collectively refer to as the "regulins"[82,103,104,107]. Individually, these regulators are known as myoregulin (MLN), another-regulin (ALN), endoregulin (ELN), and DWORF (Dwarf open reading frame). The focus of my thesis research has been on MLN and ALN[104,116].

MLN was discovered through a bioinformatic screen scanning uncharacterized skeletal muscle genes[104]. The gene was identified as a long non-coding RNA transcript which encoded a 138-nucleotide sequence and was found to be translated into a 46 amino acid peptide. Briefly, this peptide was found to be an interactor and regulator of SERCA in fast-twitch skeletal muscle, implicating it in calcium cycling and skeletal muscle function. Moreover, when MLN was knocked out in mice, the knock-out mice showed an overall significant increase in running distance and duration compared to WT mice. Knock-out mice also showed an increase in SR calcium levels, indicating that more calcium can be pumped across the membrane in the absence of MLN[104]. While there is no specific physiological or disease-associated role for MLN in humans yet, these *in vivo* studies first implemented MLN as a functional SR peptide. These studies showed that skeletal muscle performance increased when MLN was removed from the calcium transport system in skeletal muscle[41,42,117,118]. With this, MLN could be a potential

therapeutic target for skeletal muscle diseases where calcium cycling and muscle performance is impaired.

Proper calcium homeostasis is essential for skeletal muscle function and a disruption to this process underlies different muscle diseases like Brody myopathy and muscular dystrophies[41,42]. Brody myopathy is excessive muscle stiffening or cramping with minimal relaxation during exercise as a result of SERCA1a not being completely active[41,117]. Muscular dystrophies are classified as degenerative muscle disorders[117]. Interestingly, one study done in mice showed that muscle performance increased with increased expression of SERCA1a[104]. Knowing that SERCA is important in calcium transport in muscle and that its regulation is important for proper muscle function, the new SERCA regulator, MLN, could be an important target in finding a therapy for these diseases. For example, there is the potential to pharmacologically disrupt the interaction between MLN and SERCA with the goal of improving muscle function, especially considering MLN knock-out mice showed enhanced exercise performance[119,120].

While the exact physiological role of MLN in calcium cycling remains unknown, details into its gene control, expression, and function have already been explored. The components involved in calcium regulation, SERCA, MLN, and RyR, are all co-regulated by the transcription factor, MyoD (myogenic differentiation 1), which has been implicated in muscle cell differentiation[119,120] This suggests an overall core genetic element controlling calcium movement in skeletal muscle. Additionally, the MLN gene showed two highly conserved binding sites for MyoD and for MEF2 (myocyte enhancement factor)[104]. MEF2 has been implicated in muscle cell differentiation and development[121]. Overall, MLN is likely targeted by transcription factors with roles in skeletal muscle development[104].

MLN is mainly expressed in skeletal muscle and co-localizes in the SR membrane with SERCA1a. Real-time PCR analysis showed that MLN is expressed the most with SERCA1a in

skeletal muscle[104]. The same analysis also showed that PLN is co-expressed with SERCA2, the cardiac isoform, and that SLN is co-expressed with both SERCA1 and SERCA2. Of note, even though both MLN and SLN are expressed in skeletal muscle, SLN is downregulated in adult skeletal muscles in mice[104]. MLN appears to be the highest expressing peptide in skeletal muscle[104]. That said, these expression analyses were completed in mice, so further studies to confirm these expression levels and patterns in humans need to be completed.

Additionally, MLN was shown to interact with SERCA and adopt the same general structure and function as PLN and SLN. When a series of residues within the TM domain of MLN were each mutated to alanine, the interaction observed with co-immunoprecipitation experiments was abolished. Also, docking studies using ClusPro software predicted that MLN and SLN occupy the same binding groove in SERCA1[107]. Lastly, a series of functional studies involving the transfection of a regulatory peptide and SERCA into HEK293 cells and measurements of calcium uptake rate demonstrated an effect of MLN on SERCA activity. From this, it was shown that PLN, SLN, and MLN all decreased calcium uptake, corresponding to a decreased calcium affinity of SERCA[107]. While these are important experiments, the use of HEK293 cells has been criticized in the field as they have yielded inconsistent results for the effect of peptide regulators on SERCA[77].

While the discovery of MLN has expanded the field of calcium regulation in skeletal muscle, another newly identified regulator of SERCA, another-regulin (ALN), was also studied in my thesis research. The same group that identified MLN and DWORF as functional regulators of SERCA also carried out a bioinformatic screen of the mouse genome for uncharacterized peptides with the same SERCA-binding motif as the other regulators. Two genes were identified through this screen and they were named endoregulin (ELN) and ALN, with the latter being the focus of this work. The most striking finding of these peptides is that they are the first SERCA regulators to be expressed in non-muscle tissues[95,98]. Like MLN, there is no current

physiological or disease-associated role for ALN, though the identification of SERCA regulators in non-muscle cell types adds to our understanding and to the importance of the tight regulation of Ca^{2+} ions in cells.

Like the muscle-specific regulators, ALN shares the same SERCA-binding site, localizes to the SR membrane, and is a helical transmembrane peptide[107]. In SERCA, a space is formed between the M2, M6, and M9 helices where PLN and SLN have been shown to bind, so the question was raised if ALN also bound to this space[107]. Competition studies where PLN and ALN were labelled and expressed equally in COS-7 cells showed that when PLN levels were increased, less ALN was seen to associate with SERCA[107]. While this did not directly show the interaction between ALN and SERCA, it showed that ALN likely binds to the same place as PLN. In addition to this, subcellular distribution studies involving labelled SERCA isoforms and the various regulators showed that both components localized to the SR membrane[45,107,122,123]. ALN does have some similarities to the other regulators, but the most intriguing difference lies in their tissue expression patterns.

To gain understanding of the expression patterns of ALN and various SERCA isoforms, mRNA expression was measured during development and in adult mice[107]. From this, ALN was found to be expressed in a pattern similar to SERCA2b, the ubiquitously expressed isoform of SERCA[107]. Quantitative RT-PCR also showed corresponding expression patterns between SERCA2b and ALN, making ALN the only ubiquitously expressed regulator. Important to note is that ALN alone was detected in a variety of tissues from skeletal and cardiac muscle to endothelium. With that, the question was raised of whether ALN would serve a redundant or compensatory role, especially in tissues where it was co-expressed with other SERCA isoforms and regulators[70,71,97]. An additional unique difference with ALN and SERCA isoforms is the change in calcium affinity and activity; ALN was found to decrease the calcium affinity of SERCA2b and SERCA3, but not alter the maximal activity[124].

Another interesting aspect of ALN is its potential to be regulated by phosphorylation. ALN contains a PKA recognition motif (RxxS) in the cytoplasmic region, which also happens to be a key regulatory feature of PLN's effect on SERCA. It has been well established that upon phosphorylation, PLN loses its ability to inhibit SERCA and that a structural change is induced in PLN so that it becomes disordered and can no longer inhibit SERCA[107]. From a physiological perspective, this puts PLN under control of β-adrenergic signalling[111]. With the existence of the PKA phosphorylation motif in ALN, it is possible that these two peptides share a conserved mechanism to control their regulatory effect on SERCA[105]. Nonetheless, the identification of these new regulatory peptides and their implication in regulating SERCA throughout the body has opened many doors towards gaining a fuller understanding of intracellular calcium homeostasis.

Even though MLN and ALN have been identified as functional regulators, key kinetic details into this regulatory effect remain undefined. Previous functional studies used whole-cell homogenates, which do not allow for this system to be studied in isolation. Additionally, these studies were completed using the mouse sequences of the peptides, which have some differences from the human sequence and potential roles in human physiology and disease. Thus, the goal of my thesis research was to characterize the effect of MLN and ALN on SERCA activity in reconstituted proteoliposomes. More specifically, this work aimed to carefully optimize the reconstitution method and measure the maximal activity (V_{max}), apparent calcium affinity (K_{Ca}), and cooperativity (nH) of SERCA in the absence and presence of MLN and ALN. Based on previous work by others, it was hypothesized that MLN and ALN will regulate SERCA by lowering the calcium affinity without altering the maximal activity.

3.2: Results: MLN and ALN depress the V_{max} of SERCA

3.2.1: MLN

When reconstituted at a 1:5 molar ratio of SERCA to peptide, both MLN and ALN were seen to lower the maximal activity (V_{max}) of SERCA (Figures 15, 16, and Table 3). For MLN, the greatest depression in V_{max} was seen in the 1:5 molar ratio reconstitution, where activity dropped to 3.41 μmol/min/mg from 3.98 μmol/min/mg when SERCA was reconstituted alone. A depression in maximal activity was also seen with SERCA:MLN reconstitutions at 1:2.5 and 1:7.5 molar ratios, though to a lesser extent than at 1:5. Activity dropped from 3.98 μmol/min/mg to 3.67 μmol/min/mg and 3.57 μmol/min/mg for 1:2.5 and 1:7.5 molar ratios, respectively. Regarding the 1:7.5 molar ratio, it is possible that not all MLN was incorporated into the proteoliposome or that the maximal amount of peptide was added to the proteoliposome, leading to a less dramatic effect despite the addition of more regulatory peptide. Additionally, for each of these ratios and reconstitutions, there was no significant change to SERCA's apparent calcium affinity or cooperativity in the presence of MLN (Figure 16, Table 3). Thus, MLN's main regulatory effect on SERCA is to depress the maximal activity. This finding is unique to MLN, since the other well-studied regulators, PLN and SLN, have been found to decrease SERCA's affinity for calcium, as seen by an increase in K_{Ca} (Figure 16), as the main mode to regulating SERCA.

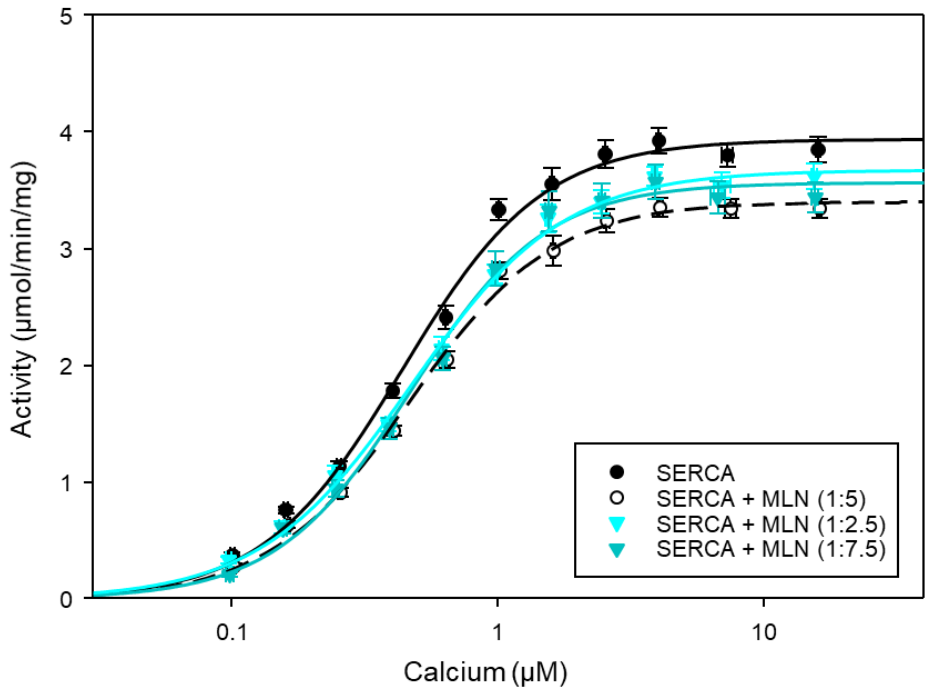

Figure 15: ATPase activity measurements of SERCA reconstituted with MLN at various molar ratios

Activity measurements are shown over a range of calcium concentrations for SERCA reconstituted alone (black circles), with MLN at 1:5 (clear circles), at 1:2.5 (blue triangles), at 1:7.5 (teal triangles) molar ratios. N values (separate reconstitutions) and n values (number of assays) are N=8, n=39 for 1:5, N=4, n=14 for 1:2.5, N=3, n=14 for 1:7.5.

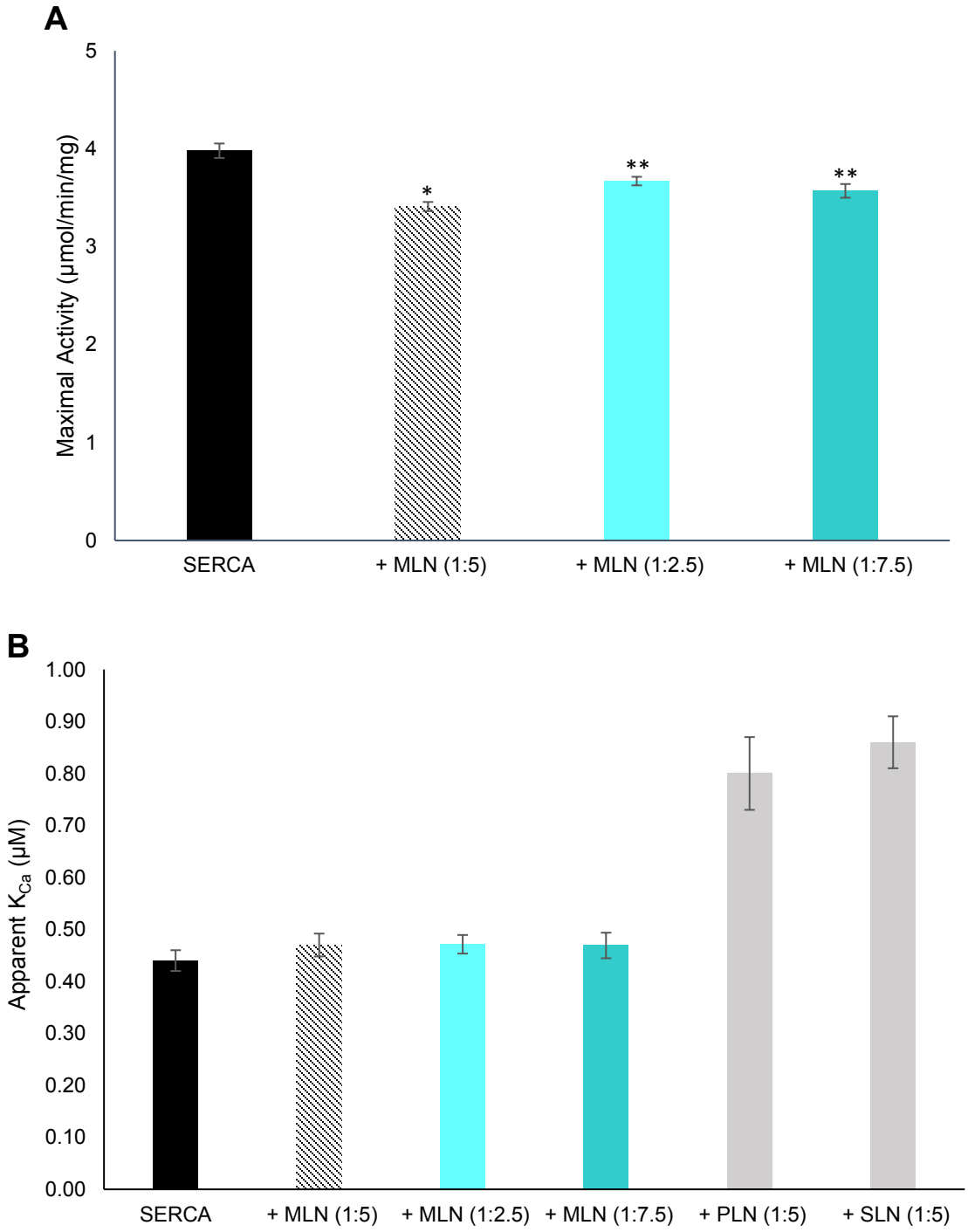

Figure 16: Maximal activity and apparent calcium affinity values of SERCA reconstituted with MLN

(A) Maximal activity, V_{max} and (B) Apparent calcium affinity, K_{Ca}, of SERCA reconstituted with MLN. Apparent calcium affinity values for SERCA reconstituted with phospholaman (PLN) and sarcolipin (SLN) are also shown to emphasize how MLN does not affect K_{Ca} as greatly as other well-studied peptides.

Table 3: Kinetic parameters of SERCA reconstituted with MLN at different molar ratios

	V_{max} (μmol/min/mg)	**Apparent K_{Ca} (μM)**	**Hill coefficient**
SERCA	3.98 ± 0.07	0.44 ± 0.02	1.65 ± 0.10
SERCA + MLN (1:2.5)	3.67 ± 0.05 *	0.47 ± 0.02 (NS)	1.55 ± 0.08 (NS)
SERCA + MLN (1:5)	3.41 ± 0.05 **	0.47 ± 0.02 (NS)	1.62 ± 0.09 (NS)
SERCA + MLN (1:7.5)	3.57 ± 0.07 **	0.47 ± 0.02 (NS)	1.69 ± 0.13 (NS)

Note: * indicates P<0.05 and ** indicates P<0.001

3.2.2: ALN

When reconstituted with ALN at a 1:5 molar ratio, both the Vmax and apparent calcium affinity (K_{Ca}) were lowered (Figures 17,18). Reconstitution with ALN led to a drop in V_{max} from 4.07 μmol/min/mg to 3.37 μmol/min/mg and an increase in K_{Ca} or decrease in apparent calcium affinity from 0.44 μM to 0.58 μM (Table 4). There was no significant change to the cooperativity. From these experiments, it was found that ALN's regulatory effect on SERCA is to depress maximal activity and calcium affinity.

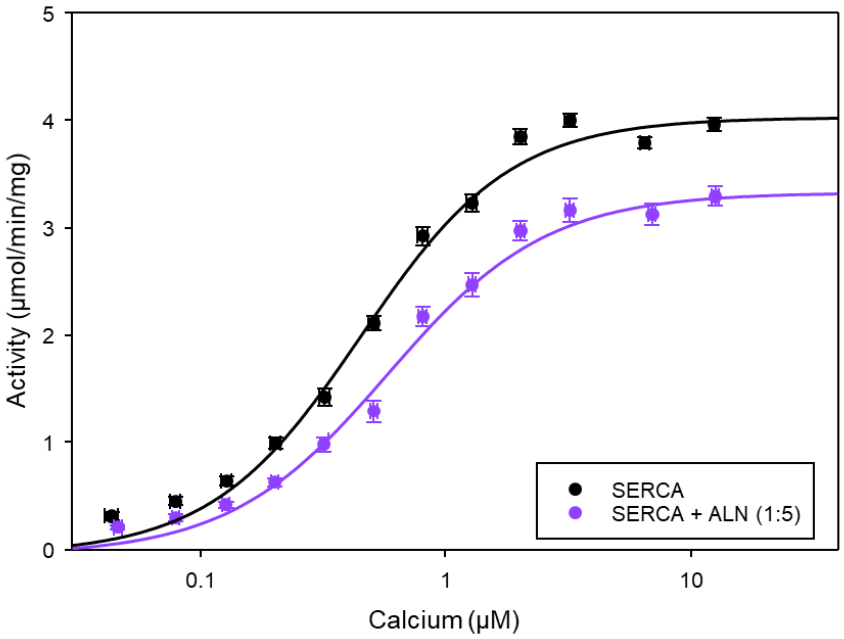

Figure 17: ATPase activity measurements of SERCA reconstituted with ALN
Measurements are for SERCA reconstituted alone (black circles) or with ALN (purple circles) at a 1:5 molar ratio. A slight decrease in maximal activity and rightward shift of the curve can be seen when SERCA is reconstituted with ALN. N values (separate reconstitutions) and n values (individual assays) are N=4, n=32 for ALN 1:5

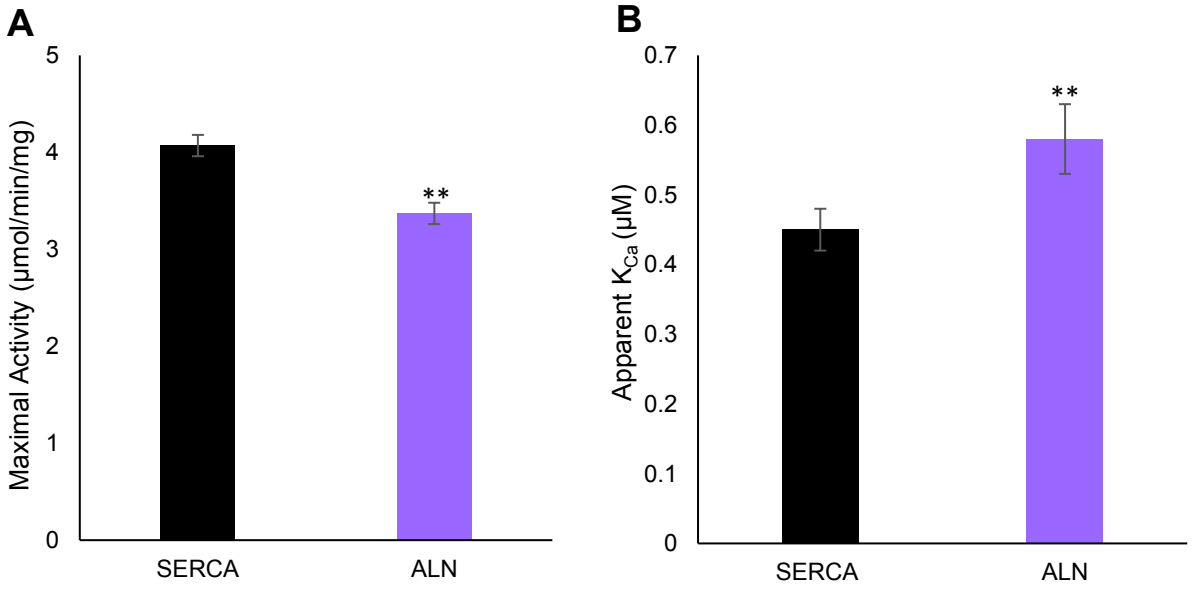

Figure 18: Maximal activity and apparent calcium affinity of SERCA reconstituted alone or with ALN
(A) Maximal activity and (B) apparent K_{Ca} values from SERCA reconstituted alone (black) or with ALN (purple) at a 1:5 molar ratio. ALN depresses the maximal activity and increases the apparent K_{Ca} of SERCA, meaning that ALN inhibits SERCA.

Table 4: Kinetic parameters of SERCA reconstituted with ALN

	V_{max} (μmol/min/mg)	**Apparent K_{Ca} (μM)**	**Hill coefficient**
SERCA	4.07 ± 0.11	0.45 ± 0.03	1.42 ± 0.12
SERCA + ALN (1:5)	3.37 ± 0.11**	0.58 ± 0.05**	1.34 ± 0.13 (NS)

Note: ** indicates P<0.001

3.3: MLN also depresses the V_{max} of SERCA when detergent is incorporated at different steps

The effect of MLN on SERCA was further explored by altering the reconstitution process. In this set of experiments, reconstitutions were prepared by adding half of the total amount of detergent at the same time the thin lipid films were formed. The remaining amount of detergent was added when lipid films were resuspended in water and buffer. Proteoliposomes were formed and isolated in the same manner as the other method mentioned previously.

Following this method, the greatest effect on ATPase activity was seen when SERCA was reconstituted with MLN at a 1:7.5 molar ratio (Figures 19, 20). Here, maximal activity dropped from 4.02 μmol/min/mg to 2.95 μmol/min/mg in the presence of MLN. Decreases in maximal activity were also seen at 1:2.5 and 1:5 ratios, dropping from 4.02 μmol/min/mg to 3.62 and 3.65 μmol/min/mg, respectively. Like the trend seen in the first reconstitution method, there was no significant change to calcium affinity or cooperativity of SERCA when reconstituted with MLN (Figure 20, Table 5).

Additionally, for the 1:7.5 molar ratio reconstitution for this method, the difference in maximal activity from when SERCA was reconstituted alone was about 1 μmol/min/mg- a greater difference than any change seen for the first method of reconstitution. This is potentially due to more MLN being solubilized with the addition of detergent at the initial lipid film step, leading to a greater amount of MLN to be incorporated into the proteoliposome.

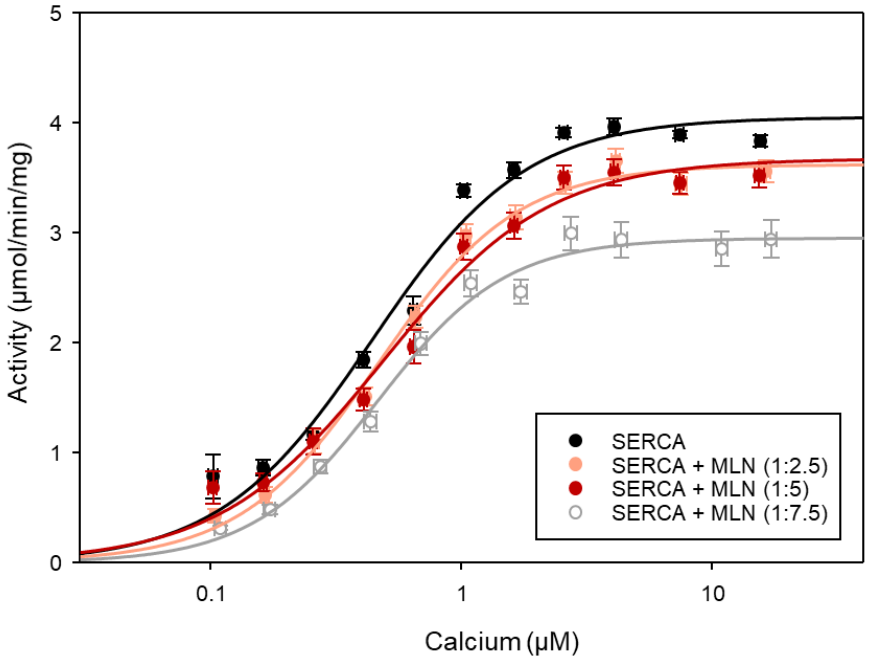

Figure 19: Activity measurements for SERCA reconstituted with MLN using a new method

For these experiments, half of the detergent was added at the initial lipid film step and the remainder was added during thin film solubilization. Activity measurements are shown for SERCA reconstituted alone (black circles), SERCA reconstituted with MLN at 1:2.5 (orange circles), 1:5 (red circles), and 1:7.5 (open grey circles) molar ratios. The most dramatic change is seen with a decrease in maximal activity when SERCA was reconstituted with MLN at 1:7.5. Small decreases in maximal activity were also seen at the other ratios. N values (separate reconstitutions) and n values (individual assays) are N=5, n=23 for 1:5, N=4, n=14 for 1:2.5, N=3, n=9 for 1:7.5.

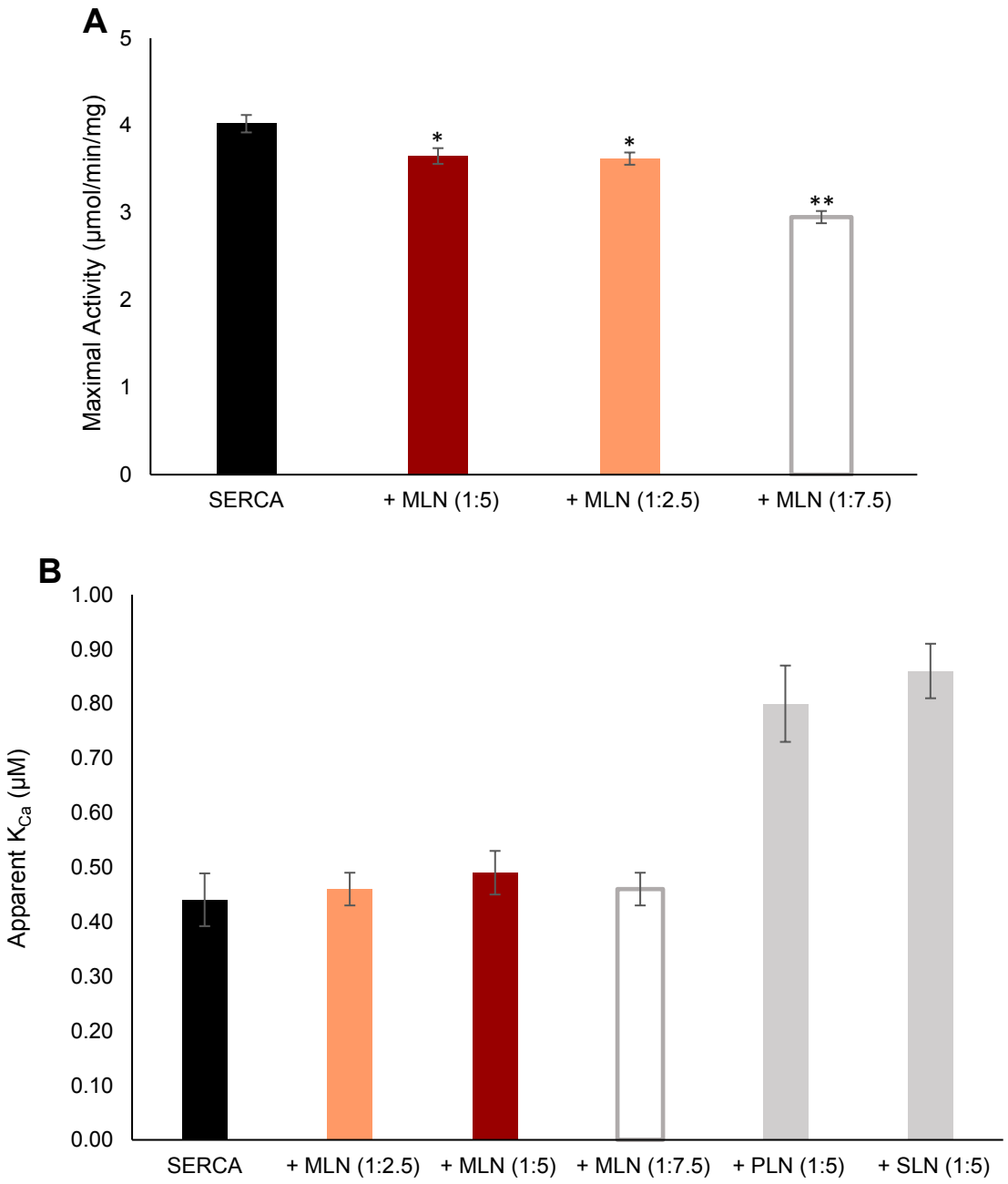

Figure 20: Maximal activity and apparent calcium affinity values for SERCA reconstituted with MLN (new method)
(A) Maximal activity of SERCA reconstituted alone (black) or with MLN at 1:2.5 (orange), 1:5 (red), or 1:7.5 (grey outline) molar ratios. (B) Apparent calcium affinity for the same groups as in A, but with the added groups of PLN and SLN at 1:5 molar ratios to highlight the lack of K_{Ca} effect compared to MLN.

Table 5: Kinetic parameters for SERCA reconstitued with MLN following the new reconstitution method

	V_{max} (µmol/min/mg)	Apparent K_{Ca} (µM)	Hill coefficient
SERCA	4.02 ± 0.10	0.44 ± 0.03	1.53 ± 0.14
SERCA + MLN (1:2.5)	3.62 ± 0.07 *	0.46 ± 0.03 (NS)	1.57 ± 0.11 (NS)
SERCA + MLN (1:5)	3.65 ± 0.09 *	0.49 ± 0.04 (NS)	1.40 ± 0.13 (NS)
SERCA + MLN (1:7.5)	2.95 ± 0.07 **	0.46 ± 0.03 (NS)	1.68 ± 0.16 (NS)

Note: * indicates P<0.05 and ** indicates P<0.001

3.4: Observing the incorporation of protein into proteoliposomes

3.4.1: Incorporation of MLN using both reconstitution methods

In order to confirm that MLN and ALN were being incorporated into the proteoliposome and to compare the amount of peptide incorporated through different reconstitution methods, the reconstitution process was observed via SDS-PAGE. MLN, with calculated molecular weight of 5.2 kDa, is seen between the 5 and 11 kDa standards. SERCA is also present in isolated proteoliposomes at levels compared to the expected amount and is not lost during the reconstitution process (Figure 21). SDS-PAGE protein quantitation showed that about 60-70% of SERCA or MLN was present in isolated proteoliposomes relative to the starting material or 'before biobead' sample of the reconstitution process (Figure 21). Important to note is that an equal or similar amount of SERCA and MLN was maintained relative to the starting material, meaning that the final ratio of SERCA to MLN was not perturbed.

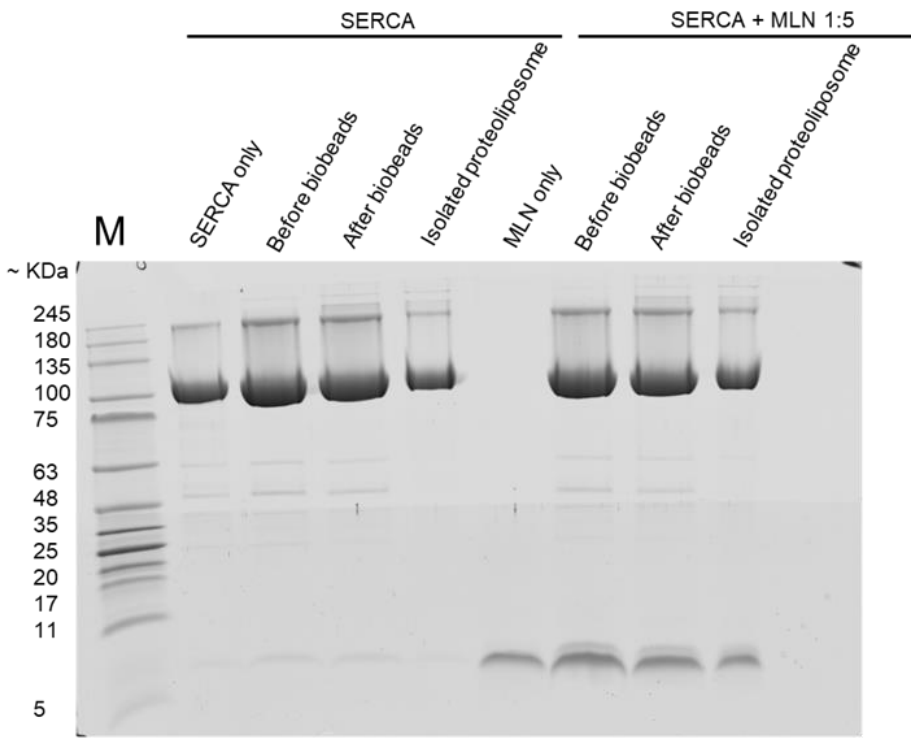

Figure 21: SDS-PAGE showing the incorporation of MLN and SERCA
10 µL of sample was loaded for each condition. (A) Observations of the incorporation of MLN through the first method of reconstitution at a 1:5 molar ratio. MLN does not appear to be lost at any step. SERCA only and MLN only refer to amounts of pure protein expected in isolated proteoliposomes.

Regarding the second method of reconstitution, SDS-PAGE protein quantitation showed that SERCA and MLN were both lost to a small degree through the reconstitution process and it appeared as though more MLN was present in the 1:7.5 molar ratio condition compared to the other molar ratios (Figure 22A). In fact, when comparing samples from each method to an expected amount for the 1:7.5 molar ratio condition, more MLN was present in the sample from the second method compared to the expected amount of protein (Figure 22B). Also, important to note is that SERCA is also lost through the reconstitution process, meaning that the final desired ratio of SERCA:MLN is more likely to be maintained in the isolated proteoliposome. Protein quantitation estimated that roughly 50% of SERCA was retained and that about 45% of MLN for the 1:2.5 and 1:5 ratios was retained. More MLN was retained for the 1:7.5 ratio, where 60% was estimated to be retained. Ultimately, enough SERCA and MLN were retained to maintain the desired ratios.

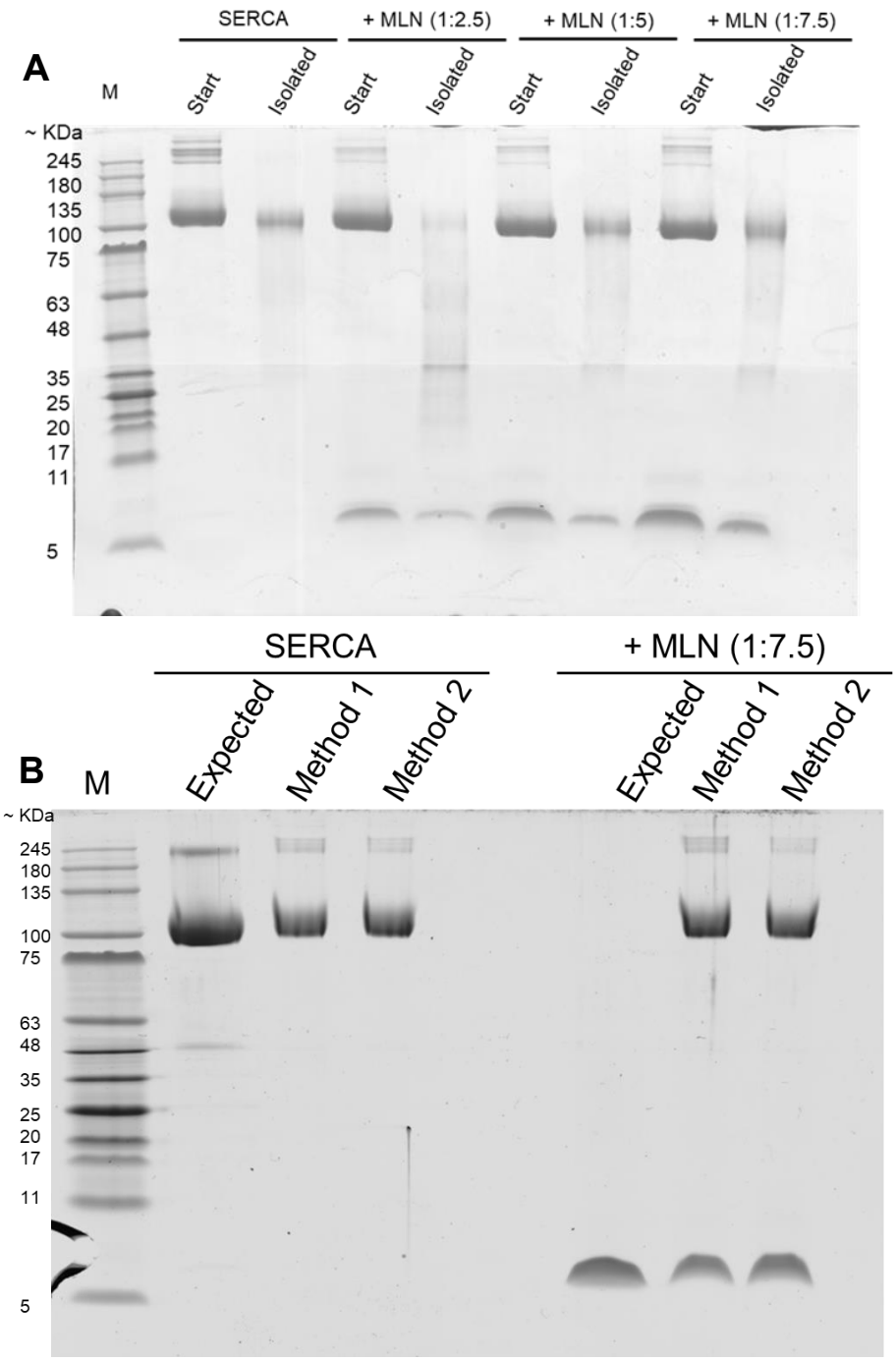

Figure 22: SDS-PAGE analysis showing the incorporation of MLN (new method)
For these experiments, half of the total amount of detergent was added at the initial lipid step. (A) Observations of the incorporation of MLN at varying molar ratios to SERCA through the second method of reconstitution (where detergent was added at the start). Start refers to the stage in reconstitution before biobeads are added and isolated refers to a sample from isolated proteoliposomes. MLN does not appear to be lost through the reconstitution process of this method. (B) Comparison of 1:7.5 molar ratio reconstitution condition between reconstitution methods to show that more MLN is incorporated with the new method.

3.4.2: Observing the incorporation of ALN into proteoliposomes

Similar to MLN, ALN was also shown to be present in the final reconstitution and can be seen between the 5 and 11 KDa molecular weight markers at two different molecular weights (Figure 23). This was also seen when pure ALN was separated via SDS-PAGE (Figure 23B). The pattern of these bands does not obviously correspond to a monomer-dimer pattern for ALN, but it is possible for this to be the oligomeric profile of ALN. It is also possible that peptide fragments were generated as a result of the synthesis process. It is also not likely for the smaller of the two bands to be SLN (which can be co-purified with SERCA), as it is not seen in the SERCA-only reconstitutions. SDS-PAGE protein quantitation analysis estimated that about 27% was retained for the larger band and 40% for the smaller band. When both bands were quantified together, about 31% was retained (as quantified using Image Studio Lite). Additionally, quantitation also showed that some SERCA appeared to be lost through the process and it was estimated that about 60% of SERCA was retained through the reconstitution process. In combination, these quantitative estimates show that more ALN was lost through the reconstitution process compared to SERCA, indicating that the desired final 1:5 ratio of SERCA:ALN was not maintained. With the results here, it is likely that the final ratio may be between 1:2.5 and 1:5, hinting that future optimization will be required beyond the completion of this thesis.

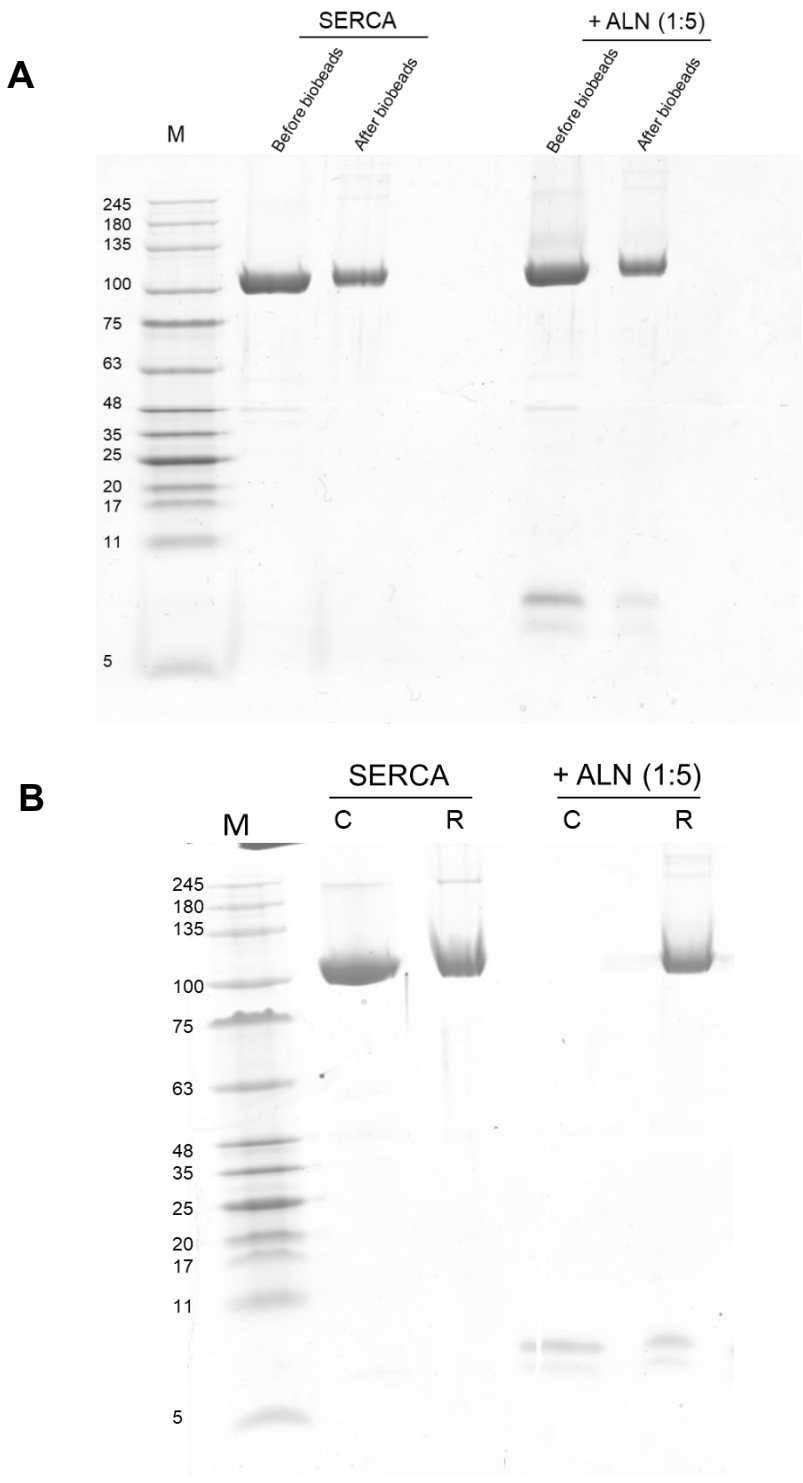

Figure 23: SDS-PAGE analysis showing the incorporation of ALN into proteoliposomes
(A) Comparison of ALN reconstitutions before and after the addition of biobeads. It can be seen that SERCA and ALN are not completely incorporated into the proteoliposome. (B) A comparison of pure SERCA and ALN to samples of reconstituted proteoliposomes. C refers to the control sample and R refers to a reconstituted sample.

3.5: Determining if lipids have a role in the way MLN regulates SERCA

Another aspect of regulation that was probed was to determine if lipid composition of the liposome may have an impact on the way MLN regulates SERCA. Thus far, all reconstitutions were carried out using a 9:1 ratio of egg yolk phosphatidylcholine and phosphatidic acid, respectively. Since MLN has a cluster of negative charges close to the membrane surface, we predicted that the negative charges from EYPA headgroup may impede the interaction between MLN and SERCA, and thus prevent it from regulating (Figure 24). In these experiments, the lipid composition was altered so that only EYPC or a 9:1 ratio of EYPC to EYPE (egg yolk phosphatidylethanolamine), a zwitterionic lipid, was used. In both conditions, the negative charge present on the surface of the membrane is removed.

MTGKNWILISTTTPKSLEDE**IVGRLLKILFVIFVDLISIIYVV**ITS

Figure 24: Primary sequence of MLN highlighting the negative residues near the transmembrane domain
Bold letters indicate the transmembrane domain and the cluster of negative residues are highlighted in grey.

When reconstituted with EYPC only, MLN's regulatory affect on SERCA was unchanged from what was previously observed (Figure 24, 25, Table 6). There is a slight decrease in maximal activity when SERCA is reconstituted with MLN in EYPC proteoliposomes, however the difference is not as dramatic as with previous conditions. Similarly, with EYPC/EYPE proteoliposomes, no significant change to maximal activity was seen when SERCA was reconstituted with MLN (Figure 25B, 26). For both of these lipid conditions, no significant change to apparent calcium affinity was observed (Figure 25, 26, Table 6).

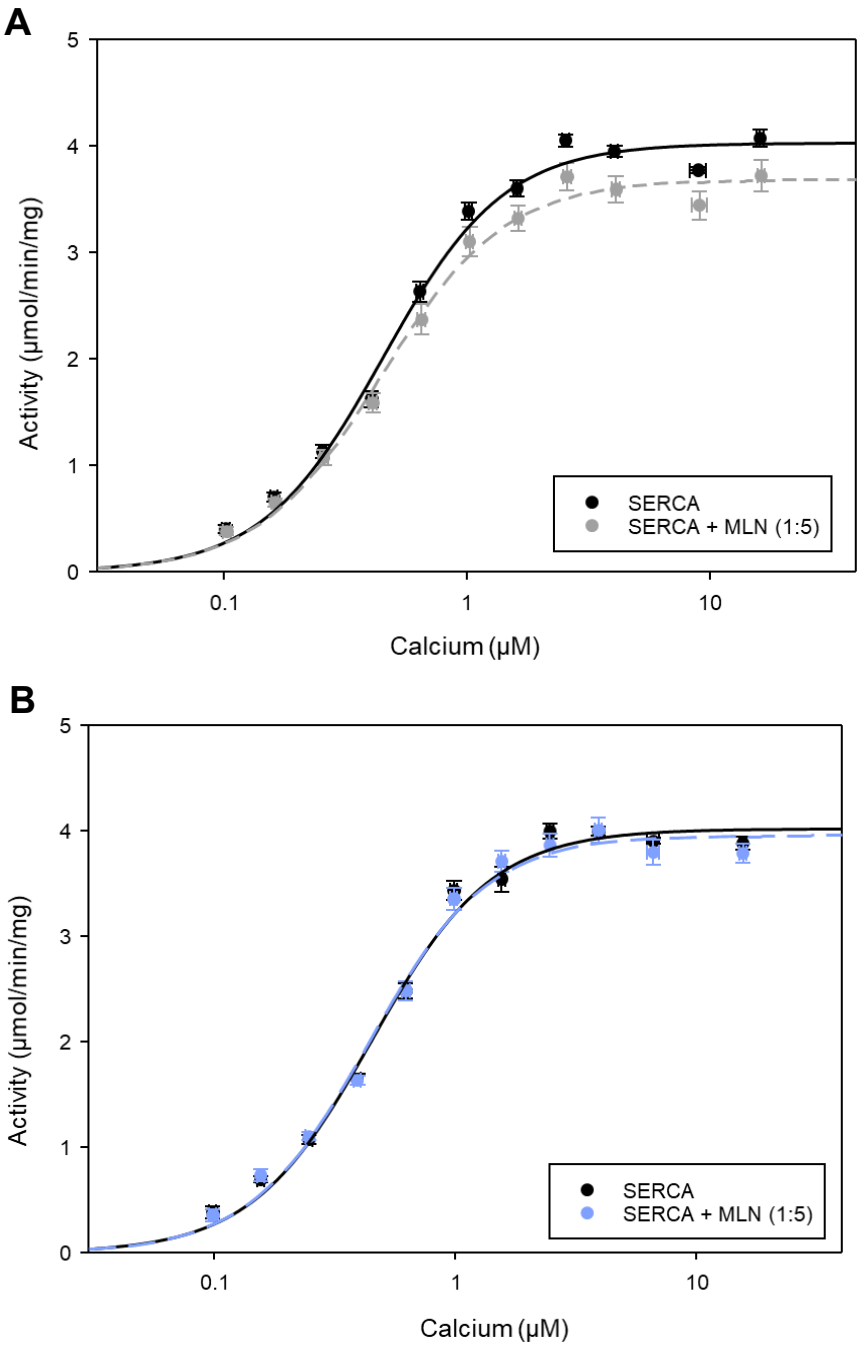

Figure 25: ATPase activity measurements from reconstitutions using varied lipid conditions

(A) Activity measurements of SERCA reconstituted alone (black circles) or with MLN at a 1:5 molar ratio (grey circles) in liposomes with only EYPC. N values (separate reconstitutions) and n values (individual assays) are N=4, n=21 (B) Activity measurements of SERCA reconstituted alone (black circles) or with MLN at a 1:5 molar ratio (light purple circles) in liposomes with EYPC and EYPE. N values (separate reconstitutions) and n values (individual assays) are N=3, n=22.

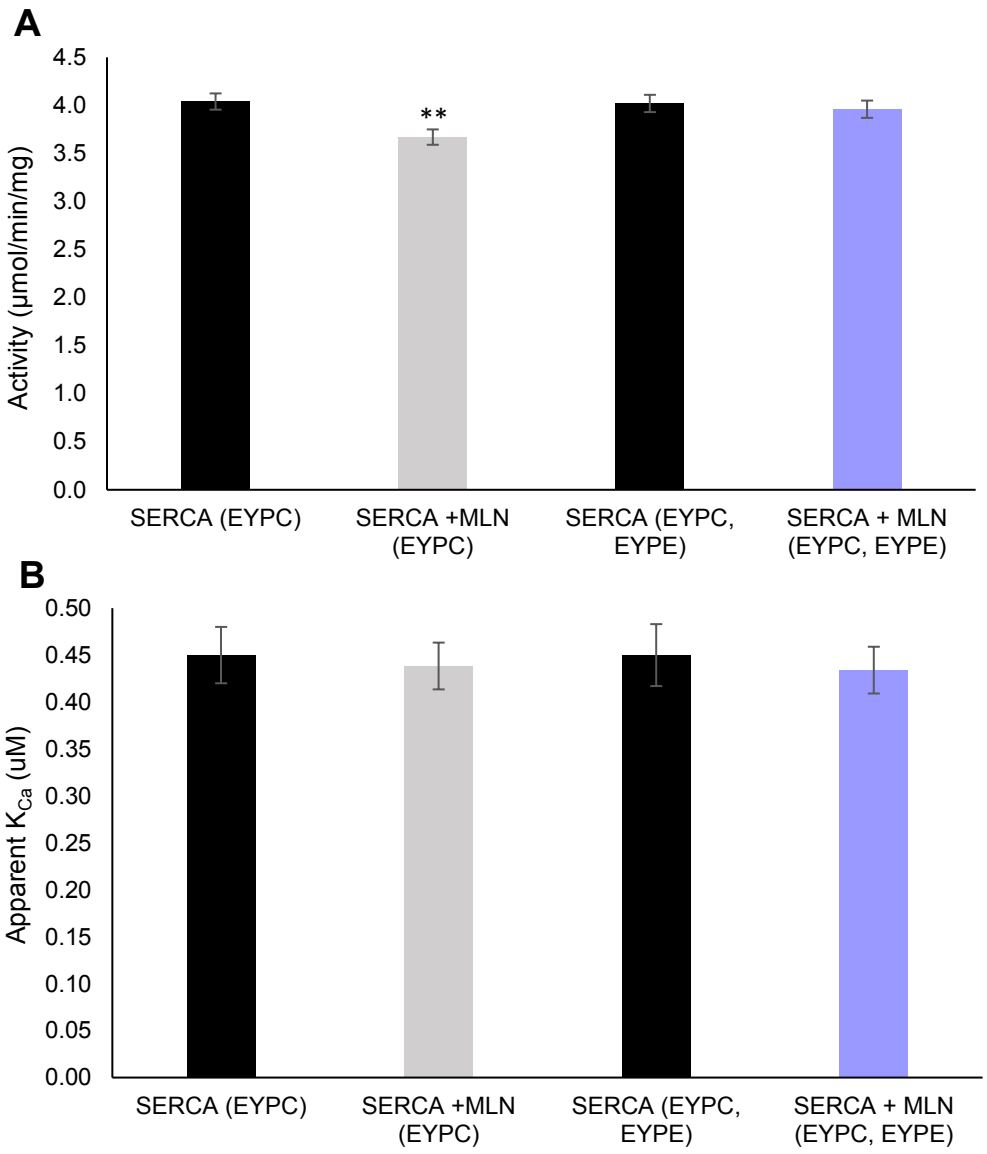

Figure 26: Maximal activity and apparent calcium affinity for reconstitutions using varied lipid conditions

(A) Maximal activity (V_{max}) for and (B) apparent calcium affinity (K_{Ca}) values for SERCA:MLN reconstitutions composed of EYPC only or EYPC and EYPE

Table 6: Kinetic parameters for SERCA reconstituted with MLN using varied lipids

	V_{max} (μmol/min/mg)	Apparent K_{Ca} (μM)	Hill coefficient
Reconstitution with EYPC only			
SERCA	4.04 ± 0.09	0.45 ± 0.03	1.74 ± 0.16
SERCA + MLN (1:5)	3.67 ± 0.08**	0.44 ± 0.03 (NS)	1.71 ± 0.14 (NS)
Reconstitution with EYPC and EYPE			
SERCA	4.02 ± 0.09	0.45 ± 0.03	1.74 ± 0.15
SERCA + MLN (1:5)	3.96 ± 0.09 (NS)	0.43 ± 0.03 (NS)	1.77 ± 0.17 (NS)

Note: ** indicates P<0.001

3.6: Biotinylation of MLN to determine orientation in proteoliposomes

In addition to altering reconstitution conditions to elucidate the effect of MLN on calcium pumping by SERCA, the orientation of MLN in the proteoliposome was also determined. To do this, a biotinylation assay was employed, which took advantage of the lysine residues in the cytoplasmic domain of MLN (Figure 27). Here, NHS-linked biotin was used to label these residues, and IR-dye streptavidin was used to probe for these labelled resides in intact proteoliposomes or in proteoliposomes where the membrane was solubilized with octylglucoside, leading to complete labelling of MLN.

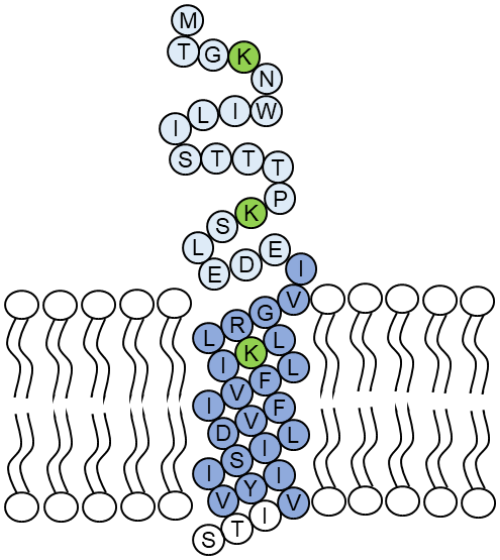

Figure 27: Topology diagram of MLN highlighting different domains and lysine residues
Highlighted are the transmembrane domain (blue) and the cytoplasmic domain (light blue) and lysine residues (green). The lysine residue located in the transmembrane domain is likely protected from labelling and experiments using unreconstituted MLN did not show comparable labelling likely due to it being insoluble in similar buffer to reconstituted conditions.

Following this reaction, MLN was found to be about 83 % correctly oriented (Figure 28). This result agreed with experiments completed for PLN, another well-characterized cardiac SERCA regulator[110,125]. Of note, experiments were also carried out using pure MLN resuspended in buffer as a control to determine complete labelling. In doing this, it was difficult to solubilize MLN in comparable buffer conditions to what was used for labelling protein in reconstituted proteoliposomes. Thus, it was difficult to carry out a control reaction with MLN at the same concentration in proteoliposomes and obtain a signal similar to that from the labelled MLN in proteoliposomes. It was assumed that lysine 27 in the TM domain of MLN was protected by the membrane and unable to be labelled.

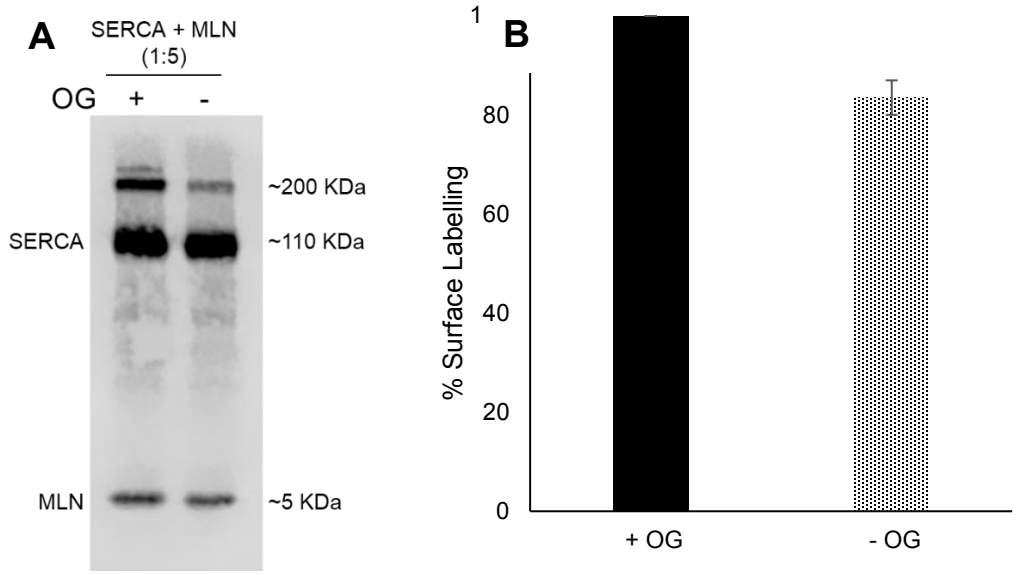

Figure 28: Surface labelling and orientation of MLN in proteoliposomes
(A) Representative blot following labelling with biotin and probing with IRdye streptavidin in the presence (+) and absence (-) of detergent. In the presence of detergent, all of SERCA or MLN should be labelled. The uppermost band seen on the western blot likely corresponds to a dimer of SERCA. For these experiments, the orientation of SERCA was not calculated as the signal was too strong relative to that obtained from MLN. (B) Percent surface labelling of MLN in proteoliposomes with OG added to show complete labelling (black) and without OG to only label protein that is oriented outside of the proteoliposome (dotted). Results were obtained from three independent labelling experiments and blots.

3.7: Circular dichroism (CD) spectroscopy and secondary structure of MLN

Circular dichroism results and calculations obtained via Dichroweb showed that MLN was 37% alpha helical, and 63 % random coil or beta sheet. These results corresponded with *in silico* results obtained to predict secondary structure. TMHMM results indicated that residues 21-43 were predicted to be alpha-helical and that residues 25-43 were the most likely residues to be alpha-helical[125,126]. An important observation to note is that the cytoplasmic domain is generally unstructured, especially between residues serine 10 and glutamate 20, which contains several serine and threonine residues which have the potential to be phosphorylation sites (Figure 29).

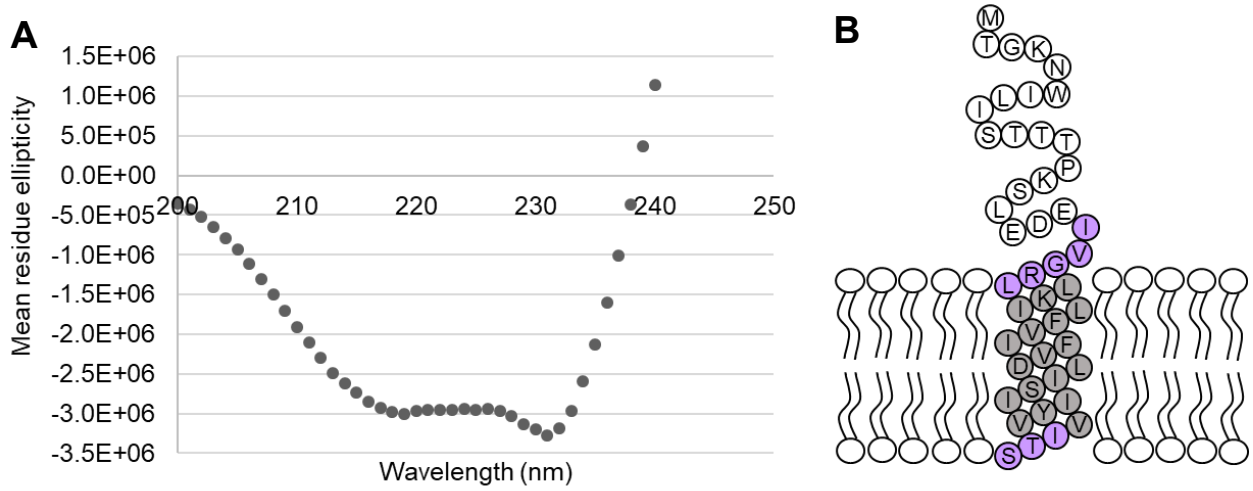

Figure 29: Secondary structure determination of MLN
(A) Circular dichroism spectra of MLN. Measurements are from 10 separate acquisitions with background noise from buffer components subtracted. (B) Topology diagram highlighting residues strongly predicted to be alpha helical (grey), less strongly predicted to be alpha helical (purple), and disordered (white)

3.8: Discussion

The goal of this work was to determine the kinetic effect that MLN and ALN have on SERCA in isolated proteoliposomes. Moreover, because this was the first time these peptides were reconstituted, significant optimization of this process was also done to ensure they were incorporated and functional in this system. It was found that MLN decreased maximal activity but had no effect on the calcium affinity of SERCA and that ALN on the other hand decreased both parameters. It was also shown that changing the method of reconstitution alters the effect and that these peptides to incorporate into the proteoliposome in the correct orientation. These experiments begin to break the surface to show that these regulators each have a unique way of regulating SERCA, though there is still a lot left to be investigated.

Many methods of reconstitution are available, and each is valuable for studying different things. In our case, the formation of unilamellar vesicles containing pure lipid, peptide, and SERCA has been documented as the best to maintain SERCA activity and for structural studies[111]. Alterations can be made to this method and that is what was done here; the addition of $C_{12}E_8$ at two different stages of the reconstitution process led to a more dramatic effect of MLN on SERCA activity. The likely explanation is that the initial addition of detergent allowed more MLN to be solubilized and thus, be incorporated into the proteoliposome. There are other options to improve solubilization, like sonication, which have been used commonly and can serve as options to improve potentially troubling reconstitutions, especially with the unstudied regulators[127–129]. In addition to knowing that MLN does incorporate into the proteoliposome, further confirmation that the effect on SERCA is true comes from the correct orientation of MLN in the proteoliposome. Previous orientation studies with PLN and SERCA in proteoliposomes show that about 70-80% of PLN is correctly oriented, which is comparable to the results obtained here[130].

One thing that was not explored in this work was a method to identify a direct interaction between MLN or ALN and SERCA. Previous studies employing FRET have shed light on the reaction mechanism of SERCA, binding affinity of PLN to different SERCA isoforms, and the effect that phosphorylation of PLN has on the reaction mechanism[131]. Given that these systems have provided detailed information for PLN, it would be useful to study the other regulators in this context as well. In fact, experiments to determine oligomerization and binding affinity of MLN and ALN to SERCA have already begun[131,132]. Another technique that may be useful to investigate the interaction between SERCA and its various regulators is microscale thermophoresis, or MST. This relatively new technique measures the motion of molecules through fluorescence along at temperature gradient created by an infrared laser. MST is sensitive to changes that occur in the experimental set up from protein unfolding to the binding of two biomolecules, as these changes lead to varied movement along the created temperature gradient[104]. This technique does not have some of the challenges that others have; it can be used label-free if intrinsic fluorescence is sufficient and it removes the requirement for a tag or immobilization, thus removing multiple steps that require optimization[133]. Regarding label-free MST with membrane proteins, the greatest challenges would come from the solubility of the proteins involved and from the level of intrinsic fluorescence that can be obtained. Nonetheless, these techniques could provide a plethora of information to supplement activity studies with SERCA and its regulatory peptides.

When comparing the results of experiments obtained here with those completed by Anderson et al. (2015), there is a striking difference in how MLN regulates SERCA. In these experiments it was found that MLN did not change SERCA's calcium affinity and decreased maximal activity whereas it was previously found that MLN decreased the calcium affinity with no effect on maximal activity[70,71,124,134,135]. One explanation for this could be that isolated proteoliposomes and whole-cell homogenate are such different sources of material. It is

possible that in a whole-cell system, a post-translational modification occurred allowing for MLN to regulate SERCA by decreasing calcium affinity. It is also possible that the levels of MLN to SERCA are different from those obtained in an isolated proteoliposome system. Additionally, it is currently unclear of what role the TM domain plays in comparison with the cytoplasmic domain of MLN with regard to regulation. It is possible that the regulatory function of MLN lies within one of these domains, and further experiments to clarify this will be necessary. With this, by looking at the primary sequence of MLN, particularly in the cytoplasmic region, it appears to be a candidate for phosphorylation by casein kinase 2 (CK2) and glycogen synthase 3 (GSK3) (Figure 30).

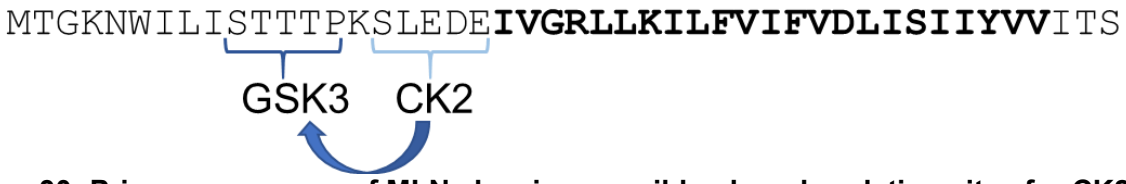

Figure 30: Primary sequence of MLN showing possible phosphorylation sites for CK2 and GSK3
The transmembrane domain is also represented (bold). The CK2 recognition site requires acid residues C-terminal to the modification site and the general GSK3 site that is phosphorylated is SXXXP[133].

It is known that PLN's inhibitory action on SERCA is regulated through phosphorylation via protein kinase A (PKA, or cAMP-dependent kinase) and through dephosphorylation by protein phosphatase 1 (PP1)[136,137]. Knowing this, it is possible that MLN's effect on SERCA is also regulated through phosphorylation; however, rather than the effect being diminished as with PLN, phosphorylation of MLN would lead to inhibitions as seen in activity studies done in whole-cell homogenate. MLN has several threonine and serine residues in the cytoplasmic domain, making it an ideal candidate for phosphorylation (Figure 30). Notably, it has two motifs that would allow for synergistic phosphorylation by CK2 which would prime for phosphorylation

by GSK3 (Figure 30)[138,139]. Physiologically, CK2 is a ubiquitous, constitutively active enzyme with a vast number of substrates like signalling proteins, transcription factors, regulators, and structural proteins[70,124]. GSK3 is also involved in a variety of pathways from glucose metabolism to developmental pathways and recent research has specified one isoform of GSK3 to have a specific role in glucose metabolism in muscle[140]. While it may be too early to make any direct conclusions, these observations provide a novel future direction for the regulation of MLN and consequently, SERCA in skeletal muscle.

ALN also appears to have the potential to be phosphorylated. One site that has the potential to be phosphorylated is RRXS, which is the recognition motif in PLN that is recognized by PKA (Figure 31). As mentioned, phosphorylation by PKA removes PLN's inhibitory effect on SERCA and is under control of β-adrenergic signalling[141]. Of note, this motif is different between the human and mouse sequence of ALN, meaning that this site may not be of great importance for phosphorylation, or that this difference does not affect phosphorylation (Figure 31). Additionally, ALN also appears to have a recognition motif for AMP-activated kinase (AMPK) (Figure 31)[142].

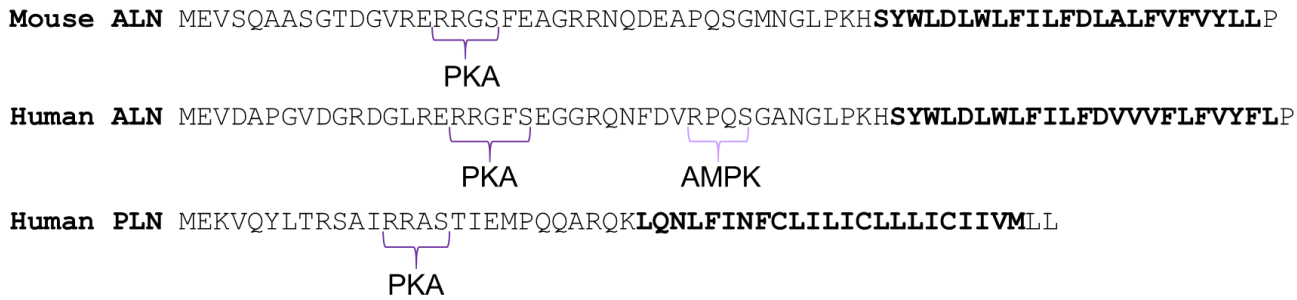

Figure 31: ALN and PLN primary sequences indicating potential and known phosphorylation sites
Primary sequences of mouse ALN (top), human ALN (middle), and human PLN (bottom) highlighting potential protein kinase A (PKA) and AMP-activated protein kinase (AMPK) phosphorylation sites in ALN and known phosphorylation sites in PLN.

Physiologically, PKA is also ubiquitous enzyme with many substrates involved in cardiac and endocrine function and in cancer[104]. AMPK also has a central role as mediating energy homeostasis and thus has been implicated in many different tissues and diseases[83,86–88,90,96]. Again, while the results of these experiments are preliminary, these connections provide a source of speculation for ALN's place in the body. Since ALN is ubiquitously expressed, perhaps it may have a central role in energy homeostasis or perhaps it has a role in regulating Ca^{2+} pumping activity by SERCA when the other regulators are incapable of doing so. Additionally, current experiments do not hint at whether phosphorylation will be an inhibiting or activating action, or if it could be controlled. Nonetheless, with the existence of kinase recognition motifs and the knowledge that other regulators are phosphorylated, the phosphorylation of ALN remains something to be explored.

Currently, our lab has an established protocol to phosphorylate transmembrane peptides *in vitro* by PKA, so it could be used with the other regulators as well. This protocol also allows for proteoliposome reconstitution and activity assays to be carried out afterwards to determine if there is any effect on activity. This protocol could be adapted for the other kinases like CK2, GSK3 and AMPK. Additionally, phosphomimetic mutations of the predicted target serine or threonine residues could be made. Because of challenges in expressing and purifying these regulators and because of the cost of obtaining hydrophobic peptides, the latter option may not be the most immediately fruitful. Other approaches could be taken to observe phosphorylation, and these include the use of phospho-specific antibodies which could detect phosphorylated protein in whole-cells or cell lysates[143].

Another question to ask is the reason that skeletal muscle would evolve to have two transmembrane peptide regulators of SERCA. Perhaps these regulators are involved in different pathways, are regulated separately, or maybe MLN and SLN have a compensatory or additive role in altering calcium cycling in skeletal muscle (Figure 32). With recent studies, it is known

that MLN has a role in muscle performance and potentially myogenesis because its expression is regulated by the transcription factors, MyoD and MEF2[144]. SLN however, has been implicated in a variety of systems in recent years, from non-shivering thermogenesis, to mitochondrial biogenesis, to proper functioning of the atria of the heart[104]. With these vastly different roles, it is possible that SLN and MLN are part of separate physiological and regulatory systems in skeletal muscle. Another aspect that is yet to be answered is the relative expression levels between MLN and SLN at different stages of life. It has been mentioned that SLN is downregulated in adult skeletal muscle, leaving MLN to be dominantly expressed[66,89,96]. It may also be that other environmental or physiological factors could alter levels of MLN or SLN. For example, if muscle performance needed to be regulated or if new muscle is generated, MLN would be more greatly expressed. If a body needs to generate heat through thermogenesis, then SLN would be more greatly expressed. While this is speculative, it will be exciting for another aspect of skeletal muscle function to be mapped out.

Although MLN has not been directly related to any disease or specific physiological process, it is interesting to think of MLN's role in calcium handling in skeletal muscle which may be related to muscle performance or to energy homeostasis (Figure 32). Another future path for these regulators is their potential to be therapeutic targets. Knowing that MLN has a direct role in skeletal muscle performance and that the removal of MLN leads to enhanced muscle performance in mice, the disruption of the interaction between SERCA and MLN could be a pharmacological target for degenerative muscle diseases[50,58,122]. Also, studies have implicated SERCA activity to have a role in energy homeostasis in skeletal muscle, opening questions that MLN may also play a part in this process[65,66]. These questions are entirely unexplored and answering them will eventually paint a clear picture of the workings of skeletal muscle.

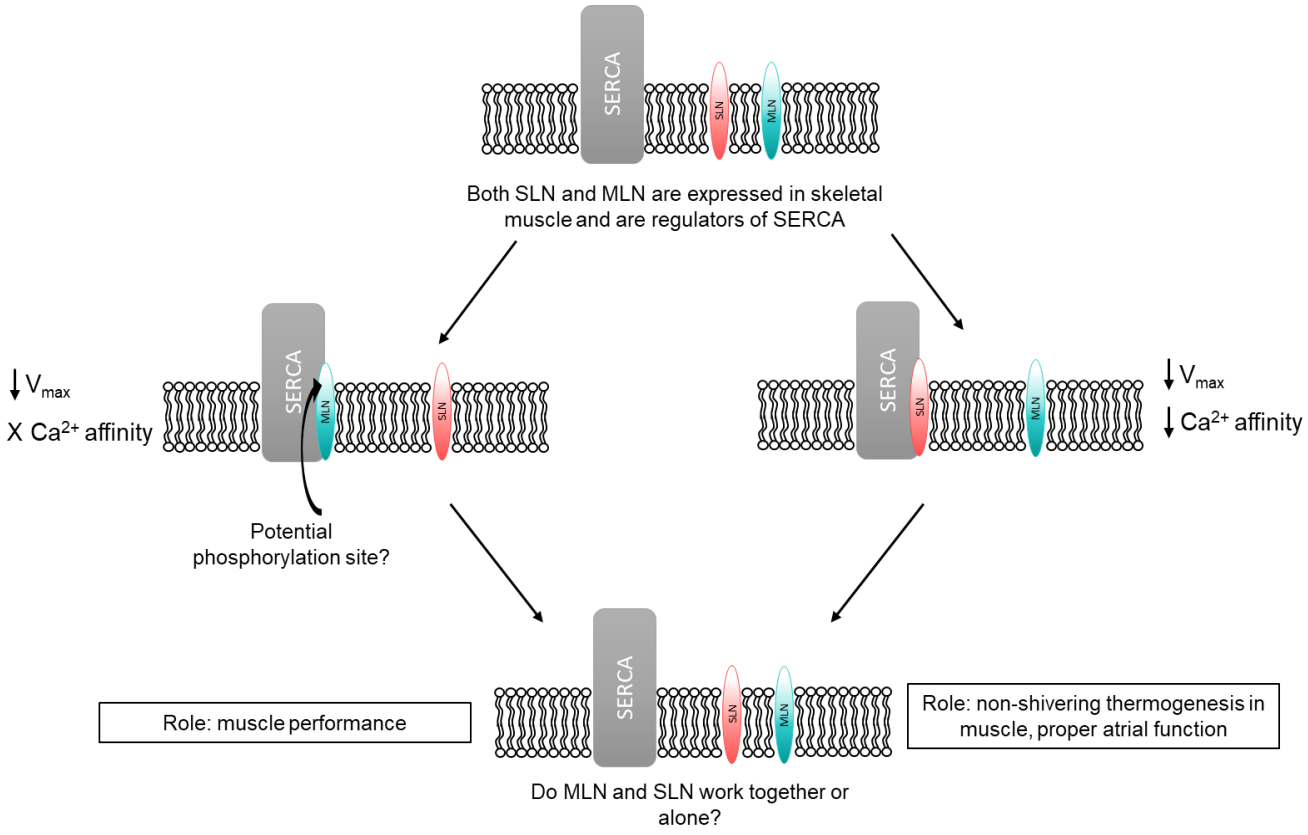

Figure 32: Schematic showing MLN, SLN, and SERCA in the SR membrane with potential roles for these proteins

Our current outlook is that MLN and SLN have independent effects on SERCA, but further research could bridge the gap between the regulatory effects on SERCA. Perhaps each peptide acts under a completely different system for a different purpose. This last notion may be likely because of MLN's and SLN's currently known physiological functions

Many of the same questions surround the existence of ALN. Being the only known ubiquitously expressed regulator, it could be that it is an overall compensatory mechanism for intracellular calcium cycling and that it serves an otherwise redundant role if a body is in homeostasis or a healthy state (Figure 33). In the case of non-muscle tissues, SERCA2b and 3 have been implicated in cell death and survival pathways along with store-operated calcium entry[16,37]. Additionally, altered calcium cycling and SERCA expression levels have been implicated in diabetes, but role of these regulators, especially in the context of non-muscle tissues, is yet to be investigated[145]. Our current knowledge does not allow for conclusions regarding ALN, so future combinatory or loss-of-function studies both *in vitro* and *in vivo* will help to patch the gaps in our understanding. Another limitation to this study was that the skeletal muscle isoform of SERCA was used rather than the ubiquitously expressed isoform SERCA2b, which is the main isoform that ALN is expressed with. It is known that different isoforms of SERCA do have different kinetic properties, so further experiments matching different regulators with other SERCA isoforms could be done to fill in these gaps[101,146]. What's more, is that the identification of these new SERCA regulators and of regulatory peptides of other enzymes is likely just touching the surface of all the functional regulators that exist.

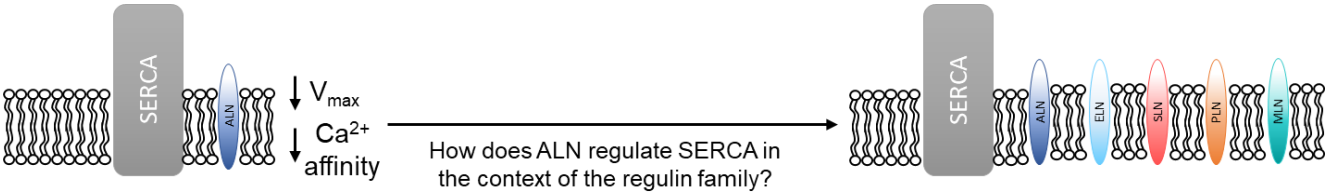

Figure 33: ALN decreases the maximal activity and calcium affinity of SERCA, but its physiological role remains undetermined
These results show that ALN alone decreases the maximal activity and calcium affinity of SERCA, however future experiments will need to show what is the role of ALN.

Chapter 4: Sarcolamban and the effect of sequence variation on SERCA regulation

4.1: An introduction to sarcolamban

Sarcolambans (SLB) are a group of peptides that initially sparked interest in long non-coding RNAs as a source of small open reading frames. The long non-coding RNAs were found to encode functional peptides, which eventually lead further discoveries and the family of SERCA-regulatory peptides that is known today[147]. SLB peptides were identified as small open-reading frames (smORFs) through a bioinformatic screen of long non-coding RNA[145,146,148–151]. Prior to this study, it was known that smORFs were abundant in plant and animal genomes, though little knowledge into their relevance or function in these living systems was known due to difficulties with identifying, validating, and studying short peptide sequences[101]. Nonetheless, multiple studies were done in the context of insect, mouse, and human genomes to identify new, small, and functional genes, extensively demonstrating that smORFs are not an aspect of life to be ignored[101].

SLB peptides are considered the invertebrate orthologues of mammalian SERCA-regulatory peptides, with some similarities to their mammalian counterparts[101]. Upon the identification of potentially functional smORFs in the fly genome located in the putative non-coding RNA003 in 2L (pncr003:2L), it was found that they were expressed in somatic muscle and the post-embryonic heart of *Drosophila*[101]. Moreover, these encoded peptides were localized to the area between the sarco-endoplasmic reticulum membrane and plasma membrane of the sarcomeres, shedding light on a potential role for these peptides. With this, it was proposed that these peptides may have a role in facilitating the transfer of voltage stimulation to calcium release from the sarcoplasmic reticulum and consequent muscle contraction[101].

While a BLAST search only identified other fly SLBs, a search based on structural homologues showed that human sarcolipin (SLN), a regulator of SERCA in atrial and skeletal tissue, was a match[68,82,83,152]. Also, sequence alignments and the generation of a phylogenetic tree showed that SLB, SLN, and the longer mammalian peptide, PLN, all originated from a single smORF, making this study the first to show the conservation and evolution of a smORF[102,153,154]. With this and the knowledge that SLN and PLN function to regulate SERCA's ability to pump calcium across the SR membrane, the role for SLB in regulating SERCA-dependent calcium transport and has become an important point to investigate[101].

The equivalent of mammalian SERCA in insects, referred to as Ca-P60A, is about 70% identical to mammalian SERCA isoforms 1 and 2, has an identical hydropathy profile, and has the same essential residues responsible for Ca^{2+} binding in mammalian SERCA[101]. Combinatory experiments using PLN, SLN, and Ca-P60A showed that either mammalian peptide localizes and interacts with Ca-P60A[155–157]. Additionally, when PLN was expressed with Ca-P60A in *Drosophila* (where endogenous SLB is mutated to be non-functional), cardiac function and measured calcium levels return close to trends seen with WT *Drosophila* SLB. These results, in combination with modelling studies of the structure of Ca-P60A with bound PLN and SLN, show that these regulatory peptides share a common mechanism in regulating Ca-ATPases. Another point to note is that because of the similarities to SLN and PLN, these names were combined to create the name sarcolamban[155].

In insects, Ca-P60A is an important player in calcium homeostasis. Studies have shown that the removal or alteration of Ca-P60A leads to dysregulation of calcium signalling, disrupted protein trafficking to the membrane, and many homozygous mutations are lethal in early stages of development[105]. It is highly expressed in the central nervous system. muscles, and shows ubiquitous low-level expression, suggesting both specific and maintenance functions[105]. Proper calcium cycling is essential throughout eukaryotic life; this is reflected by the facts that calcium

cycling is centrally important in insect and mammalian cells and that SERCA and Ca-P60A have about 70% sequence identity. With this, studying the unknown aspects of these regulatory systems becomes hugely important to further our understanding of the ever-important process of calcium cycling in the cell.

Since it was observed that mammalian peptide regulators affect invertebrate Ca-ATPases, the opposite scenario becomes open for investigation as well. With this, the goal of my work was to investigate how four different SLB peptides effect the maximal activity, calcium affinity, and cooperative calcium binding of mammalian SERCA. Furthermore, we wanted to investigate the role that sequence variation amongst peptide regulators may have on SERCA regulation. While PLN and SLN are highly conserved amongst mammals, invertebrate SLBs exhibit broad sequence variation that ranges from more PLN-like to more SLN-like. To examine this sequence variation, four different SLB peptides from four different invertebrate species were generated as recombinant MBP-fusion proteins and purified via affinity chromatography (see Chapter 2). Specifically, *Bombus terrestris*, *Drosophila melanogaster*, *Daphnia pulex*, and *Triops cancriformis* were used (Figure 34). Purified peptides, lipids, and SERCA were co-reconstituted into proteoliposomes, which were used to measure the effect each peptide had on SERCA's calcium handling. In doing this, it was found that each SLB peptide had a unique effect on SERCA, showing that sequence variation does have a role in the regulation of SERCA. More broadly, this work shows how the regulatory function of these peptides is conserved across species and that the level or type of variation (maximal activity or calcium affinity) can vary greatly.

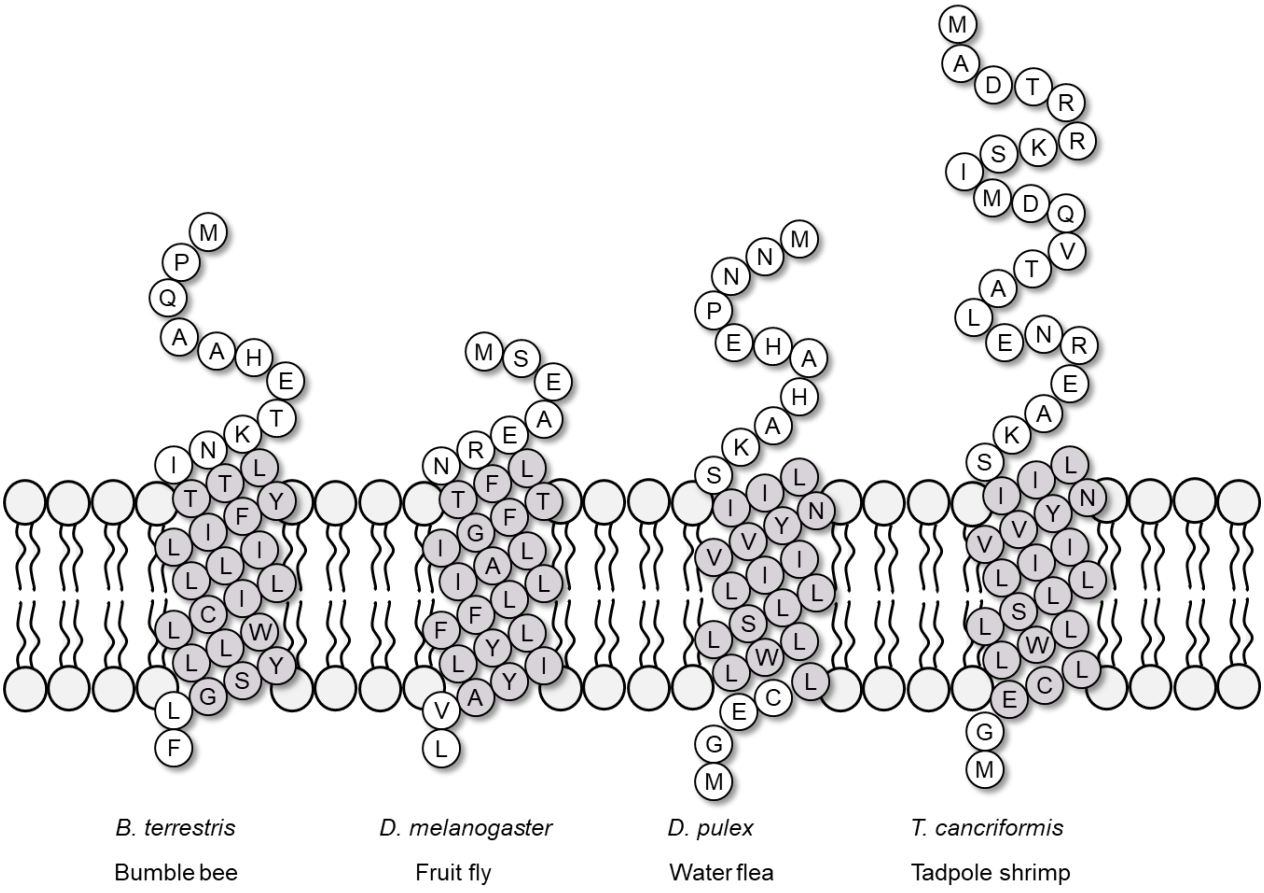

Figure 34: Topology diagram of the various SLB peptides
Sequences from four different species are shown. Transmembrane domains (grey circles) were predicted using TMHMM software[72,158].

4.2: Sequence variation of regulatory peptides changes the way SERCA is regulated

Four different insect orthologues of SERCA-regulatory peptides were used to observe how sequence variation may have a role in the regulation of calcium pumping by SERCA. Two regulators, *B. terrestris* and *T. cancriformis* SLB, were seen to be strong inhibitors of SERCA. When reconstituted at a 1:5 SERCA-SLB molar ratio, both regulators significantly depressed the maximal activity from 4.1 μmol/min/mg to 1.1 and 2.3 μmol/min/mg, respectively (Figure 35, 36, Table 7). Additionally, the apparent K_{Ca} increased from 0.44 μM calcium to 1.82 and 2.05 μM, for *B. terrestris* and T. *cancriformis*. *D. pulex* SLB also increased the apparent K_{Ca}

of SERCA when reconstituted at a 1:5 molar ratio, increasing this value from 0.44 μM calcium to 1.53 μM (Figure 35, 36, Table 7). Interestingly, this regulator also showed a slight increase in maximal activity, increasing from 4.08 μmol/min/mg for SERCA alone to 4.80 μmol/min/mg in the presence of *D. pulex* SLB. In contrast with the other peptides, *D. melanogaster* SLB did not appear to alter SERCA's maximal activity or apparent K_{Ca} (Figure 35, 36, Table 7).

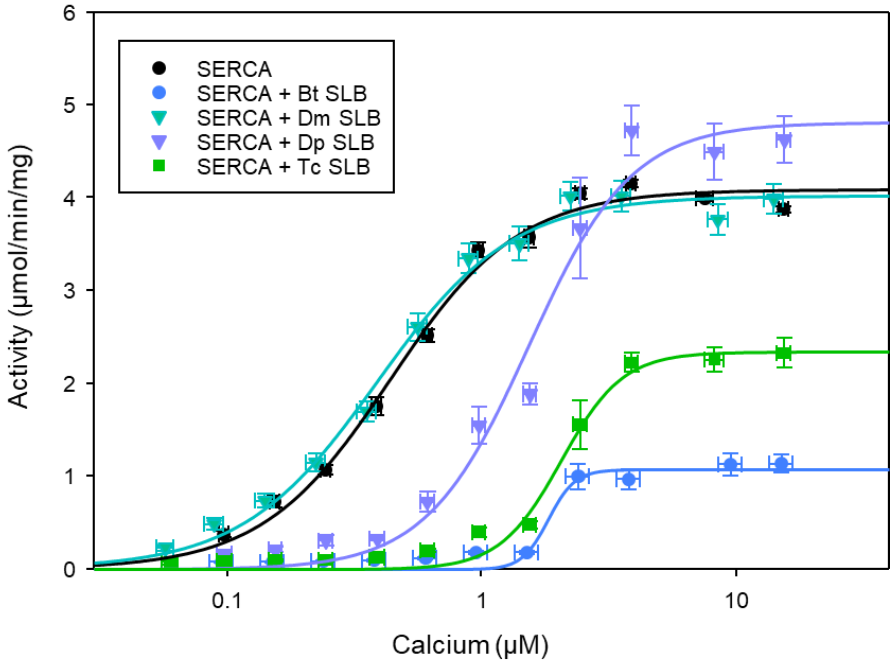

Figure 35: ATPase activity measurements for SERCA reconstituted with SLB peptides Measurements for SERCA reconstituted alone (black circles), with *B. terrestris* SLB (Bt, blue cirlces), with *D. melanogaster* SLB (Dm, teal triangles), with *D. pulex* SLB (Dp, purple triangles), and with *T. cancriformis* SLB (Tc, green squares) are shown. N values (separate reconstitutions) are N=3 for each SLB peptide and n values (individual assays) are n=15 for Bt and Dm and n=10 for Dp and Tc.

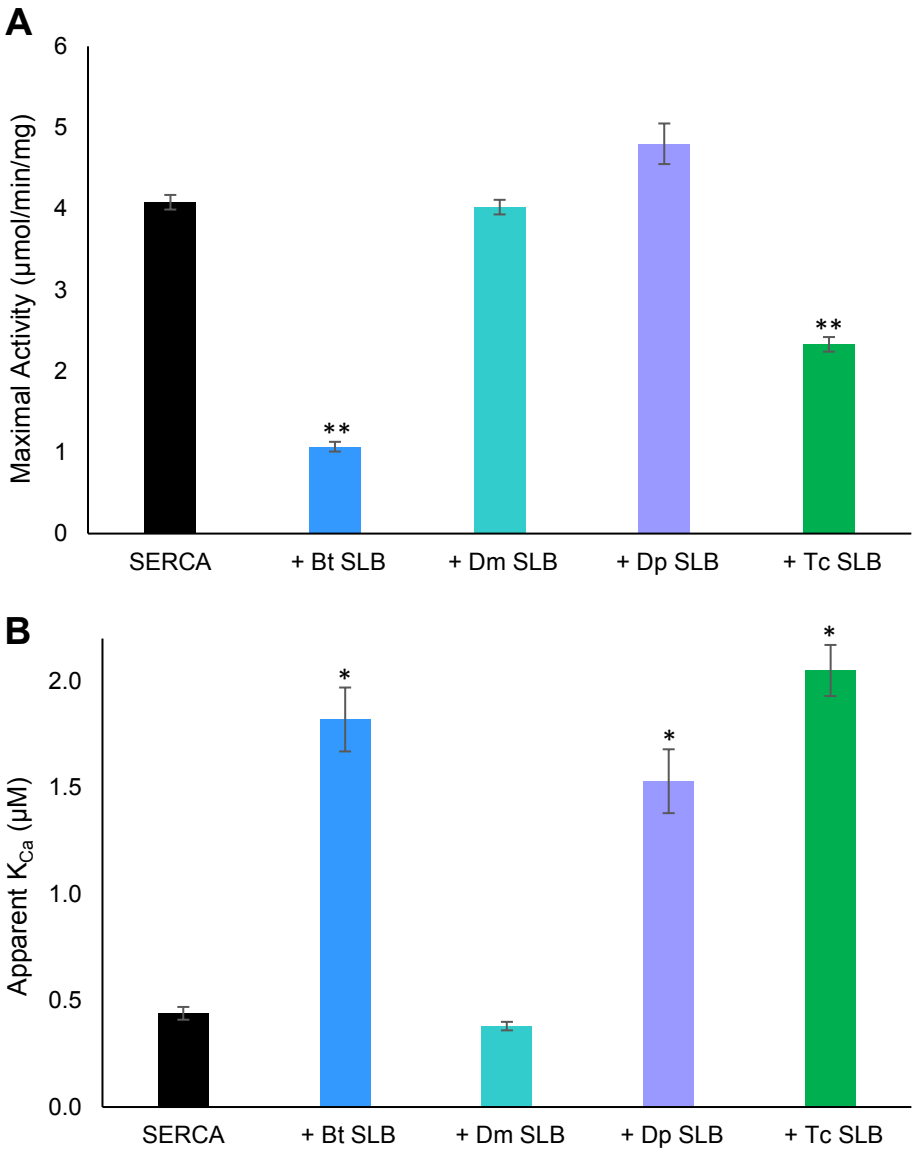

Figure 36: Maximal activity and apparent calcium affinity values for SLB reconstitutions Values are shown for SERCA reconstituted alone (black), with *B. terrestris* SLB (Bt, blue), *D. melanogaster* SLB (Dm, teal), *D. pulex* SLB (Dp, purple), and *T. cancriformis* SLB (Tc, green).

Table 7: Kinetic parameters for SERCA reconsituted with the various SLB peptides

	V_{max} (µmol/min/mg)	**Apparent K_{Ca} (µM)**
SERCA	4.08 ± 0.09	0.44 ± 0.03
SERCA + Bt SLB	1.07 ± 0.06**	1.82 ± 0.15*
SERCA + Dm SLB	4.02 ± 0.09	0.38 ± 0.02
SERCA + Dp SLB	4.80 ± 0.25	1.53 ± 0.15*
SERCA + Tc SLB	2.33 ± 0.09**	2.05 ± 0.12*

Note: * indicates P<0.05 and ** indicates P<0.001

4.3: Observing the incorporation of SLB peptides into proteoliposomes with SERCA

Similar to the peptide studies discussed above, reconstitutions containing SERCA and SLB peptides were separated and analyzed via SDS-PAGE. Regarding *B. terrestris* SLB, silver staining showed the incorporation of the peptide between 5-11 kDa, close to the expected mass of 3.8 kDa (Figure 37). Additionally, image quantification through Image Studio Lite showed that about 30% of the peptide was retained through the reconstitution process. For *D. melanogaster* SLB, the peptide was difficult to observe on both methods of staining the gel at the expected mass of 3.3 kDa (Figure 37). *D. pulex* and *T. cancriformis* were also seen to be present in isolated proteoliposomes, adding to the point that these peptides reconstituted with SERCA in proteoliposomes (Figure 37). For the peptides that are visible in either method of staining, multiple bands can be seen between 5 and 17 kDa around the expected masses for each respective peptide (Figure 37). These additional bands likely correspond to oligomers of the peptide, as PLN and SLN are known to oligomerize[97]. Again, image quantification of the intensity of the bands though Image Studio Lite revealed that these main bands corresponded to about 20-30% incorporation.

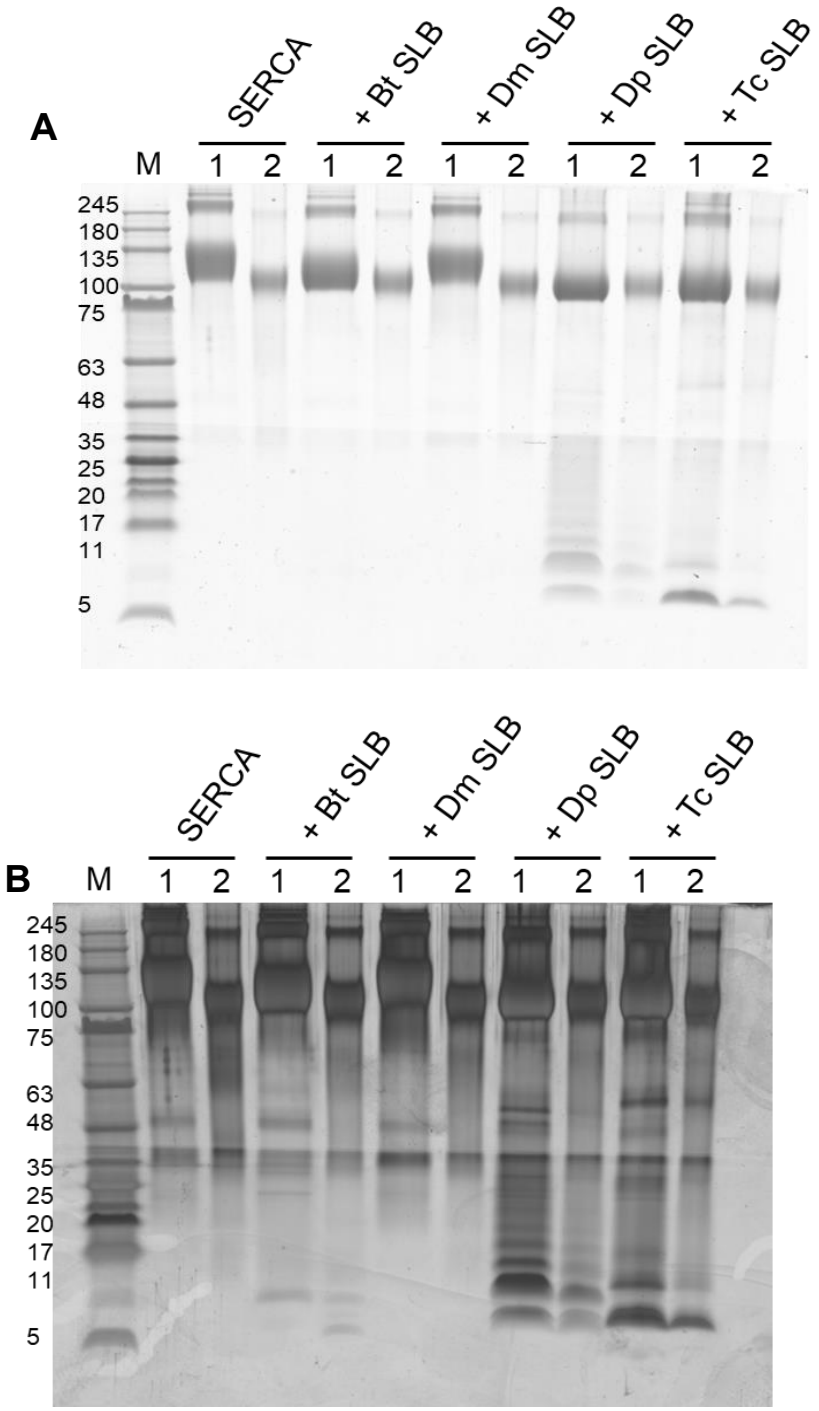

Figure 37: SDS-PAGE analysis of reconstitutions containing SERCA and different SLB peptides

1 refers to a sample taken before the addition of biobeads and proteoliposome reconstitution and 2 refers to a sample taken from isolated proteoliposomes. (A). Coomassie stained gel showing the incorporation of *D. pulex* SLB (Dp), and *T. cancriformis* SLB (Tc) with SERCA in proteoliposomes. (B) Silver stained gel from A, showing the incorporation of *B. terrestris* SLB with SERCA in proteoliposomes.

4.4: Discussion

The goal of this work was to elucidate how sequence variation in regulatory transmembrane peptides alters the action of SERCA to pump calcium across a membrane. This was carried out by reconstituting four different insect Ca-ATPase regulators, or sarcolamban (SLB) peptides, with SERCA into proteoliposomes and measuring changes in ATPase activity of SERCA. From these experiments, it was found that each SLB peptide regulated SERCA in a unique way. Two peptides, *B. terrestris* and *T. cancriformis* SLB, were both strong inhibitors of SERCA as they greatly depressed maximal activity and calcium affinity of SERCA. *D. melanogaster* SLB did not alter SERCA activity and *D. pulex* SLB slightly increased maximal activity and decreased the calcium affinity of SERCA. Bringing these functional results in context with the functional effect of PLN and SLN, it appears as though *B. terrestris* and *T. cancriformis* are more SLN-like and *D. pulex* is more PLN-like.

While each SLB peptide behaved independently of the other, some also behave like their mammalian counterparts. For example, *D. pulex* SLB increased maximal activity and decreased calcium affinity, which is the same effect seen from WT PLN when reconstituted and measured in the same way[101]. Also*, T. cancriformis* SLB decreased both maximal activity and calcium affinity, the same overall trend seen for WT SLN[159,160]. It is also important to note that these experiments were completed at the same molar ratio of peptide to SERCA and overall lipid to protein ratio. Thus, the functional differences observed between the various SLB peptides are less likely to be from dramatic differences in peptide-SERCA-lipid ratio, which is known lead to varied effects in a reconstituted system. Moreover, when aligning the different groups of SLN-like or PLN-like peptides to SLN or PLN, some conserved or similar residues do exist, though there is no obvious pattern or region that is conserved. For the SLN-like peptides, there is a conserved “WLL” motif towards the C-termini of the sequences, though the exact functional importance of these residues in SLN has not been determined (Figure 38). Also, the

highly conserved “RSYQY” motif in mammalian SLN that is responsible for its inhibitory action is not present in *B. terrestris* or *T. cancriformis* SLB (Figure 38). For the PLN-like peptide, *D. pulex* SLB, there are also conserved residues, but no obvious conserved motif between these sequences (Figure 38). The majority of conserved residues reside in the TM region, so these residues may be important for both peptides to carry out their inhibitory action on SERCA, or they may be conserved because they are in the TM region. Also noteworthy is that while these peptides can be separated into functional groups, the length of the peptide and the TM regions vary in length. With this, it is difficult to determine the exact residue or region of the peptides that is responsible for the effect observed here. One approach to clarify this could be to conduct alanine-scanning mutagenesis of the conserved residues in each peptide and then follow through with activity studies. Overall, this sequence variation could have an interesting application, which will be discussed in the following paragraphs.

Regarding *D. melanogaster*, it is was difficult to observe via SDS-PAGE and Coomassie staining, so it is possible that it did not efficiently and effectively reconstitute with this method, explaining why it seemed to have no effect on SERCA’s maximal activity or calcium affinity. This process could be improved for future experiments by changing the initial solubilization of *D. melanogaster* SLB, perhaps using the same method as in Chapter 3 where detergent was added twice through the reconstitution process. Despite this unusual result, phylogenetic and bioinformatic analysis of mammalian and invertebrate peptide regulators showed that each peptide likely originated from a single ancestor of about 30 amino acids[106]. A common ancestor amongst these peptides could explain why some invertebrate peptides may act like mammalian PLN or SLN and why some may act with a unique effect. Knowing this, it is possible that *D. melanogaster* SLB could be categorized as SLN or PLN-like following optimization to protocols used here. Individual sequence alignments between *D. melanogaster* SLB and PLN or SLN do show identical or similar residues between the different sequences, however, some of these

residues are also conserved between PLN and SLN (Figure 38). With similarities to both PLN and SLN, it could be that *D. melanogaster* SLB lowers the calcium affinity of SERCA, though any alteration to be maximal activity remains in question. It is also possible that *D. melanogaster* does not have as dramatic of an effect on SERCA as it would Ca-P60A.

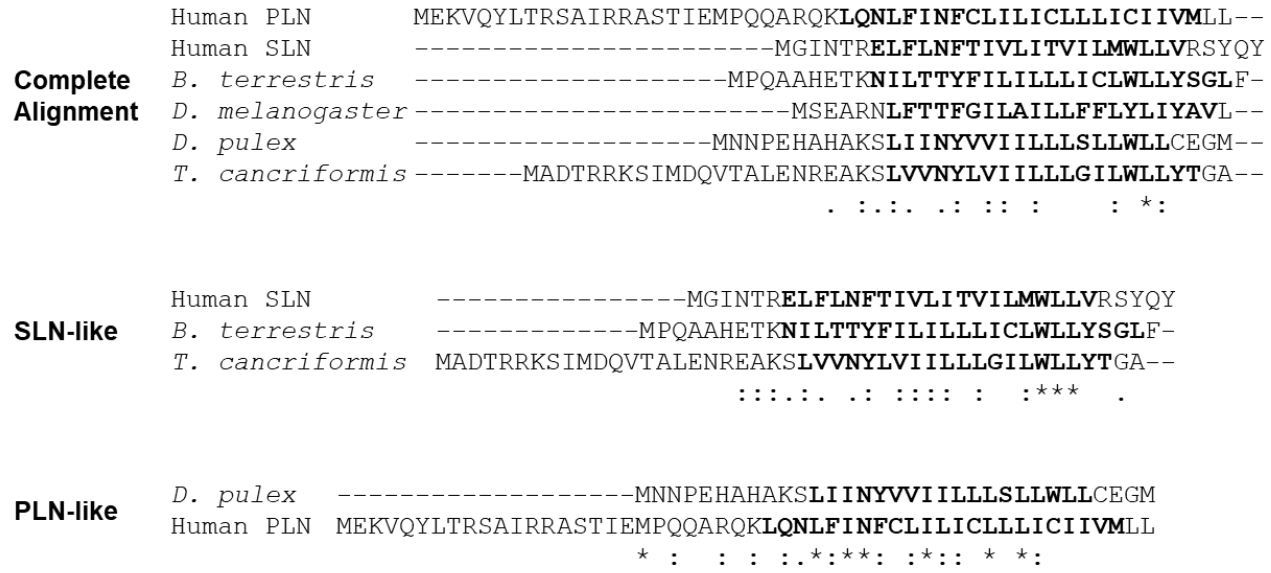

Figure 38: Sequence alignment of mammalian and invertebrate peptide regulators
Alignments were completed using Clustal Omega and then adjusted manually to maximize the amount of overlap over the transmembrane domains (bold font)[105]. Transmembrane domains were predicted for SLB peptides using TMHMM[160]. A period indicates weakly similar properties, a colon indicates strongly similar properties, and an asterisk indicates nearly identical properties between sequences.

Broadly, these sequences are varied so it is difficult to determine if part of a sequence is important, especially with these experiments (Figure 38). With the well-studied regulator, PLN, it is known that single amino acid changes can have a dramatic effect on the peptide's regulation of SERCA, rendering it either non-functional or as a super-inhibitor. For example, R9C and R14del mutations to PLN have been implicated in lethal dilated cardiomyopathy[160]. From these studies, it was concluded that hydrophobic balance in the cytoplasmic domain of PLN is important for proper regulation of SERCA in a physiological context[161–164]. In light of these small sequence changes, it is not surprising that completely different sequences have varied effects

on SERCA's activity. From these activity experiments, it is difficult to determine what specific part of each SLB peptide is responsible for the effect seen, thus, future experiments could probe into identifying structural elements. That said, these activity experiments show that sequences that deviate from PLN and SLN can regulate SERCA activity in a similar manner.

In line with this, SERCA's site to bind regulatory peptides is not very specific and has been screened for a variety of site-specific molecules to be used as potential therapeutics in diseases where SERCA regulation is disrupted[97]. With the results of these experiments showing that sequence variation is essential in the way SERCA is regulated, it is possible that other peptides or effector molecules could be designed and tailored for a specific effect on SERCA based on the sequences of known regulators. Three different studies using AAV gene therapy were carried out with the aim of improving heart failure by increasing the amount of SERCA2a and upregulating calcium cycling[156,157]. Currently, none of these trials have been successful, leaving the opportunity for another approach, which could be to design and use tailored peptide regulators as a means to upregulate calcium cycling in a diseased state. These regulators could be designed as activators of SERCA so that calcium cycling is upregulated. This approach would be challenging to design and implement, yet gene therapy may be more effective with a small peptide compared to the much larger SERCA2a only- which is already present in cardiac tissue. Despite this, the idea that sequence variation is important and that peptide regulators can be designed with specific functionality remains open for investigation in the future.

While one perspective is to think about peptide variation and how that could be implicated in a human context, there is another perspective- the importance of these regulators in an invertebrate system and their overall role in calcium signalling within these organisms. As mentioned previously, it is known that Ca-P60A is essential for calcium homeostasis in an invertebrate[101,102]. It has also been observed that diminished Ca-P60A function leads to temperature sensitivity, decreased heartbeat and altered rhythm, and that heat exposure leads

to paralysis or seizure-like behaviour in *D. melanogaster* because of altered calcium signalling[165,166]. Currently, no conclusions have been made as to why Ca-P60A needs to be regulated, but perhaps this allows the organism to conserve energy and to survive in higher temperatures. It has also been observed that too much or no SLB leads to arrhythmias and altered calcium transients, and that no SLB (and consequently unregulated Ca-ATPase activity) can be rescued by decreasing Ca-P60A activity[166]. Thus, both players need to be present and functional for proper calcium homeostasis. One potential, speculative application of this is to use gene editing as a method to control insect populations or to impart vulnerable populations more resistant to changing environmental temperatures. Gene editing of insects thus far has mostly been to control populations by altering development and reproductive systems[166]. Additionally, completing and implementing the results of these experiments is challenging as there are not well-defined regulations to using genetically modified insects[107]. Despite that, it is interesting to think of a different application of this system

Chapter 5: Conclusions and future directions

The goal of this thesis was to investigate the effects of various transmembrane regulators of SERCA in an isolated system. To date, MLN, ALN, and the various SLB peptides in the context of sequence variation have not been studied in this system before. The research completed here found that each of these regulators has a unique mode of regulation; MLN lowers the maximal activity, ALN lowers both the maximal activity and apparent calcium affinity, and the SLB peptides are unique amongst themselves (Tables 8 and 9). Specifically, *B. terrestris* SLB and *T. cancriformis* SLB lower the calcium affinity and maximal activity greatly, *D. pulex* SLB lowered the calcium affinity, and *D. melanogaster* SLB did not appear to regulate SERCA (Table 9). Overall, it was found each regulatory peptide has a distinct function and that sequence variation is an important factor in the regulatory effect on SERCA, as shown by the SLB peptides. Also, most of these regulators reconstitute to expected levels, though further optimization could be carried out to improve this process. While some interesting conclusions were drawn from these studies and while some questions were answered, these results ultimately led to many more future questions.

Table 8: Summary of mammalian SERCA regulators

Regulin	Peptide size (KDa)	Tissue Expression	Coexpressed SERCA Isoform	Action on SERCA
PLN	6.1	Cardiac, slow-twitch skeletal muscle	SERCA2a	↓ Ca^{2+} affinity
SLN	3.8	Atria, skeletal muscle	SERCA2a	↓ Ca^{2+} affinity
DWORF	3.8	Atria	SERCA2a	↑ Ca^{2+} affinity
ALN	7.6	Ubiquitous	SERCA2b	↓ Ca^{2+} affinity, V_{max}
ELN	7.0	Endothelial and epithelial tissue	SERCA3	↓ Ca^{2+} affinity
MLN	5.2	Skeletal muscle	SERCA1a	↓ V_{max}

Note: underlined regulators studied in this thesis

Table 9: Summary of invertebrate Ca-ATPase regulators

SLB (insect orthologue)	Peptide size (KDa)	Tissue and isoform coexpression	Action on SERCA
B. terrestris	3.9	Cardiac muscle, Ca-P60A	↓ Ca^{2+} affinity, V_{max}
D. melanogaster	3.3		--
D. pulex	3.8		↓ Ca^{2+} affinity, ↑ V_{max}
T. cancriformis	5.1		↓ Ca^{2+} affinity, V_{max}

Note: underlined regulators studied in this thesis

5.1: Transmembrane peptide regulators at large

SERCA is not the only P-type ATPase that is regulated by transmembrane peptides. Complicating the regulatory system even further, the known SERCA regulators can interact with other peptide regulators. One example of this is HAX1 and PLN, where it is thought that HAX1, a mitochondrial protein with antiapoptotic function, inhibits SERCA alone or through PLN, thus implicating it in calcium cycling[167]. Another example of this is SLN and small ankyrin 1, which have all been shown to interact with SERCA and modulate its activity[168]. Seipin is another small regulator that has been identified recently with a potential role in mediating fat storage through interacting with SERCA[169]. While all these interactions have been identified, a complete map of the relevant complexes and their importance is yet to be determined and remains for future researchers to investigate.

Other P-type ATPases, like Na^+/K^+ ATPase and MgtA, have regulatory subunits as well. Regulators of the Na^+/K^+ ATPase, known as the FXYD family because of an associated motif, act in excitable and osmoregulatory tissues and are highly conserved amongst species[170]. MgtA, a bacterial Mg^{2+} transporter, is regulated by MgtR, which has been shown to limit the expression of MgtA at low Mg^{2+} levels[170]. Ultimately, this field has grown into a very complex network of peptides that act through intracellular ion transport in a variety of cells and tissues in a species-specific manner. It will be exciting to see what the future holds and to continue to map out the complicated web of interactions that control life.

Seeing as there are many different P-type ATPases, it is interesting to think about how many other regulatory peptides or subunits exist to control the transport of ions by this class of biomolecules. What's more, is the identification of other interactors with the SERCA-regulatory peptide pair or with just the regulatory peptide, as with HAX-1. Ultimately, technological advances in bioinformatic screening and the newfound importance of smORFs has opened a vast area of research towards mapping out these interactions, structures, and specific functions.

The research carried out for my thesis began to answer some questions while bringing up new ones, paving the way for future research into SERCA-regulators and potentially, other regulatory peptides discovered through smORFs. Perhaps the system used here could be adapted to study other regulatory peptide/enzyme pairs.

5.2: Tip of the iceberg? Future paths to explore the depth of SERCA regulation

Since the discovery of these regulators, the opportunity and potential to learn about another level of calcium regulation in the body has grown. Branching out from the work done here and from the first studies for these regulators, studies combining co-expressed regulatory peptides with the corresponding isoform of SERCA would be a start and might provide insight into difference between experimental systems. This could be carried out either by proteoliposome reconstitution or co-transfection into mammalian cells. There are limitations to the expression levels of peptides or SERCA that can be achieved in mammalian systems, so some optimization may be required for effective comparison to reconstitution methods. One approach is to add regulatory components that may be present in whole cells (e.g. kinases) that to reconstitute the full regulatory pathway in isolated proteoliposomes. An example of this was mentioned previously and would involve phosphorylating peptides *in vitro*, then reconstituting and measuring activity. Mass spectrometry (MS) can also be used to determine whether or not a protein is phosphorylated and improvements to identification search tools for MS data mean that this may also be an appropriate technique to explore phosphorylation[171].

Mutagenesis studies and perhaps the generation of chimeras will also be key in answering questions about important residues or motifs found in these new regulators. Building from the previous points, phosphomimetic mutants could be generated to study any potential effect of phosphorylation on these peptides. Additionally, alanine-scanning mutagenesis could be done to determine the importance of individual residues in the peptide. Another area yet to

be investigated that would give insight into the important domains for regulation by these peptides is the effect of the transmembrane domains alone. Also, important to note is that this work discussed ALN and MLN, but ELN is yet to be studied in this system. Previous work has shown that ELN lowers maximal activity and calcium affinity of SERCA when co-transfected into mammalian cells[45]. However, as seen with MLN, different methods of studying the effect of these peptides, can lead to different observations as well as the hypothesis that some of these peptides may be further regulated by post-translational modifications (e.g. phosphorylation). Furthermore, reconstitution of the exact SERCA isoform that is co-expressed with a specific peptide would need to be done. Previous work has shown that SERCA1a purified from rabbit tissue is a suitable model for the cardiac isoform of SERCA because it is the most understood isoform and that the sequences between isoforms are nearly identical[18]. However, it is known that different isoforms of SERCA do show variations in their kinetics, thus it would be most suitable to use the appropriate SERCA/regulin pair for activity studies[172,173]. Overall, this has opened a large area to be explored in the context of calcium regulation in tissues.

Another aspect that is yet to be explored in detail is the structure of these peptides alone and in complex with SERCA. The structure of the peptides has been predicted using *in silico* analysis and CD spectroscopy could be done to understand the secondary structure components. However, since these peptides are small, NMR could be used to gain more detailed insight into their structure. This technique has been used previously to determine the structure of PLN in membrane environments, so it is likely that the same or similar approaches could be used for these new regulators[98]. Co-crystallization studies of PLN and SERCA as well as SLN and SERCA have been done and have shed light on the binding site on SERCA[29,129]. Various studies using FRET have also furthered our understanding of the reaction mechanism of SERCA alone and in the context of peptide regulators of SERCA[174]. Since each of these

approaches has been useful in obtaining structural information about PLN and SLN, it is likely that they will be valuable to understand the relationship between the regulins and SERCA.

The exact physiological role or disease-association of most of these peptides also remains elusive. PLN and SLN have been well implicated in heart function and disease and MLN is thought to have a role in muscle performance. ALN and ELN however, do not have specific roles yet. Speculations could be made based on their expression patterns, though *in vivo* knock-out studies would be most useful in determining a physiological role. Additionally, it is known that single-point mutations in PLN can lead to heart disease, so it will be interesting to see if the same relationship will be true with the other regulins. To date, SERCA and its regulators have been mostly studied in the context of cardiac or skeletal muscle, though SERCA has also been implicated in diabetes and cell death and survival. With this, it is possible that the regulators in non-muscle tissue, ALN and ELN, may have a part in calcium regulation in these processes. Moving forward, expression levels of these regulators in humans, both individually and relative to one another, need to be investigated. Future studies into these peptides will certainly elucidate details into the place these peptides have in calcium signalling in non-muscle tissues, deepening our understanding of the metaphorical “tip of the iceberg” of SERCA-regulation.

References

1. Crichton, R. Chapter 11 - Calcium – Cellular Signalling. in *Biological Inorganic Chemistry* (ed. Crichton, R.) 215–228 (Elsevier B.V, 2019). doi:10.1016/B978-0-444-53782-9.00011-5

2. Pchitskaya, E., Popugaeva, E. & Bezprozvanny, I. Calcium signaling and molecular mechanisms underlying neurodegenerative diseases. *Cell Calcium* **70**, 87–94 (2018).

3. Tu Levin Jacqueline B. Hamilton Andrew M. Borodinsky Laura N, M. K. Calcium signaling in skeletal muscle development, maintenance and regeneration. *Cell Calcium* **59**, 91–97 (2016).

4. Rottingen, I. Ruled by waves? Intracellular and intercellular calcium signalling. *Acta Physiologica Scandinavica* **169**, 203–219 (2000).

5. Berridge, M. J., Bootman, M. D. & Roderick, H. L. Calcium signalling: dynamics, homeostasis and remodelling. *Reviews* **4**, 517–529 (2003).

6. Berridge, B. R., Bolon, B. & Herman, E. Chapter 10 - Skeletal Muscle System. in *Fundamentals of Toxicologic Pathology* (eds. Wallig, M. A., Haschek, W. M., Rousseaux, C. G. & Bolon, B.) 195–212 (Elsevier Inc, 2018). doi:10.1016/B978-0-12-8098417.00010-1

7. Berchtold, M. W., Brinkmeier, H. & Müntener, M. Calcium Ion in Skeletal Muscle: Its Crucial Role for Muscle Function, Plasticity, and Disease. *Physiological Reviews* **80**, 1215–1265 (2000).

8. Nabeebaccus, A. & Shah, A. M. Biochemistry and physiology of cardiac muscle. *Medicine* **46**, 431–436 (2018).

9. Medical gallery of Blausen Medical 2014. *WikiJournal of Medicine* **1**, (2014).

10. Creative Commons Legal Code. Available at: https://creativecommons.org/licenses/by/3.0/legalcode. (Accessed: 22nd August 2019)

11. Lee, E. H. Ca2+ channels and skeletal muscle diseases. *Progress in biophysics and molecular biology* **103**, 35–43 (2010).

12. Catterall, W. A. Structure and Regulation of Voltage-gated Ca2+ channels. *Annual Review of Cell and Developmental Biology* **16**, 521–555 (2000).

13. Meissner, G. Ryanodine receptor/Ca2+ release channels and their regulation by endogenous effectors. *Annual Reviews of Physiology* 485–508 (1994).

14. Franzini-Armstrong, C., Protasi, F. & Ramesh, V. Shape, Size, and Distribution of Ca2+ Release Units and Couplons in Skeletal and Cardiac Muscles. *Biophysical Journal* **77**, 1528–1539 (1999).

15. Thogersen, L. & Nissen, P. Flexible P-type ATPases interacting with the membrane. *Current Opinion in Structural Biology* **22**, 491–499 (2012).

16. Periasamy, M. & Kalyanasundaram, A. SERCA pump isoforms: Their role in calcium transport and disease. *Muscle & Nerve* **35**, 430–442 (2007).

17. Palmgren, M. G. & Nissen, P. *P-Type ATPases*. *Methods in Molecular Biology* **1377**, (Springer New York, 2016).

18. Kühlbrandt, W. Biology, structure and mechanism of P-type ATPases. *Nature Reviews Molecular Cell Biology* **5**, 282–295 (2004).

19. Bublitz, M., Poulsen, H., Morth, J. P. & Nissen, P. In and out of the cation pumps: P-Type ATPase structure revisited. *Current Opinion in Structural Biology* **20**, 431–439 (2010).

20. Lahiri, S. D., Zhang, G., Dunaway-Mariano, D. & Allen, K. N. The Pentacovalent Phosphorus Intermediate of a Phosphoryl Transfer Reaction. *Science* **299**, 2067–2071 (2003).

21. Vuister, G. W. *et al.* ATP-induced conformational changes of the nucleotide-binding domain of Na,K-ATPase. *Nature Structural Biology* **10**, 468–474 (2003).

22. Ogawa, H., Nakasako, M., Toyoshima, C. & Nomura, H. Crystal structure of the calcium pump of sarcoplasmic reticulum at 2.6 resolution. *Nature* **405**, 647–655 (2000).

23. Nomura, H. & Toyoshima, C. Structural changes in the calcium pump accompanying the dissociation of calcium. *Nature* **418**, 605–611 (2002).

24. Yu, X., Carroll, S., Rigaud, J. & Inesi, G. H+ countertransport and electrogenicity of the sarcoplasmic reticulum Ca2+ pump in reconstituted proteoliposomes. **64**, 1232–1242 (1993).

25. Apell, H.-J. How do P-Type ATPases transport ions? *Bioelectrochemistry* **63**, 149–156 (2004).

26. Møller, J. v, Olesen, C., Winther, A.-M. L. & Nissen, P. The sarcoplasmic Ca2+-ATPase: design of a perfect chemi-osmotic pump. *Quarterly Reviews of Biophysics* **43**, 501–566 (2010).

27. Xu, C., Rice, W. J., He, W. & Stokes, D. L. A structural model for the catalytic cycle of Ca 2+-ATPase. *Journal of Molecular Biology* **316**, 201–211 (2002).

28. Toyoshima, C. Structural aspects of ion pumping by Ca2+-ATPase of sarcoplasmic reticulum. *Archives of Biochemistry and Biophysics* **476**, 3–11 (2008).

29. Dyla, M. *et al.* Dynamics of P-type ATPase transport cycle revealed by single-molecule FRET. *Nature* **551**, 346–351 (2017).

30. Juette, M. F. *et al.* Single-molecule imaging of non-equilibrium molecular ensembles on the millisecond timescale. *Nature methods* **13**, 341–344 (2016).

31. Brandl, C. J., deLeon, S., Dr, M. & MacLennan, D. H. Adult Forms of the Ca2+ATPase of Sarcoplasmic Reticulum. *The Journal of Biological Chemistry* **262**, 3768–3774 (1987).

32. Zwaal, R. R. *et al.* The Sarco-Endoplasmic Reticulum Ca2+ ATPase Is Required for Development and Muscle Function in Caenorhabditis elegans. *Journal of Biological Chemistry* **276**, 43557–43563 (2001).

33. Sanyal, S., Jennings, T., Dowse, H. & Ramaswami, M. Conditional mutations in SERCA, the Sarco-endoplasmic reticulum Ca2+-ATPase, alter heart rate and rhythmicity in Drosophila. *Journal of Comparative Physiology B* **176**, 253–263 (2006).

34. Lompré AM Levitsky D, A. M. Sarco(endo)plasmic reticulum calcium pumps in the cardiovascular system: function and gene expression. *Journal of Molecular Cell Cardiology* **26**, 1109–1121 (1994).

35. Sumbilla, C. *et al.* Comparison of SERCA1 and SERCA2a expressed in COS-1 cells and cardiac myocytes. *American journal of physiology. Heart and circulatory physiology* **277**, H2381 (1999).

36. Verboomen, H., Wuytack, F., van den Bosch, L., Mertens, L. & Casteels, R. The functional importance of the extreme C-terminal tail in the gene 2 organellar Ca2+-transport ATPase (SERCA2a/b). *Biochemical Journal* **303**, 979–984 (1994).

37. Verboomen, H., Wuytack, F., de Smedt, H., Himpens, B. & Casteel, R. Functional difference between SERCA2a and SERCA2b: Ca2+ pumps and their modulation by phospholamban. *Biochemical Journal* **286**, 591–596 (1992).

38. Bobe, R. *et al.* Identification, Expression, Function, and Localization of a Novel (Sixth) Isoform of the Human Sarco/Endoplasmic Reticulum Ca2+ATPase 3 Gene. *Journal of Biological Chemistry* **279**, 24297–24306 (2004).

39. Zhao, Y. *et al.* Functional analysis of SERCA1b, a highly expressed SERCA1 variant in myotonic dystrophy type 1 muscle. *Biochimica et biophysica acta* **1852**, 2042–2047 (2015).

40. Agrawal, A., Suryakumar, G. & Rathor, R. Role of defective Ca2+ signaling in skeletal muscle weakness: Pharmacological implications. *Journal of Cell Communication and Signaling* **12**, 645–659 (2018).

41. Allen DG Yeung EW Whitehead NP, G. O. L. Calcium and the damage pathways in muscular dystrophy. *Canadian Journal of Physiology and Pharmacology* **88**, 83–91 (2010).

42. V, G. & NC, V. Fourty-Four Years of Brody Disease: It is Time to Review. *Journal of Genetic Syndromes & Gene Therapy* **4**, (2013).

43. Odermatt, A. *et al.* Mutations in the gene–encoding SERCA1, the fast–twitch skeletal muscle sarcoplasmic reticulum Ca2+ ATPase, are associated with Brody disease. *Nature genetics* **14**, 191–194 (1996).

44. Treves, S., Jungbluth, H., Voermans, N., Muntoni, F. & Zorzato, F. Ca2+ handling abnormalities in early-onset muscle diseases: Novel concepts and perspectives. *Seminars in Cell and Developmental Biology* **64**, 201–212 (2017).

45. Wuytack, F., Raeymaekers, L. & Missiaen, L. Molecular physiology of the SERCA and SPCA pumps. *Cell Calcium* **32**, 279–305 (2002).

46. Zádor Vangheluwe Peter Wuytack Frank, E. The expression of the neonatal sarcoplasmic reticulum Ca2+ pump (SERCA1b) hints to a role in muscle growth and development. *Cell Calcium* **41**, 379–388 (2006).

47. Pan, Y. *et al.* Targeted Disruption of the ATP2A1 Gene Encoding the Sarco(endo)plasmic Reticulum Ca2+ ATPase Isoform 1 (SERCA1) Impairs Diaphragm Function and Is Lethal in Neonatal Mice. *Journal of Biological Chemistry* **278**, 13367–13375 (2003).

48. Shareef, M. A., Anwer, L. A. & Poizat, C. Cardiac SERCA2A/B: Therapeutic targets for heart failure. *European Journal of Pharmacology* **724**, 1–8 (2014).

49. Periasamy, M. *et al.* Impaired Cardiac Performance in Heterozygous Mice with a Null Mutation in the Sarco(endo)plasmic Reticulum Ca2+-ATPase Isoform 2 (SERCA2) Gene. *Journal of Biological Chemistry* **274**, 2556–2562 (1999).

50. Redondo, P. C., Salido, G. M., Pariente, J. A., Sage, S. O. & Rosado, J. A. SERCA2b and 3 play a regulatory role in store-operated calcium entry in human platelets. *Cellular Signalling* **20**, 337–346 (2008).

51. Tuusa, J. T., Markkanen, P. M. H., Apaja, P. M., Hakalahti, A. E. & Petäjä-Repo, U. E. The Endoplasmic Reticulum Ca2+-pump SERCA2b Interacts with G Protein-coupled Receptors and Enhances their Expression at the Cell Surface. *Journal of molecular biology* **371**, 622–638 (2007).

52. Wang, L. *et al.* High expression of sarcoplasmic/endoplasmic reticulum Ca2 +-ATPase 2b blocks cell differentiation in human liposarcoma cells. *Life sciences* **99**, 37–43 (2014).

53. Llewelyn Roderick, H., Lechleiter, J. D. & Camacho, P. Cytosolic Phosphorylation of Calnexin Controls Intracellular Ca2+ Oscillations via an Interaction with Serca2b. **149**, (2000).

54. Savignac, M., Edir, A., Simon, M. & Hovnanian, A. Darier disease : A disease model of impaired calcium homeostasis in the skin. *Biochimica et biophysica acta* **1813**, 1111–1117 (2014).

55. Sakuntabhai, A. *et al.* Mutations in ATP2A2, encoding a Ca2+ pump, cause Darier disease. *Nature genetics* **21**, 271–277 (1999).

56. Munro, C. S. The phenotype of Darier's disease: penetrance and expressivity in adults and children. *The British journal of dermatology* **127**, 126–130 (1992).

57. Tavadia, S., Tait, R. C., McDonagh, T. A. & Munro, C. S. Platelet and cardiac function in Darier's disease. *Clinical & Experimental Dermatology* **26**, 696–699 (2001).

58. Chemaly, E. R., Troncone, L. & Lebeche, D. SERCA control of cell death and survival. *Cell Calcium* **69**, 46–61 (2018).

59. Liu, L. H. *et al.* Defective Endothelium-dependent Relaxation of Vascular Smooth Muscle and Endothelial Cell Ca 2+ Signaling in Mice Lacking Sarco(endo)plasmic Reticulum Ca 2+ -ATPase Isoform 3. *Journal of Biological Chemistry* **272**, 30538–30545 (1997).

60. Arredouani, A. *et al.* SERCA3 Ablation Does Not Impair Insulin Secretion but Suggests Distinct Roles of Different Sarcoendoplasmic Reticulum Ca2+ Pumps for Ca2+ Homeostasis in Pancreatic -cells. *Diabetes* **51**, 3245–3253 (2002).

61. Mountian, I. *et al.* Expression patterns of sarco/endoplasmic reticulum Ca2+-ATPase and inositol 1,4,5-trisphosphate receptor isoforms in vascular endothelial cells. *Cell Calcium* **25**, 371 (1999).

62. Gilon, P., Chae, H.-Y., Rutter, G. A. & Ravier, M. A. Calcium signaling in pancreatic β-cells in health and in Type 2 diabetes. *Cell calcium* **56**, 340–361 (2014).

63. Tengholm, A., Hellman, B. & Gylfe, E. Glucose regulation of free Ca(2+) in the endoplasmic reticulum of mouse pancreatic beta cells. *The Journal of biological chemistry* **274**, 36883–36890 (1999).

64. Varadi, A., Molnar, E., Ostenson, C. & Ashcroft, S. J. H. Isoforms of endoplasmic reticulum Ca2+-ATPase are differentially expressed in normal and diabetic islets of Langerhans. *Biochemical Journal* **319**, 521–527 (1996).

65. Zarain-Herzberg Gerardo Estrada-Avilés Rafael, A. G.-R. & Zarain-Herzberg Gerardo|Estrada-Avilés Rafael, A.-R. Regulation of SERCA pumps expression in diabetes. *Cell Calcium* **56**, 302–310 (2014).

66. Eshima, H., Poole, D. C. & Kano, Y. In vivo calcium regulation in diabetic skeletal muscle. *Cell Calcium* **56**, 381–389 (2014).

67. Kranias, E. G. & Hajjar, R. J. The Phospholamban Journey 4 Decades after Setting Out for Ithaka. *Circulation Research* **120**, 781–783 (2017).

68. Kirchberber, M. A., Tada, M. & Katz, A. M. Phospholamban: a regulatory protein of the cardiac sarcoplasmic reticulum. *Recent advances in studies on cardiac structure and metabolism* **5**, 103–115 (1975).

69. Simmerman, H. K. B. & Jones, L. R. *Phospholamban: Protein Structure, Mechanism of Action, and Role in Cardiac Function*. *PHYSIOLOGICAL REVIEWS* **78**, (1998).

70. Chen, Z., Akin, B. L. & Jones, L. R. Mechanism of Reversal of Phospholamban Inhibition of the Cardiac Ca2+-ATPase by Protein Kinase A and by Anti-phospholamban Monoclonal Antibody 2D12. *J Biol Chem* **282**, 20968–20976 (2007).

71. Wegener, A. D., Simmerman, H. K. B., Lindemann, J. P. & Jones, L. R. Phospholamban Phosphorylation in Intact Ventricles: functional comparisons between isoforms of the sarcoplasmic or endoplasmic reticulum family of calcium pumps. *J Biol Chem* **264**, 11468–11474 (1988).

72. Simmerman, H. K. B., Collins, J. H., Theiberts, J. L., Wegeners, A. D. & Jonesst, L. R. Sequence Analysis of Phospholamban: identification of phosphorylation sites and two major structural domains. *The Journal of Biological Chemistry* **261**, 1386

73. Engelhardt, S. b-Adrenergic Receptors in Heart Failure. *Heart Failure Clin* **1**, 183–191 (2005).

74. Luo, W. *et al.* Targeted ablation of the phospholamban gene is associated with markedly enhanced myocardial contractility and loss of β-agonist stimulation. *Circulation Research* **75**, 401–409 (1994).

75. Epstein, F. H. & Morgan, J. P. Abnormal intracellular modulation of calcium as a major cause of cardiac contractile dysfunction. *New England Journal of Medicine* **325**, 625–632 (1991).

76. Young, H. S., Ceholski, D. K. & Trieber, C. A. Deception in simplicity: Hereditary phospholamban mutations in dilated cardiomyopathy. *Biochemistry and Cell Biology* **93**, 1–7 (2015).

77. Haghighi, K. *et al.* A mutation in the human phospholamban gene, deleting arginine 14, results in lethal, hereditary cardiomyopathy. *Proceedings of the National Academy of Sciences of the United States of America* **103**, 1388–1393 (2006).

78. Medeiros, A. *et al.* Genetics Mutations in the human phospholamban gene in patients with heart failure. (2011). doi:10.1016/j.ahj.2011.07.028

79. Smith, S. O., Kawakami, T., Liu, W., Ziliox, M. & Aimoto, S. Helical structure of phospholamban in membrane bilayers. *Journal of Molecular Biology* **313**, 1139–1148 (2001).

80. Simmerman, H. K. B., Eugene Lovelace, D. & Jones, L. R. Secondary structure of detergent-solubilized phospholamban, a phosphorylatable, oligomeric protein of cardiac sarcoplasmic reticulum. *Biochimica et Biophysica Acta (BBA)/Protein Structure and Molecular* **997**, 322–329 (1989).

81. Gorski, P. A., Ceholski, D. K. & Young, H. S. Structure-function relationship of the serca pump and its regulation by phospholamban and sarcolipin. in *Advances in Experimental Medicine and Biology* **981**, 77–119 (Springer New York LLC, 2017).

82. Wawrzynow, A. *et al.* Sarcolipin, the “proteolipid” of skeletal muscle sarcoplasmic reticulum, is a unique, amphipathic, 31-residue peptide. *Archives of Biochemistry and Biophysics* **298**, 620–623 (1992).

83. Odermatt, A. *et al.* Sarcolipin regulates the activity of SERCA1, the fast-twitch skeletal muscle sarcoplasmic reticulum Ca2+-ATPase. *The Journal of Biological Chemistry* **273**, 12360–12369 (1998).

84. Asahi, M. *et al.* Cardiac-specific overexpression of sarcolipin inhibits sarco(endo)plasmic reticulum Ca2+ ATPase (SERCA2a) activity and impairs cardiac function in mice. *Proceedings of the National Academy of Sciences of the United States of America* **101**, 9199–9204 (2004).

85. Bhupathy Gopal J.|Periasamy Muthu, P. Sarcolipin and phospholamban as regulators of cardiac sarcoplasmic reticulum Ca2+ ATPase. *Journal of Molecular and Cellular Cardiology* **42**, 903–911 (2007).

86. Xie, L.-H. *et al.* Ablation of sarcolipin results in atrial remodeling. *American Journal of Physiology - Cell Physiology* **302**, C1762–C1771 (2012).

87. Babu, G. J. *et al.* Ablation of sarcolipin enhances sarcoplasmic reticulum calcium transport and atrial contractility. *Proceedings of the National Academy of Sciences* **104**, 17867–17872 (2007).

88. Maurya, S. K. & Periasamy, M. Sarcolipin is a novel regulator of muscle metabolism and obesity. *Pharmacol Res* **102**, 270–275 (2015).

89. Bal, N. C. *et al.* Sarcolipin is a newly identified regulator of muscle-based thermogenesis in mammals. *Nat Med* **18**, 1575–1579 (2012).

90. Maurya, S. K. *et al.* Sarcolipin Signaling Promotes Mitochondrial Biogenesis and Oxidative Metabolism in Skeletal Muscle. *Cell Rep* **24**, 2919–2931 (2018).

91. Asahi, M. *et al.* Cardiac-specific overexpression of sarcolipin inhibits sarco(endo)plasmic reticulum Ca2+ ATPase (SERCA2a) activity and impairs cardiac function in mice. *Proceedings of the National Academy of Sciences of the United States of America* **101**, 9199–9204 (2004).

92. Mall, S. *et al.* The presence of sarcolipin results in increased heat production by Ca 2+-ATPase. *Journal of Biological Chemistry* **281**, 36597–36602 (2006).

93. Smith, W. S., Broadbridge Robert, East, J. M. & Lee, A. G. Sarcolipin uncouples hydrolysis of ATP from accumulation of Ca2+ by the Ca2+-ATPase of skeletal-muscle sarcoplasmic reticulum. *Biochemical Journal* **361**, 277–286 (2002).

94. Sahoo, S. K., Shaikh, S. A., Sopariwala, D. H., Bal, N. C. & Periasamy, M. Sarcolipin Protein Interaction with Sarco(endo)plasmic Reticulum Ca2+ATPase (SERCA) Is Distinct from Phospholamban Protein, and Only Sarcolipin Can Promote Uncoupling of the SERCA Pump. *The Journal of biological chemistry* **288**, 6881–6889 (2013).

95. Toyoshima, C. *et al.* Modeling of the inhibitory interaction of phospholamban with the Ca2 ATPase. *Proc Natl Acad Sci U.S.A.* **100**, 467–472 (2003).

96. Pant, M., Bal, N. C. & Periasamy, M. Sarcolipin: A Key Thermogenic and Metabolic Regulator in Skeletal Muscle. *Trends Endocrinol Metab* **27**, 881–892 (2016).

97. Gorski, P. A., Glaves, J. P., Vangheluwe, P. & Young, H. S. Sarco(endo)plasmic Reticulum Calcium ATPase (SERCA) Inhibition by Sarcolipin Is Encoded in Its Luminal Tail. *J Biol Chem* **288**, 8456–8467 (2013).

98. Toyoshima, C. *et al.* Crystal structures of the calcium pump and sarcolipin in the Mg2+-bound E1 state. *Nature* **495**, 260–264 (2013).

99. Saghatelian, A. & Couso, J. P. Discovery and Characterization of smORF-Encoded Bioactive Polypeptides. *Nature chemical biology* **11**, 909–916 (2015).

100. Oehler, D. & Haas, J. Hide and Seek: Protein-coding Sequences Inside “Non-coding” RNAs. *Genomics, Proteomics and Bioinformatics* **14**, 179–180 (2016).

101. Magny, E. G. *et al.* Conserved Regulation of Cardiac Calcium Uptake by Peptides Encoded in Small Open Reading Frames. *Science* **341**, 1116–1120 (2013).

102. Chorna, T. & Hasan, G. The genetics of calcium signaling in Drosophila melanogaster. *BBA-Gen Subjects* **1820**, 1269–1282 (2012).

103. Nelson, B. R. *et al.* A peptide encoded by a transcript annotated as long noncoding RNA enhances SERCA activity in muscle. *Science* **351**, 271–275 (2016).

104. Anderson, D. M. *et al.* A Micropeptide Encoded by a Putative Long Noncoding RNA Regulates Muscle Performance. *Cell* **160**, 595–606 (2015).

105. Moller, S., Croning, M. D. R. & Apweiler, R. Evaluation of methods for the prediction of membrane spanning regions. *Bioinformatics* **17**, 646–653 (2001).

106. Madeira, F. *et al.* The EMBL-EBI search and sequence analysis tools APIs in 2019. *Nucleic acids res* **47**, W636–W641 (2019).

107. Anderson, D. M. *et al.* Widespread control of calcium signaling by a family of SERCA-inhibiting micropeptides. *Science signaling* **9**, ra119 (2016).

108. Stokes, D. L. & Green, N. M. Three-dimensional crystals of CaATPase from sarcoplasmic reticulum. Symmetry and molecular packing. *Biophysical Journal* **57**, 1–14 (1990).

109. Douglas, J. L., Trieber, C. A., Afara, M. & Young, H. S. Rapid, high-yield expression and purifcation of Ca2+-ATPase regulatory proteins for high-resolution structural studies. **40**, 118–125 (2005).

110. Young, H. S., Reddy, L. G., Jones, L. R. & Stokes, D. L. Co-reconstitution and Co-crystallization of Phospholamban and Ca2+-ATPase. 103–115 (1998).

111. Trieber, C. A., Afara, M. & Young, H. S. Effects of Phospholamban Transmembrane Mutants on the Calcium Affinity, Maximal Activity, and Cooperativity of the Sarcoplasmic Reticulum Calcium Pump. *Biochemistry* **48**, 9287–9296 (2009).

112. Whitmore, L. & Wallace, B. A. DICHROWEB, an online server for protein secondary structure analyses from circular dichroism spectroscopic data. *Nucleic Acids Research* **32**, W66–W673 (2004).

113. Whitmore, L. & Wallace, B. A. Protein secondary structure analyses from circular dichroism spectroscopy: Methods and reference databases. *Biopolymers* **89**, 392–400 (2008).

114. Andrade, M. A., Chacón, P., Merelo, J. J. & Morán, F. Evaluation of secondary structure of proteins from UV circular dichroism spectra using an unsupervised learning neural network. **6**, 383–390 (1993).

115. Miles, A. J. & Wallace, B. A. Circular dichroism spectroscopy of membrane proteins. *Chemical Society reviews* **45**, 4859–4872 (2016).

116. Tonkin, J. & Rosenthal, N. One Small Step for Muscle: A New Micropeptide Regulates Performance. *Cell Metabolism* **21**, 515–516 (2015).

117. Goonasekera, S. A. *et al.* Mitigation of muscular dystrophy in mice by SERCA overexpression in skeletal muscle. *The Journal of clinical investigation* **121**, 1044–1052 (2011).

118. Karpati, G., Charuk, J., Carpenter, S., Jablecki, C. & Holland, P. Myopathy caused by a deficiency of Ca2+-adenosine triphosphatase in sarcoplasmic reticulum (Brody's disease). *Annals of neurologyeurology* **20**, 38–49 (1986).

119. Tapscott, S. J. The circuitry of a master switch: Myod and the regulation of skeletal muscle gene transcription. *Development* **132**, 2685–2695 (2005).

120. Fong, A. P. *et al.* Genetic and Epigenetic Determinants of Neurogenesis and Myogenesis. *Developmental Cell* **22**, 721–735 (2012).

121. Pon, J. R. & Marra, M. A. MEF2 transcription factors: developmental regulators and emerging cancer genes. *Oncotarget* **7**, 2297–2312 (2016).

122. Vandecaetsbeek, I., Vangheluwe, P., Raeymaekers, L., Wuytack, F. & Vanoevelen, J. The Ca2+ Pumps of the Endoplasmic Reticulum and Golgi Apparatus. **3**, a004184 (2011).

123. Clausen, J. D., Vandecaetsbeek, I., Wuytack, F., Vangheluwe, P. & Andersen, J. P. Distinct Roles of the C-terminal 11th Transmembrane Helix and Luminal Extension in the Partial Reactions Determining the High Ca2+Affinity of Sarco(endo)plasmic Reticulum Ca2+-ATPase Isoform 2b (SERCA2b). *J Biol Chem* **287**, 39460–39469 (2012).

124. Lindemann, J. P., Jones, L. R., Hathaway, D. R., Henry, B. G. & Watanabe, A. M. Beta-Adrenergic Stimulation of Phospholamban Phosphorylation and Ca2+-ATPase Activity in Guinea pig Ventricles. **258**, 464–471 (1982).

125. Skrzypek, R., Iqbal, S. & Callaghan, R. Methods of reconstitution to investigate membrane protein function. *Methods* **147**, 126–141 (2018).

126. Seddon, A. M., Curnow, P. & Booth, P. J. Membrane proteins, lipids and detergents: not just a soap opera. *BBA - Biomembranes* **1666**, 105–117 (2004).

127. Hou, Z. & Robia, S. L. Relative Affinity of Calcium Pump Isoforms for Phospholamban Quantified by Fluorescence Resonance Energy Transfer. *J Mol Biol* **402**, 210–216 (2010).

128. Pallikkuth, S. *et al.* Phosphorylated Phospholamban Stabilizes a Compact Conformation of the Cardiac Calcium-ATPase. *Biophys J* **105**, 1812–1821 (2013).

129. Dong, X. & Thomas, D. D. Time-resolved FRET reveals the structural mechanism of SERCA–PLB regulation. *Biochem Biophys Res Com* **449**, 196–201 (2014).

130. Singh, D. R. *et al.* Oligomerization of Micropeptides that Regulate SERCA. in *Biophysical Journal* **116**, 30a–31a (Elsevier BV, 2019).

131. Seidel SA Lea WA van den Boggart G Jerabek-Willemsen M Lazic A Joseph JS Srinivasan P Baaske P Simeonov A Katritch I Melo FA Ladbury JE Schreiber G Watts A Braun D Duhr S, D. P. M. Microscale thermophoresis quantifies biomolecular interactions under previously challenging conditions. *Methods* **59**, 301–315 (2013).

132. Seidel, S. A. I. *et al.* Label-Free Microscale Thermophoresis Discriminates Sites and Affinity of Protein–Ligand Binding. *Angew Chem* **51**, 10656–10659 (2012).

133. Fiol, C. J., Mahrenholz, A. M., Wangg, Y., Roeske, R. W. & Roach, P. J. Formation of Protein Kinase Recognition Sites by Covalent Modification of the Substrate. *J Biol Chem* **262**, (1987).

134. Glaves, J. P., Trieber, C. A., Ceholski, D. K., Stokes, D. L. & Young, H. S. Phosphorylation and mutation of phospholamban alter physical interactions with the sarcoplasmic reticulum calcium pump. *Journal of molecular biology* **405**, 707–723 (2011).

135. James, P., Inui, M., Tada, M., Chiesit, M. & Carafoli, E. Nature and site of phospholamban regulation of the Ca2+ pump of sarcoplasmic reticulum. *Nature* **342**, 90–92 (1989).

136. Guerra, B. & Issinger, O. G. Protein kinase CK2 and its role in cellular proliferation, development and pathology. *Electrophoresis* **20**, 391–408 (1999).

137. Meggio, F. & Pinna, L. A. One-thousand-and-one substrates of protein kinase CK2? *FASEB J* **17**, 349–368 (2003).

138. Patel, P. & Woodgett, J. R. *Chapter 8: Glycogen Synthase Kinase 3: A Kinase for All Pathways? Current Topics in Developmental Biology* **123**, (Elsevier, 2017).

139. Theeuwes, W. F. *et al.* Inactivation of glycogen synthase kinase-3β (GSK-3β) enhances skeletal muscle oxidative metabolism. *BBA - Molecular Basis of Disease* **1863**, 3075–3086 (2017).

140. Marin, T. L. *et al.* Identification of AMP-activated protein kinase targets by a consensus sequence search of the proteome. *BMC Syst Biol* **9**, 13 (2015).

141. Turnham, R. E. & Scott, J. D. Protein kinase A catalytic subunit isoform PRKACA: History, function and physiology. *Gene* **577**, 101–108 (2016).

142. Carling, D., Mayer, F. v, Sanders, M. J. & Gamblin, S. J. AMP-activated protein kinase: nature's energy sensor. *Nat Chem Biol* **7**, 512–518 (2011).

143. Kaufmann, H., Bailey, J. E. & Fussenegger, M. Use of antibodies for detection of phosphorylated proteins separated by two-dimensional gel electrophoresis. *Proteomics* **1**, 194–9 (2001).

144. Tupling AR Gupta SC Hussain D Vigna C Bloemberg D Quadrilatero J Trivieri MG Babu GJ Backx PH Periasamy M MacLennan DH Gramolini AO, B. E. Enhanced [Ca2+] transport and muscle relaxation in skeletal muscle from sarcolipin-null mice. *Am J Physiol* **301**, C841 (2011).

145. Pueyo, J. I., Magny, E. G. & Couso, J. P. New Peptides Under the s(ORF)ace of the Genome. *Trends Biochem Sci* **41**, 665–678 (2016).

146. Ladoukakis, E., Pereira, V., Magny, E. G., Eyre-Walker, A. & Couso, J. P. Hundreds of putatively functional small open reading frames in Drosophila. *Genome Biol* **12**, R118 (2011).

147. Basrai, M. A., Hieter, P. & Boeke, J. D. Small Open Reading Frames: Beautiful Needles in the Haystack. *Genome Res* **7**, 768–771 (1997).

148. Galindo, M. I., Pueyo, J. I., Fouix, S., Bishop, S. A. & Couso, J. P. Peptides Encoded by Short ORFs Control Development and Define a New Eukaryotic Gene Family. *PLOS Biol* **5**, 1052–1062 (2007).

149. Kessler, M. M. *et al.* Systematic Discovery of New Genes in the Saccharomyces cerevisiae Genome. *Genome Res* **13**, 264–271 (2003).

150. Kastenmayer, J. P. *et al.* Functional genomics of genes with small open reading frames (sORFs) in S. cerevisiae. *Genome Res* **16**, 365–373 (2006).

151. Mackowiak, S. D. *et al.* Extensive identification and analysis of conserved small ORFs in animals. *Genome Biol* **16**, 179 (2015).

152. Koss, K. L. & Kranias, E. G. Phospholamban: A Prominent Regulator of Myocardial Contractility. *Circulation research* **79**, 1059–1063 (1996).

153. Magya, A. & Varadi, A. Molecular cloning and chromosomal localization of a sarco/endoplasmic reticulum Ca2+ ATPase of Drosophila melanogaster. **173**, 872–877 (1990).

154. Valberg, S. J. *et al.* Coding sequences of sarcoplasmic reticulum calcium ATPase regulatory peptides and expression of calcium regulatory genes in recurrent exertional rhabdomyolysis. *Journal of Veterinary Internal Medicine* **33**, 933–941 (2019).

155. Magyar, A., Bakos, E. & Váradi, A. Structure and tissue-specific expression of the Drosophila melanogaster organellar-type Ca(2+)-ATPase gene. *Biochem J* **310**, 757–763 (1995).

156. Vazquez-Martinez, O., Canedo-Merino, R., Diaz-Munoz, M. & Riesgo-Escovar, J. R. Biochemical characterization, distribution and phylogenetic analysis of Drosophila melanogaster ryanodine and IP3 receptors, and thapsigargin-sensitive Ca2+ ATPase. *J Cell Sci* **116**, 2483–2494 (2003).

157. Periz, G. & Fortini, M. E. Ca(2+)-ATPase function is required for intracellular trafficking of the Notch receptor in Drosophila. *EMBO J* **18**, 5983–5993 (1999).

158. Hellstern, S. *et al.* Sarcolipin, the Shorter Homologue of Phospholamban, Forms Oligomeric Structures in Detergent Micelles and in Liposomes. *Journal of Biological Chemistry* **276**, 30845–30852 (2001).

159. Liu, G.-S. *et al.* A novel human R25C-phospholamban mutation is associated with super-inhibition of calcium cycling and ventricular arrhythmia. *Cardiovasc Res* **107**, 164–174 (2015).

160. Ceholski, D. K., Trieber, C. A. & Young, H. S. Hydrophobic Imbalance in the Cytoplasmic Domain of Phospholamban Is a Determinant for Lethal Dilated Cardiomyopathy. *J Biol Chem* **287**, 16521–16529 (2012).

161. Greenberg, B. *et al.* Calcium upregulation by percutaneous administration of gene therapy in patients with cardiac disease (CUPID 2): a randomised, multinational, double-blind, placebo-controlled, phase 2b trial. *Lancet (London, England)* **387**, 1178–1186 (2016).

162. Ylä-Herttuala, S., Bhardwaj, S. & Roy, H. Cardiovascular Gene Therapy: past, present, and future. *Mol Ther* **25**, 780–792 (2017).

163. AAV1-CMV-SERCA2a Gene Therapy Trial in Heart Failure. **2019**, (2017).

164. Investigation of the Safety and Feasibility of AAV1/SERCA2a Gene Transfer in Patients With Chronic Heart Failure. **2019**, (2016).

165. Reid, W. & O'Brochta, D. A. Applications of genome editing in insects. *Curr Opin Insect Sci* **13**, 43 (2016).

166. Gantz, V. & Akbari, O. Gene editing technologies and applications for insects. *Current Opin Insect Sci* **28**, 66–72 (2018).

167. Desmond, P. F. *et al.* Interactions between small ankyrin 1 and sarcolipin coordinately regulate activity of the sarco(endo)plasmic reticulum Ca2+-ATPase (SERCA1). *Journal of Biological Chemistry* **292**, 10961–10972 (2017).

168. Bi, J. *et al.* Seipin promotes adipose tissue fat storage through the ER Ca 2+-ATPase SERCA. *Cell Metabolism* **19**, 861–871 (2014).

169. Pirkmajer, S. *et al.* Early vertebrate origin and diversification of small transmembrane regulators of cellular ion transport. *The Journal of Physiology* **595**, 4611–4630 (2017).

170. Choi, E., Lee, K. Y. & Shin, D. The MgtR regulatory peptide negatively controls expression of the MgtA Mg 2+ transporter in Salmonella enterica serovar Typhimurium. *Biochemical and Biophysical Research Communications* **417**, 318–323 (2012).

171. Zhang, M. *et al.* PhoPepMass: A database and search tool assisting human phosphorylation peptide identification from mass spectrometry data. *Journal of Genetics and Genomics* **45**, 381–388 (2018).

172. Zamoon, J., Mascioni, A., Thomas, D. D. & Veglia, G. NMR solution structure and topological orientation of monomeric phospholamban in dodecylphosphocholine micelles. *Biophysical Journal* **85**, 2589–2598 (2003).

173. Gustavsson, M., Traaseth, N. J. & Veglia, G. Probing ground and excited states of phospholamban in model and native lipid membranes by magic angle spinning NMR spectroscopy. *Biochimica et Biophysica Acta - Biomembranes* **1818**, 146–153 (2012).

174. Larsen, E. K. *et al.* Intrinsically disordered HAX-1 regulates Ca2+ cycling by interacting with lipid membranes and the phospholamban cytoplasmic region. *Biochimica et Biophysica Acta (BBA) - Biomembranes* 183034 (2019). doi:10.1016/j.bbamem.2019.183034

Appendix

Information on proline mutations made to phospholamban and sarcolipin

In this appendix, information regarding some preliminary experiments is presented. In these experiments, the effect on SERCA activity was compared when an essential asparagine residue in phospholamban and sarcolipin was mutated to a proline, mirroring the proline present in SERCA's activator, DWORF. Some changes to the methodology as described in the main text were made and are described below.

Instead of LB media M9 minimal media was used and cultures were left for 40 hours after induction rather than 24 hours.

Instead of guanidine hydrochloride extraction to remove MBP, organic extraction was used. For extraction by chloroform-isopropanol, cleaved peptide was diluted to 5 mg/mL, mixed with 60% TCA to precipitate all the protein present, and incubated on ice for 30 minutes. Precipitated protein was isolated by centrifugation in a clinical centrifuge for 1 hour. The pellet containing precipitated protein was washed with water three times, then covered with a layer of water and incubated on ice for 10 minutes. Following this, a mixture of 1 part chloroform, to 1 part isopropanol, to 0.5 parts water was added to the pellet. The pellet was resuspended and broken into smaller pieces and transferred to a Dounce homogenizer. The mixture was homogenized once and then incubated on ice for 1 hour. Homogenization was then carried out until almost all the pellet was homogeneous in solution. The mixture was then separated into equal volumes in 6 test tubes, 1.6 mL of water was added to each tube, and tubes were left to incubate overnight at room temperature. The following day, the chloroform-isopropanol layer was transferred to new tubes and more water was added as before. Once the layers separated, the organic layer was transferred to a round-bottom flask and the solvent was evaporated using

a rotary evaporator. The remaining thin film was solubilized in 7 M guanidine hydrochloride and was ready for further refinement and purification using HPLC.

Another point to mention is that single amino acid mutations to PLN and SLN can lead to a loss of inhibition of SERCA. The reasoning behind this came from a sequence alignment between the mammalian peptides including the first endogenous activator of SERCA, DWORF (Figure)[79]. DWORF contains a proline in the same position that PLN and SLN contain an essential asparagine. When this residue in PLN and SLN is mutated to a proline, all or some of the inhibitory function of these peptides is lost. However, PLN and SLN are not turned into activators (like DWORF) and SLN still inhibits SERCA to some extent since SLN's C-terminal tail plays a main role in its inhibitory function (Figures S1-S3, Table S1). This could be because SLN's C-terminal tail has been implicated as essential to its inhibitory function[156,157]. While my experiments are preliminary, they support the notion that a single amino acid change can make a dramatic difference and that peptide regulators could be tailored and utilized in gene editing approaches.

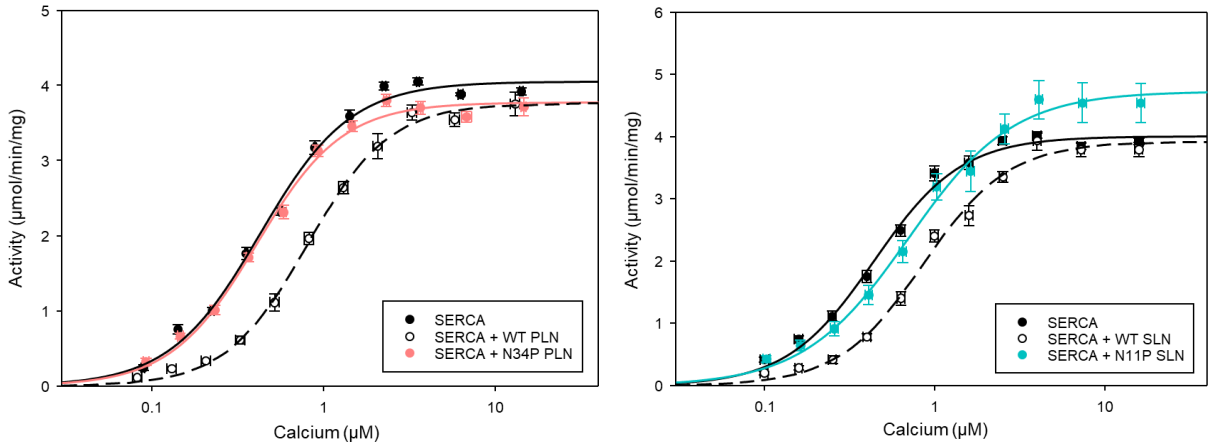

Figure S1: ATPase assay measurements of SERCA reconstituted with wild-type (WT) peptides and peptides with proline mutations. Each peptide was reconstituted with SERCA at a ratio of 1 SERCA: 5 peptide. (A) Measurements for SERCA reconstituted alone (black circles), with WT PLN (clear circles), or with N34P PLN (orange circles). N values (separate reconstitutions) and n values (individual assays) are N=4, n=17 for WT PLN and N34P PLN. (B) Measurements for SERCA reconstituted alone (black circles), with WT SLN (clear circles), or with N11P SLN (teal circles). For these conditions, N=3, n=19 for WT SLN and N11P SLN.

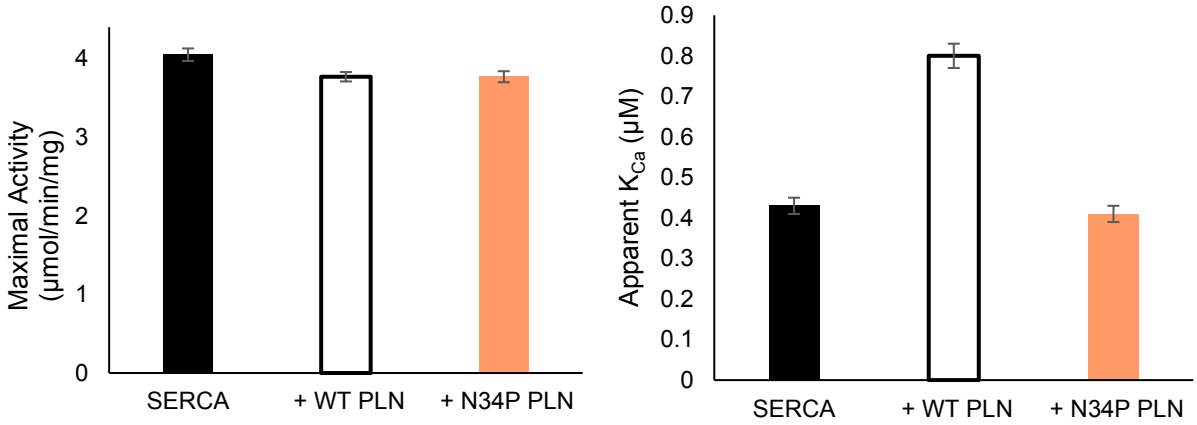

Figure S2: Maximal activity and apparent K_{Ca} values for SERCA reconstituted alone (black), with WT PLN (black outline), or with N34P PLN (orange). (A) Maximal activity values. There is a slight decrease in SERCA's maximal activity when it is reconstituted with WT PLN or N34P PLN, though it is not significant. (B) Apparent K_{Ca} values. An increase in K_{Ca} is seen when SERCA is reconstituted with WT PLN, corresponding to a decrease in calcium affinity. This change in K_{Ca} is not seen when SERCA is reconstituted with N34P PLN.

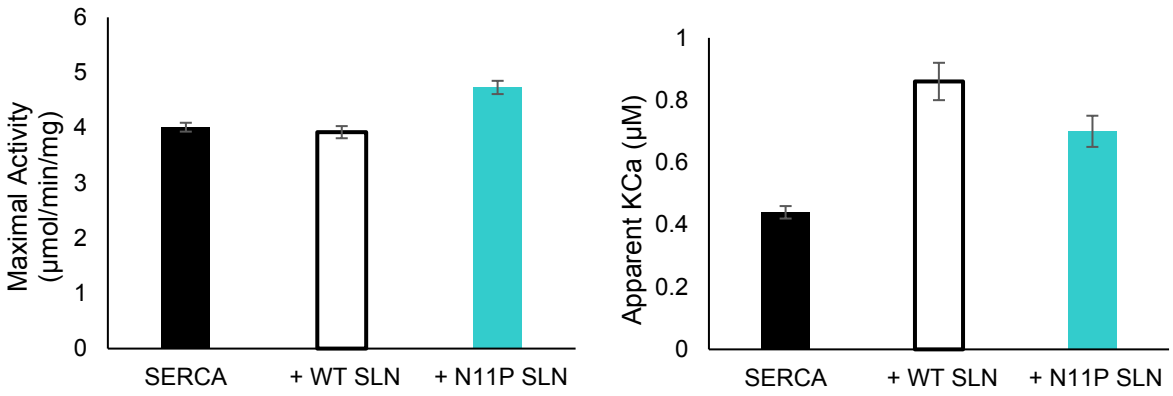

Figure S3: Maximal activity and apparent K_{Ca} values for SERCA reconstituted alone (black), with WT SLN (black outline), or with N11P SLN (teal). (A) Maximal activity values. No change is seen when reconstituted with WT SLN and an increase is seen when reconstituted with N11P SLN. (B) Apparent calcium affinity values. An increase in K_{Ca} is seen when reconstituted with WT SLN, indicating a decrease in calcium affinity of SERCA. An increase is also seen when reconstituted with N11P SLN, though not as dramatic as with WT.

Table S1: Kinetic parameters for SERCA reconstituted with WT or proline mutants of phospholamban or sarcolipin

	V_{max} (μmol/min/mg)	**Apparent K_{Ca} (μM)**	**Hill coefficient**
SERCA	4.05 ± 0.08	0.43 ± 0.02	1.65 ± 0.12
SERCA + WT PLN	3.77 ± 0.06*	0.80 ± 0.03 **	1.82 ± 0.12 (NS)
SERCA + N34P PLN	3.77 ± 0.07 (NS)	0.41 ± 0.02 (NS)	1.74 ± 0.14 (NS)
SERCA	4.01 ± 0.08	0.44 ± 0.02	1.69 ± 0.13
SERCA + WT SLN	3.92 ± 0.11 (NS)	0.86 ± 0.06 **	1.73 ± 0.16 (NS)
SERCA + N11P SLN	4.73 ± 0.12 (NS)	0.70 ± 0.05 **	1.41 ± 0.11 (NS)

Note: * indicates P<0.05 and ** indicates P<0.001